

The effect of the allelic diversity in *AvrSr35* on *Sr35*-based resistance in wheat

by

Bliss Madison Betzen

B.S., Kansas State University, 2016

A THESIS

submitted in partial fulfillment of the requirements for the degree

MASTER OF SCIENCE

Genetics Interdepartmental Program
Department of Plant Pathology
College of Agriculture

KANSAS STATE UNIVERSITY
Manhattan, Kansas

2020

Approved by:

Major Professor
Dr. Eduard Akhunov

Copyright

© Bliss Betzen 2020.

Abstract

Ug99 is the most devastating race group of wheat stem rust caused by the fungal pathogen *Puccinia graminis* f. sp. *tritici* (*Pgt*) and was originally found in Uganda in 1999 (Pretorius et al., 2000). Ug99 has since rapidly evolved giving rise to new virulent races that spread in parts of Africa and the Middle East, causing significant yield loss and food insecurity. The expansion of the Ug99 lineage provided evidence that this fungus is capable of evolving quickly to overcome resistance of a large number of wheat varieties with known wheat stem rust resistance (*R*) genes. The emergence of the Ug99 race group highlights the importance of studies aimed at understanding the evolutionary dynamic of *R* genes and their corresponding avirulence (*Avr*) factors. Here, I used a stem rust-wheat pathosystem to investigate the impact of intra-species variation in a recently identified fungal effector *AvrSr35* on the ability of stem rust resistance gene *Sr35* to recognize it and trigger defense response. We have identified the allelic variants of *AvrSr35* inducing reduced immune response in heterologous (tobacco leaves) and homologous (wheat protoplasts) transient expression systems. Missense mutations in the coding region of *AvrSr35* with potential to interfere with *AvrSr35*-*Sr35* interaction were detected by comparing allelic variants of *AvrSr35* in a diverse collection of *Sr35*-virulent and *Sr35*-avirulent *Pgt* isolates. To facilitate molecular analyses of wheat-rust pathosystem and characterization of additional *R*-*Avr* pairs, we assembled the reference genome of U.S. *Pgt* isolate 99KS76A-1 (race RKQQC). Advances in long-read sequencing technologies provide the opportunity to improve the quality of genome assemblies of many pathogens, including the complex cereal rust genomes. The assembly of the dikaryotic *Pgt* genome is challenged by the presence of two haplotypes in the dikaryon (Spatafora et al., 2017). Using Oxford Nanopore long-read sequencing in combination with error correction based on Illumina short reads, we generated a

haplotype-resolved assembly of the 99KS76A-1 isolate. We demonstrate that our assembly contains fewer gaps and shows higher N50 value than currently available reference genomes.

Table of Contents

List of Figures	viii
List of Tables	ix
Acknowledgements.....	x
Dedication	xi
Chapter 1 - Literature Review.....	1
1.1 Wheat as a global staple crop	1
1.2 Wheat stem rust overview.....	2
1.3 <i>Puccinia graminis</i> f. sp. <i>tritici</i> life cycle	3
1.4 Emergence of Ug99, stem rust recent epidemics.....	5
1.5 Identification and cloning of resistance genes	8
1.6 Adult plant resistance versus all stage resistance	10
1.7 Gene-for-gene concept.....	11
1.8 Plant immune strategies	12
1.8.1 PAMP triggered immunity.....	12
1.8.2 Effector triggered immunity.....	13
1.9 The wheat-rust pathosystem	15
1.9.1 <i>Sr35</i> gene.....	15
1.9.2 <i>AvrSr35</i> gene.....	16
1.10 Molecular approaches for studying gene-for-gene interactions.....	17
1.11 Fungal genetics and its difficulties	20
1.12 Research objectives and hypotheses	22
1.13 References.....	23
Chapter 2 - The effect of the allelic diversity in <i>AvrSr35</i> on <i>Sr35</i> -triggered hypersensitive response.....	36
2.1 Abstract.....	36
2.2 Objectives of study	37
2.3 Introduction.....	38
2.3.1 Stem rust group- Ug99.....	38
2.3.2 Wheat-stem rust pathosystem	39

2.3.3 <i>Sr35</i> gene.....	39
2.3.4 <i>AvrSr35</i> gene.....	40
2.4 Materials and Methods.....	43
2.4.1 Allelic diversity analyses of <i>AvrSr35</i> variants	43
2.4.2 <i>Agrobacterium</i> transformation.....	43
2.4.3 Gateway cloning	44
2.4.4 Transient expression in <i>Nicotiana benthamiana</i>	46
2.4.5 RNA isolation and gene expression (RT-PCR and qPCR).....	47
2.4.6 Create <i>Sr35</i> + YFP vector	49
2.4.7 Isolation and transformation of wheat protoplasts.....	50
2.4.8 Statistical analyses for wheat protoplast transformation.....	52
2.5 Results.....	53
2.5.1 <i>AvrSr35</i> allelic diversity in <i>Pgt</i> population.....	53
2.5.2 Evaluating interaction between <i>Sr35</i> and <i>AvrSr35</i> variants using the <i>N. benthamiana</i> transient expression system.....	55
2.5.3 Evaluating interaction between <i>Sr35</i> and <i>AvrSr35</i> variants by transient expression in the wheat protoplasts.....	60
2.6 Discussion.....	64
2.7 References.....	70
Chapter 3 - High-quality genome assembly and annotation of the <i>Puccinia graminis</i> f. sp. <i>tritici</i> isolate RKQQC	79
3.1 Abstract.....	79
3.2 Objectives of study	79
3.3 Introduction.....	80
3.4 Materials and Methods.....	82
3.4.1 Spore grow-up, collection, and spore mat formation.....	82
3.4.2 Fungal DNA isolation	83
3.4.3 Oxford Nanopore library prep and sequencing technology	85
3.4.4 Illumina library prep and sequencing technology.....	86
3.4.5 Programs and pipelines: Canu, Pilon	87

3.4.6 Comparison of the completeness of 99KS76A-1 (race RKQQC) and CDL75-36-700-3 (race SCCL) genome assemblies using BUSCO.	88
3.5 Results and Discussion	88
3.6 References.....	92
Chapter 4 - Conclusions.....	96
Appendix.....	98

List of Figures

Figure 1.1: Wheat rusts	3
Figure 1.2: Life cycle of <i>Puccinia graminis</i> f. sp. <i>tritici</i> (<i>Pgt</i>)	5
Figure 1.3: Gene-for-gene model depiction	12
Figure 1.4: Structure of an NBS-LRR protein	13
Figure 1.5: Boom-Bust Cycle	14
Figure 2.1: Overview of alterations made to the <i>AvrSr35</i> gene variants for Gateway cloning	45
Figure 2.2: <i>AvrSr35</i> amino acid sequence diversity	54
Figure 2.3: Evaluation of interactions between allelic variants of <i>AvrSr35</i> and <i>Sr35</i> using <i>N. benthamiana</i> infiltration system.....	56
Figure 2.4: qRT-PCR Ct values demonstrating the expression of QTHJC and control gene constructs in the <i>Agrobacterium</i> infiltrated tobacco leaves.....	58
Figure 2.5: Combined normalized protoplast absorbance per isolate at various hours post Infection (HPI)	63
Figure 2.6: Models of Host-Pathogen interaction.....	67
Figure 3.1: BUSCO comparison of RKQQC and SCCL assemblies.....	91

List of Tables

Table 1.1: Ug99 race group lineage	7
Table 2.1: Primer Sequences used throughout this study	59
Table 2.2: Summary of presence or absence of hypersensitive response (HR) seen in <i>N. benthamiana</i> infiltration system alongside the wheat protoplast system at 24 Hours Post Infection (HPI) between allelic variants of <i>AvrSr35</i> and <i>Sr35</i>	64
Table 3.1: Sequencing data statistics	89
Table 3.2: <i>Pgt</i> genome assembly statistics	90

Acknowledgements

I express my dearest gratitude to my major professor, Dr. Eduard Akhunov, for providing me with the great opportunity to work with his guidance and to grow both professionally as a scientist and grow as person. I would like to thank the esteemed faculty serving on my committee: Dr. David Cook, who provided me with the confidence to keep writing even when my anxiety was taking over; and Dr. John Fellers, who was a major collaborator in the RKQQC reference assembly and also gave me constructive criticism in a fun-loving way. I thank all of my committee for making me think more critically and ask questions to produce hypothesis-driven research.

I would like to specifically acknowledge Dr. Andres Salcedo and Dr. Wei Wang for being true mentors to me. Andres' previous research and willingness to teach me classic techniques in my study were a key role in helping me conceptualize and develop my project. In the same breath, I would also like to thank Wei for his readiness to teaching me more molecular approaches to my research.

I would like to acknowledge Dr. Robert Bowden for training me and allowing me to use the USDA-ARS equipment for spore isolations and infections.

I would also like to thank Dr. Yuanwen Guo for doing all of the bioinformatics for the RKQQC reference genome assembly with the help of Dr. Katie Jordan and Dr. Fei He. I would still be trying to code if not for their help and knowledge.

I would like to thank the Akhunov lab, both present and past, for being true friends to me as well as sharing camaraderie, kindness, and support throughout my graduate career.

Lastly, I would like to thank my loving family: my parents, Kim Foister and Ron and Karen Betzen; and my siblings, Liz, Brooklynne, Brittaney, Peter, and Taylor for always encouraging me. My fiancé John Coffin, who provides unending support and love in helping me accomplish my goals. I thank John for spending many hours/days/weeks editing dozens of drafts of this thesis and STILL wanting to marry me. I would also like to thank all my friends that have kept me sane and who have made Manhattan my home in these last few years.

Dedication

I would like to dedicate my thesis to my grandpa, Lavern Lee Drapal, who inspired me to pursue higher education and unfortunately was not able to see the end of this journey before his passing on March 19th, 2020. Lavern Drapal was an exceptional high school math teacher, an aspiring artist, a cheater at card games, a cheerleader to his three children and five grandchildren, and a cultivator of not only delicious snap peas, but also of unconditional love. Without his love and support, I guarantee I would not be submitting this compilation of work.

Chapter 1 - Literature Review

1.1 Wheat as a global staple crop

Common bread wheat (*Triticum aestivum*) is an allohexaploid ($2x=6N$), while durum wheat (*Triticum durum*) is a tetraploid wheat ($2x=4N$) (Gill & Friebe, 2002). The original progenitors of hexaploid bread wheat were two species of diploid wild grasses, *Triticum urartu* (A genome) and *Aegilops speltoides* (B genome ~S genome) (Ozkan et al., 2001; Glémin et al., 2019). After hybridization between these two species, polyploidization occurred through whole genome duplication, resulting in tetraploid *Triticum turgidum* (Ozkan et al., 2001; Gustafson et al., 2009). A subsequent hybridization event between *T. turgidum* and a diploid wild relative, *Aegilops tauschii*, led to the origin of hexaploid bread wheat that we have today (Kihara, 1994). The hexaploid nature of common bread wheat and diversity contributed by wild and domesticated ancestors provided sufficient variation for selection (Sharma & Gill, 1983). The genetic diversity of modern bread wheat is shaped by natural and human-driven selection aimed to improve wheat adaptation to diverse climates and agricultural practices (Cavanagh et al., 2013; Willcox, 2005; Venske et al., 2019).

Common wheat is the third most important staple world crop, alongside rice (*Oryza sativa*) and maize (*Zea mays*) (Shewry, 2009), and makes up an estimated 20% of the world's calorie consumption ("Wheat Nutrition," 2020). Wheat is grown throughout mid-temperate and tropic regions (Simmonds, 1979) and is a staple crop in Europe, Asia, Africa, Australia, and the Americas accounting for 215 million hectares and 761.5 million tonnes worldwide (*WHEAT in the World* » CGIAR Research Program on WHEAT, 2017; FAOSTAT, 2019). Developing countries, in areas such as Africa and the Middle East, contain some of the most food insecure and malnourished populations on Earth (Roser & Ritchie, 2013) and only account for 25 million

(Tadesse et al., 2019) and 43.8 (*Middle East : Wheat - Producing Countries (Tons)*, 2016) million tonnes of the global wheat production, respectively. This indicates that less than 10% of the wheat produced globally is in the countries that need this staple crop the most. In order to help these countries, a better understanding of how wheat interacts with biotic stresses from plant pathogens and pests is necessary for plant protection and productivity (Shewry, 2009).

1.2 Wheat stem rust overview

Among the known biotic stresses, there are three wheat rust diseases caused by fungi of the Puccinales order: leaf rust, stripe rust, and stem rust (Bushnell & Roelfs, 1984; *Rust Diseases of Wheat*, 2016), which are shown in Figure 1.1. *Puccinia triticina* (*Pt*) is the causal agent of wheat leaf rust, also known as brown rust (Park, 2015; Aktar-Uz-Zaman et al., 2017; Bolton et al., 2008). Leaf rust is commonly identified by the presence of small circular to oval brown or orange spots on infected leaves (Figure 1.1, A), but also can affect the glumes and awns (Savile, 1984; Marsalis & Goldberg, 2016). Leaf rust is the most widespread of the wheat rusts, causing yield losses up to 20% (*Wheat Leaf Rust : USDA ARS*, 2017). *P. striiformis* f. sp. *tritici* (*Pst*) causes wheat stripe rust, also known as yellow rust (Park, 2015; Schwessinger, 2017; Lin et al., 2018), and produces light yellow or orange stripes of pustules on leaves and heads that vary in size and length (Figure 1.1, B) (Bushnell & Roelfs, 1984; Marsalis & Goldberg, 2016). Stripe rust can cause a more severe disease with up to 40% of yield losses in wheat under conducive conditions (*Wheat Stripe Rust : USDA ARS*, 2017). *Pgt* causes wheat stem rust, also known as black rust (Park, 2015; Aktar-Uz-Zaman et al., 2017; Rahmatov et al., 2016), and affects many parts of the plant such as the leaves, sheaths, glumes, and awns and appears as red or brown oval to elongate lesions (Figure 1.1, C) (Singh et al., 2008; Marsalis & Goldberg, 2016). Stem rust is

one of the most destructive wheat rust diseases, causing yield losses up to 70 % under conducive conditions (FAOSTAT, 2019).



Figure 1.1: Wheat rusts. (A) Leaf rust, (B) Stripe rust, (C) Stem rust

Reprinted from “Rust diseases of Wheat”, by Jorge David Salgado, Elizabeth Roche and Pierce A. Paul, 2016.

1.3 *Puccinia graminis* f. sp. *tritici* life cycle

The visual signs of *Pgt* typically are seen as red oblong spores called urediniospores (Bushnell & Roelfs, 1984). When the pathogen matures the urediniospores turn black, giving the rust’s alternative name of black rust (*Wheat Stem Rust : USDA ARS, 2017*). *Pgt* is able to complete multiple cycles of asexual infection during the life cycle of wheat. Given the optimal temperature of 18-27°C, high dew points at night, and a susceptible host, *Pgt* is able to create millions of urediniospores during all wheat stages (*Wheat Stem Rust : USDA ARS, 2017*). *Pgt* is heteroecious, which means that it completes its life cycle on two unrelated hosts (Prentice et al.,

2002). The sexual portion of the *Pgt* life cycle is on an alternate host, barberry (*Berberis vulgaris*), and the asexual portion can be completed on important economic grass crops, such as wheat (*T. aestivum*) and barley (*Hordeum vulgare*) (*Wheat Stem Rust : USDA ARS*, 2017). The life cycle of *Pgt* is detailed in Figure 1.2 (Reprinted from Leonard & Szabo, 2005).

During the asexual stage of the *Pgt* life cycle, wheat dikaryotic uredinium grows on infected wheat and produces thin-walled urediniospores through mitosis (Figure 1.2, A). These spores are the primary inoculum of *Pgt* and spread via wind to other susceptible plants (Figure 1.2, A). Telium carrying diploid teliospores are formed from uredinium which have durable outer walls allowing the spores to overwinter on wheat stubble or volunteer wheat (Figure 1.2, B). Once conditions are favorable, the teliospores fuse together in a process called karyogamy and perform meiosis in the fungal structure called promycelium (Figure 1.2, C and D). Haploid basidiospores emerge from the promycelium to infect the barberry plants (Figure 1.2, E). Fertilization is possible via the spreading of pycnium carrying pycniospores by attracting insects for means of dispersal to other infected plants (Figure 1.2, F and G) (Bushnell & Roelfs, 1984). Sexual recombination can occur and the aecium form, carrying dikaryotic aeciospores, which completes the cycle by infecting wheat and creating uredinium (Figure 1.2, H). When there is no alternate host for the sexual portion of the life cycle, only the asexual portion is completed. Only uredinium carrying urediniospores infect wheat and continue with the sexual portion of the life cycle (Schumann & Leonard, 2000). With or without the sexual cycle, wheat stem rust is extremely detrimental to global wheat production with its quick ability to readily infect plants.

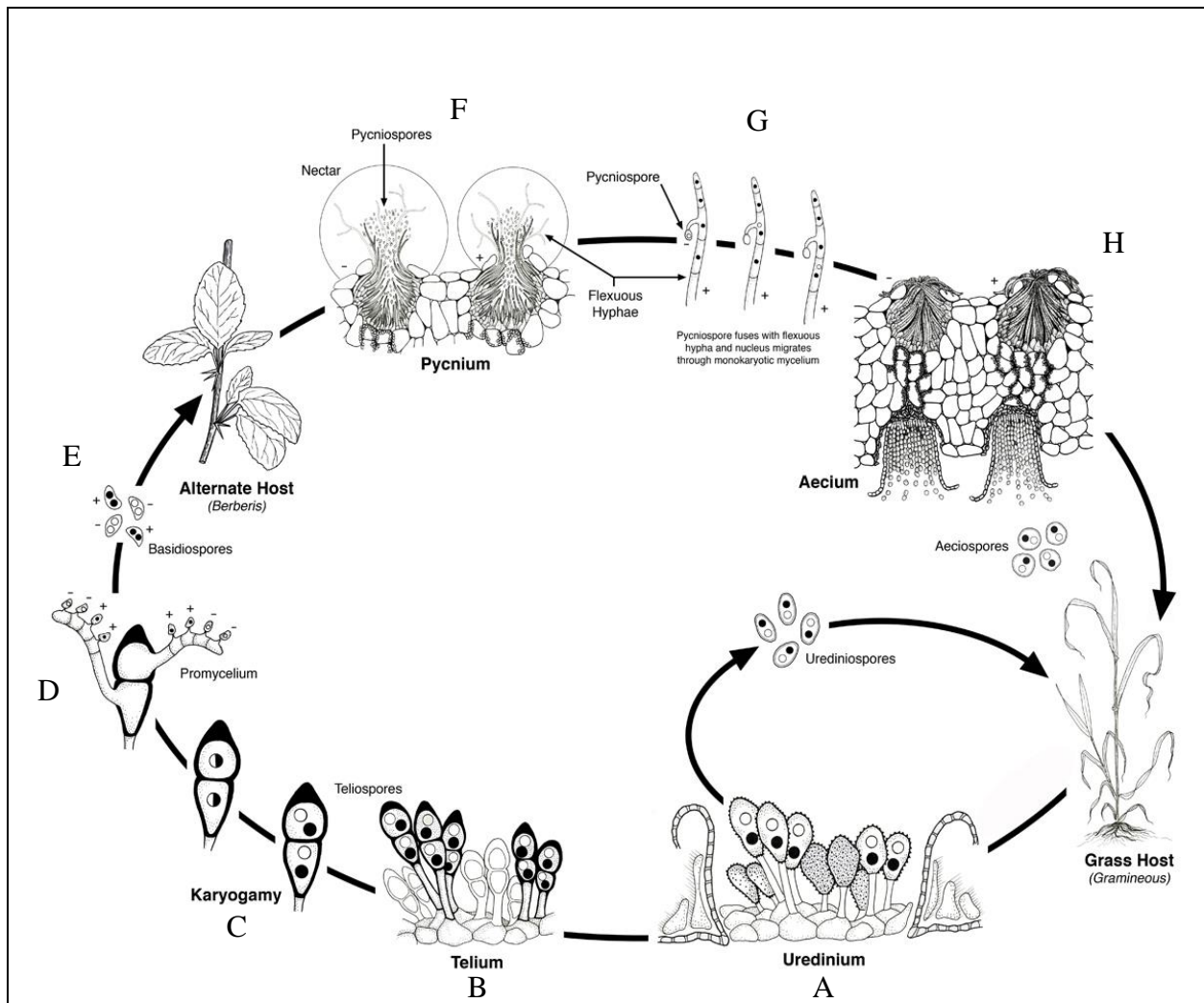


Figure 1.2: Life cycle of *Puccinia graminis* f. sp. *tritici* (Pgt). (A) Uredinium stage, (B) Telium stage, (C) Karyogamy stage, (D) Promycelium stage, (E) Basidiospores, (F) Pycnium stage, (G) Pycniospores, (H) Aecium stage

Reprint from Leonard & Szabo, 2005.

1.4 Emergence of Ug99, stem rust recent epidemics

Depictions of stem rust have been stated throughout history. The Romans celebrated the festival of Robigalia to offer sacrifices to the god Robigus in order to have healthy wheat fields, free from rust (Beard et al., 1998). Stem rust has also been noted in more recent times during the

1900's as one of the biggest global threats, which was particularly devastating to North American farmers through the 1910's-1950's (*Wheat Stem Rust : USDA ARS*, 2017). From the 1950's until 1999 the damage done by *Pgt* was relatively low due to deployment of resistance (*R*) genes in wheat, the eradication of the alternate host of barberry, and cultural agronomic practices in the field (Hartman et al., 2016; Schumann & Leonard, 2000). For roughly 45 years, global stem rust infection seemed to decline. Many stem rust (*Sr*) *R* genes had been deployed in wheat breeding lines globally making for strong resistance in wheat towards stem rust, even in the most conducive environments for pathogen fitness (Pretorius et al., 2000). However, in 1999 a new race of stem rust was identified in Uganda with high virulence against varieties with the *Sr31* gene and was coined Ug99 (Pretorius et al., 2000; Hartman et al., 2016). Numerous *R* genes such as *Sr31*, *SrTmp*, *Sr9h*, *Sr24*, *Sr31*, *Sr36* have all been overcome by the Ug99 race group. These *R* genes were highly utilized in germplasms globally and were well known as effective stem rust resistance sources (*GlobalRust.Org*, 2019). The Ug99 outbreak sparked a new wave of research by wheat breeders, plant pathologists, and geneticists. Li et al. (2019) states that the reason for this sudden pathogen outbreak was the result of the introduction of genetic diversity in *Pgt* due to nuclear exchange between dikaryotes, known as somatic hybridization, resulting in the origin of the Ug99 race lineage. Genomic comparison done by Li et al. (2019) showed that Ug99 contains one haploid nucleus from an Australian *Pgt* isolate, *Pgt21-0*, and another from an unknown isolate which brought pathogen virulence towards *Sr31*. Ug99 rapidly evolved to create a diverse group of races that have spread throughout Africa and the Middle East at an alarming rate and were able to overcome other *R* genes such as *SrTmp* (Patpour et al., 2015), *Sr9h* (Rouse et al., 2014), *Sr24* (Jin et al., 2008), and *Sr36* (Jin et al., 2009). A study done by Singh et al. (2011) tested a panel of wheat varieties commonly used in Africa and Asia and found that only

5-10% of those varieties provided adequate resistance to the Ug99 race group. Approximately, 80-90% of the cultivars currently used globally are susceptible to Ug99 and do not have adequate resistance (Hodson, 2019). The ability to overcome resistance in global wheat germplasm makes Ug99 a considerable threat to global food security. The Ug99 group has currently evolved into 13 known races: TTKSK (Ug99), TTKSF, TTKST (Ug99+Sr24), TTTSK (Ug99+Sr36), TTKSP, PTKSK, PTKST, TTKSF+, TTKTT, TTHSK, PTKTK, TTHST (Table 1.1 from https://rusttracker.cimmyt.org/?page_id=22; Hodson, 2019).

Table 1.1: Ug99 race group lineage. Including common aliases, R genes in which each race confers virulence or avirulence, year of identification, and confirmed countries in which the race is present. From https://rusttracker.cimmyt.org/?page_id=22				
Race ^a	Common Alias	Key Virulence (+) or Avirulence (-) [*]	Year of Identification	Confirmed Countries (year)
TTKSK	Ug99	+Sr31	1999	Uganda (1998/9), Kenya (2001), Ethiopia (2003), Sudan (2006), Yemen (2006), Iran (2007), Tanzania (2009), Eritrea (2012), Rwanda (2014), Egypt (2014)
TTKSF		-Sr31	2000	South Africa (2000), Zimbabwe (2009), Uganda (2012)
TTKST	Ug99+Sr24	+Sr31, +Sr24	2006	Kenya (2006), Tanzania (2009), Eritrea (2010), Uganda (2012), Egypt (2014), Rwanda (2014)
TTTSK	Ug99+Sr36	+Sr31, +Sr36	2007	Kenya (2007), Tanzania (2009), Ethiopia (2010), Uganda (2012), Rwanda (2014)
TTKSP		-Sr31, +Sr24	2007	South Africa (2007)
PTKSK		+Sr31, -Sr21	2007	[Uganda (1998/9)?], Kenya (2009), Ethiopia (2007), Yemen (2009), South Africa (2017)
PTKST		+Sr31, +Sr24, -Sr21	2008	Ethiopia (2007), Kenya (2008), South Africa (2009), Eritrea (2010), Mozambique (2010), Zimbabwe (2010)
TTKSF+		-Sr31, +Sr9h	2012	South Africa (2010), Zimbabwe (2010)
TTKTT		+Sr31, +Sr24, +SrTmp	2015	Kenya (2014)
TTKTK		+Sr31, +SrTmp	2015	Kenya (2014), Egypt (2014), Eritrea (2014), Rwanda (2014), Uganda (2014)
TTHSK		+Sr31, -Sr30	2015	Kenya (2014)
PTKTK		+Sr31, -Sr21, +SrTmp	2015	Kenya (2014)
TTHST		+Sr31, -Sr30, +Sr24	2015	Kenya (2013)

^a Some uncertainty exists over the reaction of the Sr21 gene (this influences the initial code letter being “T” (+Sr21) or “P” (-Sr21). Current table presents most plausible races
* Only key Sr genes are indicated, not the complete virulence/avirulence profile

Chemical and biological control methods are often used to control the damage and spread of stem rust. However, the most promising strategy to provide effective and sustainable protection for yield and to control the spread of disease is through genetic improvement of wheat disease resistance and the decreased use of susceptible wheat varieties (Singh et al., 2015). Several groups around the world are pioneering efforts to detect disease outbreak, as well as discover and deploy new effective stem rust *R* genes in international breeding programs. The USDA Cereal Disease Laboratory (CDL) is the lead on new *R* gene identification, while The Sainsbury Laboratory (TSL) is working on a program for rapid gene identification (Moscou & Esse, 2017; *Cereal Disease Lab : USDA ARS*, n.d.). Other groups, such as the Borlaug Global Rust Initiative (BGRI) and CIMMYT have created networks of labs to conduct global stem rust surveillance spanning 40 countries, develop specialized labs to test for new races all over the world, and to initiate the execution of early warning systems in affected areas through field data and surveys to provide a seven day forecast pipeline for stem (*GlobalRust.Org*, 2019). Now farmers are able to get ahead of disease due to early warning, early detection, and early control which are all critical for minimizing disease outbreak.

1.5 Identification and cloning of resistance genes

While modern crop management provides effective approaches for reducing the impact of disease on farmers' fields, the most sustainable strategy against stem rust is based on the exploration and utilization of genetic resistance provided by *R* genes (Mundt, 2014). The USDA-CDL among other groups have screened hundreds of wheat varieties, which has led to the identification of more than 70 stem rust *R* genes, over half of which are proven effective at some

level against one or more of the Ug99 races (*GlobalRust.Org*, 2019; *Cereal Disease Lab : USDA ARS*, n.d.; McIntosh et al., 2017; Rahmatov et al., 2019; Hodson, 2019). Researchers continue to build up and improve the arsenal of viable *R* genes, which can be implemented individually or in tandem with other *R* genes in breeding programs. Cloning of *R* genes can benefit the plant protection community by incorporating biotechnology and gene editing into developing new resistant wheat varieties and integrating genetic background knowledge to improve plant protection strategies. Seven *R* genes effective against Ug99 have been cloned: *Sr13* (Zhang et al., 2017), *Sr21* (Chen et al., 2018), *Sr22* (Steuernagel et al., 2016), *Sr33* (Periyannan et al., 2013), *Sr35* (Saintenac et al., 2013), *Sr45* (Steuernagel et al., 2016), *Sr50* (Mago et al., 2015). Traditionally, the cloning of genes has been accomplished through map-based cloning (Young, 1990) and has been used for several years to clone many rust *R* genes such as *Sr35* (Saintenac et al., 2013), *Sr50* (Mago et al., 2015), and the non-race specific *Lr34/Yr18/Sr57/Pm38* (Krattinger et al., 2009). In the past ten years there has been significant progress in improving the methods for *R* gene cloning based on the Target-sequence Enrichment and Sequencing (TEnSeq) strategies: Mutagenesis and the Resistance gene Enrichment and Sequencing (MutRenSeq) (Steuernagel et al., 2016), Mutagenesis Chromosome flow sorting and short-read Sequencing (MutChromSeq) (Sánchez-Martín et al., 2016), Targeted Chromosome-based Cloning via long-read Assembly (TACCA) (Thind et al., 2017), and Association genetics with Resistance gene Enrichment and Sequencing (AgRenSeq) (Arora et al., 2019). With TEnSeq cloning strategies, researchers are able to reduce genome complexities and perform rapid cloning of plant *R* genes without the need of large mapping populations (Zhang et al., 2020).

1.6 Adult plant resistance versus all stage resistance

Plant resistance does not imply that the plant is resistant at all growth stages. There are two broad and non-exclusive classifications for types of resistance. Non-race specific resistance consists of a number of genes conveying resistance to a wide range of pathogens. This type of resistance is typically shown as adult plant resistance (APR) and refers to plants only being able to implement effective resistance against pathogens when the plant reaches maturity (Marla et al., 2018). Adult plant resistance is especially useful for rust resistance because it is normally paired with an early season fungicide application or other *R* genes through gene pyramiding via plant backcrossing or transgenic gene cassettes (Zhang et al., 2020). APR conferred by slow-rusting genes provides partial resistance and therefore is used in tandem with other *R* genes to provide a more durable resistance. Race-specific resistance is when a gene confers resistance to a specific pathogen. Race-specific resistance is typically exhibited as seedling resistance or all stage resistance (ASR), which can maintain resistance against pathogens throughout few growing seasons (Chen & Line, 1992; Park et al., 2003; Elmansour et al., 2017). However, resistance that is race-specific can be short lived when pathogens undergo genetic evolution therefore conveying new virulence (Riaz et al., 2016; Chen & Line, 1992). Due to this observation, APR is said to be more durable than ASR (Wang et al., 2005). The continued research of plant protection strategies via deployment of *R* genes has determined that not all *R* genes are either APR or ASR; there can be aspects of both types of resistance mechanisms that apply. One prime example of the ambiguity of resistance gene classification is the wheat leaf rust resistance gene, *Lr12*, which McIntosh et al. (1995) identified as a race-specific APR gene. Another example is shown in *Lr34-Yr18-Sr57-Pm18*, which is non-race specific and encode for a putative ABC transporter in wheat; however, the resistance provided by this gene is comparable to that of a race-specific gene (Singh &

Huerta-Espino, 2003; Soria, 2019; Krattinger et al., 2009).). In plant breeding, both APR and ASR genes are utilized to provide more complex and long-lasting genetic protection against pathogens and maintain adequate gene stewardship (Zhang et al., 2020; Periyannan et al., 2017).

1.7 Gene-for-gene concept

A pathosystem encompasses a pathogen, its host, and molecular components within the system that may promote or block establishing compatible interactions between host and pathogen (Robinson, 1977). In plant pathology, the two main factors of a pathosystem are the host plant *R* genes and the corresponding fungal pathogen effectors or avirulence (*Avr*) genes. One of the most commonly utilized models describing plant-pathogen interaction is the gene-for-gene interaction model. This model is based on host-pathogen interactions of flax (*Linum usitatissimum*) and flax rust (*Melampsora lini*) by H. H. Flor (1942). Gene-for-gene theory conveys the terms of plant resistance and susceptibility through the presence and absence of host *R* genes and pathogen *Avr* genes. Only when the host plant *R* gene and the corresponding fungal *Avr* gene are both present within the pathosystem will the plant show resistant phenotype (Figure 1.3) (Flor, 1942). If the protein products of one or both of the *R* and *Avr* genes are missing, modified, or non-functional, host plant recognition of the disease will not occur, resulting in host plant susceptibility (Flor, 1942). This concept is the basis of resistance breeding against wheat stem rust using major *R* genes.

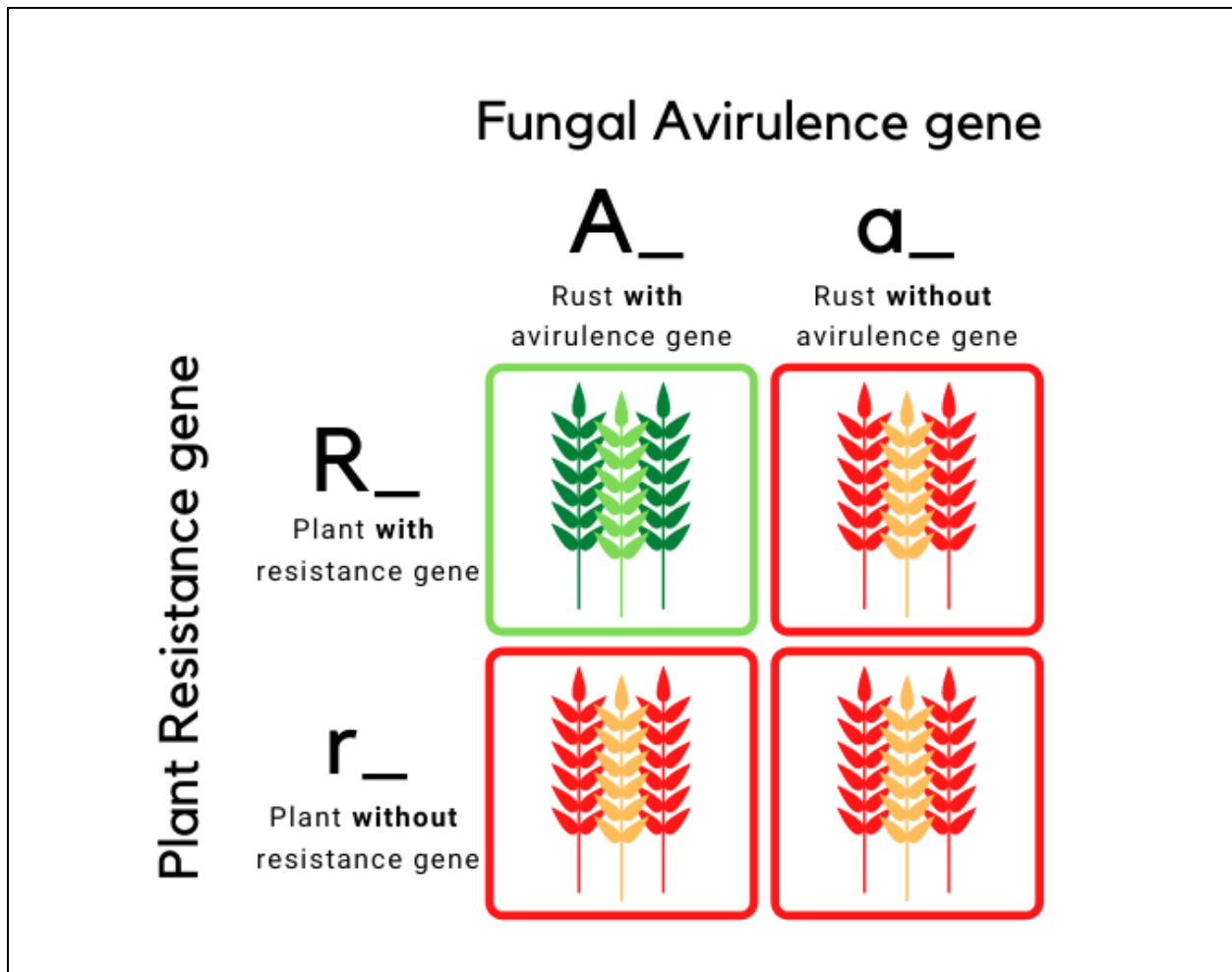


Figure 1.3: Gene-for-gene model depiction. When plants have a specific resistance (*R*) gene that correspond to one of the specific avirulence (*Avr*) genes present in the fungal pathogen there is pathogen recognition and immune system signaling.

1.8 Plant immune strategies

1.8.1 PAMP triggered immunity

Plant immunity could be triggered by recognition of microbes and their associated molecules by pattern recognition receptors (PRR) (Zhang et al., 2010), which identify microbe, pathogen, or damage-associated molecular patterns (MAMP, PAMP, DAMP) (Boller & Felix, 2009; Krol et al., 2010). This recognition, called PAMP triggered immunity (PTI), is also known as basal disease resistance or vertical resistance. PTI is fundamentally thought of as a part of innate

immunity functioning across all developmental stages (Nürnberger & Brunner, 2002; Boller & Felix, 2009). Bacterial flagellin and fungal chitin are prime examples of MAMP and PAMP (Choi & Klessig, 2016). Damages to plants such as leaf tissue injuries, changes in the plasma membrane, and biotic stresses are prime examples of DAMP (Krol et al., 2010; Ferrari et al., 2013). Once PRRs initiate PTI, a network of signaling pathways is triggered and molecular cascades result in plant resistance (Bigeard et al., 2015).

1.8.2 Effector triggered immunity

Another layer of plant immunity is called effector-triggered immunity (ETI) (Boller & Felix, 2009), previously known as *R* gene-based resistance or horizontal resistance. In plant pathology, one of the main classes of *R* genes encodes for intracellular receptor proteins that are composed of a coil-coiled (CC) or toll-interleukin receptor (TIR) like domain, nucleotide-binding site (NBS), and leucine-rich repeats (LRR) which are collectively called NLR genes (Figure 1.4) (Gu et al., 2015). The receptor protein structure is important in plant immunity for specificity in disease recognition and resistance. In plants, the NLR gene family is diverse and in common bread wheat alone there over 2000 NLR genes currently identified (Gu et al., 2015).

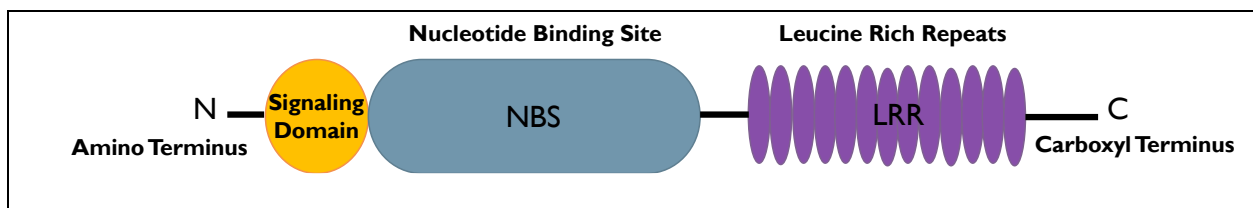
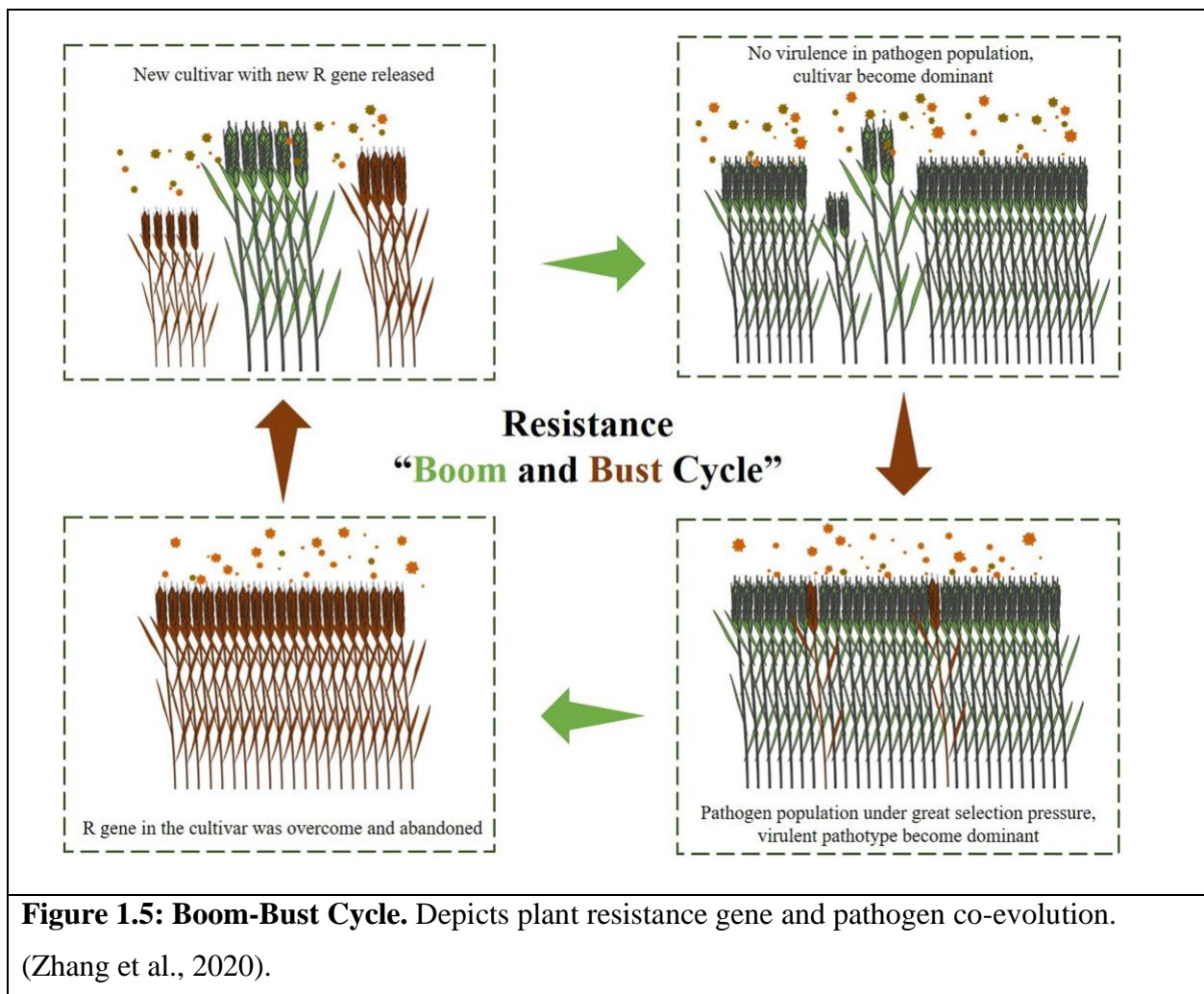


Figure 1.4: Structure of an NBS-LRR protein. Starting from the amino (N) terminus there is the intercellular signaling domain that can be one of two types: coiled-coil (CC) domain or toll-interleukin receptor (TIR) domain. In the middle of the protein there is the nucleotide binding site (NBS) and at the carboxyl (C) terminus there is the leucine rich repeats (LRR) region.

Adapted from McHale et al. 2006.

In plant pathology, ETI is based on host *R* genes' highly specific recognition of pathogens' effectors encoded by *Avr* genes (Riaz et al., 2016). *Avr* recognition triggers a hypersensitive response (HR), localized cell death, which stops the spread of the pathogen by cutting off supply of nutrients required for fungal growth (Balint-Kurti, 2019, Hogenhout et al., 2009) . Selection against avirulent variants of fungal effectors that are recognized by the host results in the origin of new effector variants that are undetectable by the host's immune system, resulting in co-evolution between host *R* genes and pathogen *Avr* genes (Jones & Dangl, 2006). Co-evolution of *Avr-R* genes is also known as an evolutionary arms race or the resistance boom and bust cycle (Figure 1.5, Reprint from Zhang et al., 2020).



1.9 The wheat-rust pathosystem

Due to the complex life cycle of cereal rusts and lack of effective methods for rust transformation, only a few *R-Avr* gene pairs have been identified so far, including *AvrSr35-Sr35* and *AvrSr50-Sr50*. (Saintenac et al., 2013; Salcedo et al., 2017; Mago et al., 2015; Chen et al., 2017). Both studies showed that *Pgt* recognition is triggered by direct interaction between the resistance genes and matching effectors, and that virulent strains of a *Pgt* population carry mutations in the *Avr* gene encoding regions. Identification of these resistance genes and matching fungal effectors provides unique opportunities for the characterization of host proteins that could be targeted by effectors. Knowledge of these interactions is also useful for investigating the mechanisms used by pathogens to establish compatible interaction and for developing novel pathogen surveillance methods. These methods allow for detecting the distribution of known avirulence genes in pathogen populations and predicting virulence of novel isolates to existing resistance genes deployed in cultivars grown in farmers' fields.

1.9.1 *Sr35* gene

The stem rust *R* gene *Sr35* was identified in *T. monococcum*, a diploid species of wheat commonly known as cultivated einkorn (McIntosh et al., 1984; Saintenac et al., 2013; Koehler et al., 2014) and is located on the long arm of chromosome 3A of *T. monococcum* (Zhang et al., 2010). The gene contains four introns and two exons, and is 4,872 base pairs (bp) long (Saintenac et al., 2013). *Sr35* has two alternative splicing variants: (1) the main isoform, in which the mature mRNA contains no intron sites, and (2) isoform 2, which still contains the third intron site (Saintenac et al., 2013). *Sr35* encodes for a coiled-coil, nucleotide-binding, leucine-rich repeat (NLR) intracellular receptor (Saintenac et al., 2013). There are three mechanisms by which NLR genes recognize pathogens: (1) direct interaction with pathogen effectors, (2)

monitoring of host target modifications, or (3) through monitoring a host target decoy that interacts with pathogen effectors (Van de Weyer et al., 2019; Kourelis & van der Hoorn, 2018). Currently, the mechanism used by *Sr35* to recognize *AvrSr35* is unknown. Some experimental data suggest that *Sr35* interacts with *AvrSr35* on the cellular membrane, suggesting the possibility of direct interaction with another host protein (Salcedo et al., 2017).

The transfer of *Sr35* into bread wheat was shown to provide resistance against stem rust (Saintenac et al., 2013). Saintenac et al. (2013) were able to produce a transgenic hexaploid wheat plant expressing *Sr35* that showed resistance against Ug99 and RKQQC races of *Pgt* (Salcedo et al., 2017). Likewise, *Sr35* transferred into hexaploid wheat via crossing and recombination was effective against several *Pgt* isolates, including isolates from the Ug99 group (McIntosh et al., 1984; Zhang et al., 2010). These studies demonstrated that *Sr35* could be used to build resistance gene complexes to provide broad spectrum resistance in breeding programs.

1.9.2 *AvrSr35* gene

The discovery of the *Sr35* gene prompted in-depth research into plant-pathogen interactions and the identification and characterization of corresponding fungal *Avr* genes. The fungal avirulence gene *AvrSr35* was one of the first *Avr* genes to be identified for cereal rusts and encodes for a secreted protein and upon recognition by *Sr35* triggers an immune response (ETI) (Saintenac et al., 2013; Salcedo et al., 2017). *AvrSr35* was found by infecting a wheat variety carrying *Sr35* with a diverse set of *Pgt* isolates along-side EMS mutagenized *Pgt* isolates known to contain *AvrSr35* (Salcedo et al., 2017). *AvrSr35*, which was found in the fungal *Pgt* race RKQQC, contains 6 introns and 7 exons, and is 1,734 bp long. Its interaction with *Sr35* was demonstrated to be critical for *Sr35*-based resistance response in wheat. In addition to the identification of *AvrSr35*, Salcedo et al. (2017) compiled a set of *Pgt* isolates from varying years and locations,

and characterized allelic diversity of the *AvrSr35* gene locus. This analysis revealed high levels of sequence diversity in the *Pgt* population affecting coding regions of *AvrSr35* and showed that most of the virulent isolates of *Pgt* carry a transposable element (TE) insertion introducing premature termination codon (Salcedo et al., 2017). However, some variants of *AvrSr35* from the *Sr35*-virulent *Pgt* isolates showed an absence of the TE insertion, suggesting that they might carry either amino-acid changing mutations that affect sites involved in interaction with *Sr35*, or additional effectors that are capable of disrupting *Sr35*-triggered defense response (Salcedo et al., 2017).

1.10 Molecular approaches for studying gene-for-gene interactions

The gene-for-gene concept was first developed in the 1940s prior to the molecular and DNA-sequencing approaches that we take for granted today. Flor (1942) performed controlled crosses between different races of *Melampsora lini* (flax rust) and used F₂ progeny of these crosses to infect sets of differential *Linum usitatissimum* (flax) lines carrying known resistance genes. By comparing the observed ratio of the F₂ progeny to the expected ratio under Mendelian inheritance (9:3:3:1), Flor was able to demonstrate flax resistance and rust avirulence appeared to be determined by the presence of complementary genes, leading him to develop the gene-for-gene concept of plant-pathogen interaction. Flor's inception of the gene-for-gene concept (1942) laid the theoretical foundation for understanding host-plant co-evolutionary dynamics; however, further advances in molecular methods of genome analyses were required to develop an empirical mechanistic understanding of these at a molecular level.

One of the limitations for studying biotrophic fungi is their dependence on the host's resources for growth and reproduction (Meadows, 2011). Due to this reason, first insights into the

molecular mechanisms of host-pathogen interactions were obtained in bacterial pathogens. For instance, the first *Avr* gene, *avrA*, was cloned from the bacteria *Pseudomonas syringae* pv. *glycinea* (bacterial blight of soybean) (Staskawicz et al., 1984; Keen, 1990) .

Yeast two-hybrid (Y2H) assay is one of the broadly used methods for characterizing interaction between two proteins. The Y2H systems is based on two plasmids expressed in yeast cells: (1) one plasmid contains a target gene sequence encoding a protein of interest called ‘bait’ fused with the binding domain (BD) and, (2) another plasmid contains the other target sequence encoding the interacting protein referred to as ‘prey’, which is fused with the activation domain (AD) (Young, 1998). Interaction between the two target proteins brings together the BD and AD activating transcription of a reporter gene that allows yeast cells to grow in media lacking certain nutrients (Young, 1998). An example of Y2H assay application for studying plant-pathogen interaction is the study of fungal effectors from *Ustilago maydis* by Alcântara et al. (2019). They found that a number of the tested effectors interacted with themselves and other *U. maydis* effectors, suggesting formation of extensive effector complexes.

Another popular method for analyzing protein-protein interactions among the host’s receptor proteins and pathogen’s effectors is immunoprecipitation. The method is often based on the usage of epitope-tagged protein fusions that allow for separating a tagged protein and its interacting partners from a complex mix of other protein molecules using antibodies against epitopes attached to a solid surface. There are many versions of immunoprecipitation methods, all of which could be used to study plant-pathogen interactions: protein immunoprecipitation (IP; see Phizicky & Fields, 1995; Kaboord & Perr, 2008; Woods Ignatoski, 2001), protein complex immunoprecipitation (Co-IP; see Phizicky & Fields, 1995; Kaboord & Perr, 2008; Weis et al., 2013), chromatin immunoprecipitation (ChIP; see (Wang et al., 2004; Nissen & Yamamoto,

2000; Mishra et al., 2017), ribonucleoproteins (RNP) immunoprecipitation (RIP; see Hassan et al., 2010; Cozzitorto et al., 2015; Marmisolle et al., 2018), and tagged proteins such as FLAG, HA, and Green Fluorescent Protein (GFP) (see Operaña & Tukey, 2007; Salim et al., 2002; Terzi & Simpson, 2009). Immunoprecipitation is often performed in concert with mass spectrometry (MS) (Hoffmann, 2005), which measures ions' mass to charge ratio of protein molecules (Hoffmann, 2005). MS in combination with other protein-protein interaction analyses methods has been successfully used in the field of plant pathology for many years (Padliya & Cooper, 2006; Ahmad et al., 2012) leading to the identification of host-pathogen protein complexes including avirulence proteins (see Dodds et al., 2006 and Luderer et al., 2001).

Many studies utilized the *Nicotiana benthamiana* transient expression via agroinfiltration for analyzing *R-Avr* gene interactions *in planta*, which produces hypersensitive response (HR) visible as cell death lesions (Ma et al., 2012). For example, McNally et al. (2018) applied transient expression in *N. benthamiana* to study interactions between *R-Avr* genes in a wheat-powdery mildew (*Blumeria graminis* f. sp. *tritici*) pathosystem. They co-infiltrated *Agrobacterium* strains expressing the *Avr* gene with strains expressing different variants of an *R* gene into *N. benthamiana* leaves. The McNally et al. (2018) study identified three *R* gene alleles —PM3A, PM3F, and PM3F^{L456P/Y458H}— that recognized the target fungal *Avr* gene, demonstrating the utility of this method in plant-pathogen interaction research.

The level of HR triggered by the co-expression of *R-Avr* genes in *N. benthamiana* leaves could be assessed by measuring electrolyte leakage from dead cells (Whitlow et al., 1992; Igarashi et al., 2013; Bolus et al., 2019). This analysis is performed by measuring electrical conductivity of an aqueous solution containing leaf tissues co-expressing *R* and *Avr* genes (Igarashi et al., 2013). As opposed to qualitative presence-absence assessment of hypersensitive response through visual

inspection of tobacco leaves, electrolyte leakage gives researchers a quantitative measurement of hypersensitive response levels. Bolus et al. (2019) successfully used the electrolyte leakage approach as a more sensitive proxy of cell death than visual inspection of tobacco leaves for studying interactions between *Sr35* and *AvrSr35*.

It is often not clear whether protein interactions detected in heterologous gene expression systems (e.g. expression of wheat genes in tobacco leaves) do occur in the native homologous system. One of the commonly used homologous transient expression systems for evaluating protein-protein interaction is based on the protoplast cells prepared from the leaves of the plant species of interest. In a study performed by Saur et al. (2019), barley protoplasts were utilized to study interaction between two *Avr* genes, *AVRa10* and *EKA_AVRa10*, from *Blumeria graminis* f. sp. *hordei* (barley powdery mildew) with their corresponding *R* gene. This study quantified *R* gene-triggered protoplast cell death by measuring luciferase activity (Saur et al., 2019; Lu et al., 2016).

Another strategy for analyzing *R-Avr* gene interaction in the homologous system is based on the infiltration of the *Avr* protein directly into the leaves of wheat plants expressing a corresponding *R* gene. This approach was successfully used by Saintenac et al. (2013) to validate interaction between *Sr35* and *AvrSr35*. Likewise, barley leaf tissues transiently expressing the *Sr35* gene from the agroinfiltrated construct were successfully used to demonstrate HR triggered by co-expression of *AvrSr35* (Bolus et al., 2019).

1.11 Fungal genetics and its difficulties

Identification of *Pgt* effectors and their host targets will remain one of the most important priorities of wheat-*Pgt* interaction research. Considering that effector-encoding genes belong to

one of the most diverse and fast-evolving classes of genes in large fungal genomes (Li et al., 2019), comprehensive analysis of effector diversity in *Pgt* populations requires developing multiple reference genomes. Only in recent years has there been progress on a *Pgt* genome assembly (Li et al., 2019; Salcedo et al., 2017; Upadhyaya et al., 2015). Currently, there are three *Pgt* reference genomes available, including the Kansas *Pgt* race RKQQC (isolate 99KS76A_1) (Rutter et al., 2017), and *Pgt* races SCCL (Duplessis et al., 2011) and Ug99 (Li et al., 2019). These genomes are characterized by different levels of contiguity and quality of assembly. For example, the reference genome of RKQQC race had high levels of discontinuity and included 168,313 contigs, with an N50 contig length of 6,292 bp (Rutter et al., 2017). A more complete stem rust reference genome assembly would provide a better resource for the identification of effector-encoding genes.

Pgt urediniospores have a sturdy, thick outer cell wall as a biological protection for overwintering and wind dispersal (Barua et al., 2018). Breaking through this wall is crucial for obtaining high-molecular weight fungal DNA. Special protocols have been developed to isolate fungal DNA either from dried urediniospores or from spore mats, which promotes the growth of fungal germination tubes and allows for extraction of nuclei from the cell (McDonald, 2017; Webb et al., 2006). Throughout the life cycle of *Pgt*, both the sexual and asexual stages produce dikaryotic spores which contain two haploid nuclei (Spatafora et al., 2017). The presence of two nuclei significantly complicates *Pgt* genome assembly. Only recently, with the development of long-read sequencing technologies and novel assembly algorithms, it has become feasible to construct haplotype-resolved contigs, where genetic material from different nuclei is correctly phased. In our study, we used these technological advances to develop a new high-quality genome assembly of the *Pgt* race RKQQC.

1.12 Research objectives and hypotheses

The main goals of this study are to determine how effectively different allelic variants of *AvrSr35* are recognized by the *Sr35* gene from the DV92 accession of *T. monococcum* and to create an updated, high-quality fungal reference genome to identify more stem rust *Avr* genes for future pathosystem studies. To accomplish these goals, I have set out the following objectives:

- 1) Determine the viability of *Sr35* as a *R* gene against various *AvrSr35* variants, including those that are detected within the Ug99 race group.
 - a) Based on previous work by Salcedo et al. (2017), I hypothesize the origin of *Sr35*-virulence in *AvrSr35* could be driven by loss of function due to miniature inverted transposable element (MITE) insertion or due to the accumulation of amino acid changes.
 - i) Investigate *Sr35*-*AvrSr35* interaction by co-expressing *Sr35* and *AvrSr35* variants in agroinfiltrated tobacco leaves.
- 2) Identify nucleotide sequence changes in *AvrSr35* that are critical for recognition by *Sr35*.
 - a) I hypothesize that the virulence of the QTHJC race to the *Sr35* gene is linked with the accumulation of amino acid changes in *AvrSr35* which can be differentiated from that of avirulent *AvrSr35* variants.
 - i) Comparison of the *AvrSr35* gene variants from the *Sr35*-virulent and *Sr35*-avirulent *Pgt* isolates will be conducted to determine critical amino acid sequence differences.
- 3) Develop a high-quality reference genome to aid in the investigation of *Pgt Avr* genes.
 - i) Assemble *Pgt* RKQQC race genome and compare the quality of this newly generated assembly with the previously published *Pgt* SCCL reference genome.

1.13 References

- Ahmad, F., Babalola, O. O., & Tak, H. I. (2012). Potential of MALDI-TOF mass spectrometry as a rapid detection technique in plant pathology: Identification of plant-associated microorganisms. *Analytical and Bioanalytical Chemistry*, *404*(4), 1247–1255. <https://doi.org/10.1007/s00216-012-6091-7>
- Aktar-Uz-Zaman, M., Tuhina-Khatun, M., Hanafi, M. M., & Sahebi, M. (2017). Genetic analysis of rust resistance genes in global wheat cultivars: An overview. *Biotechnology & Biotechnological Equipment*, *31*(3), 431–445. <https://doi.org/10.1080/13102818.2017.1304180>
- Alcântara, A., Bosch, J., Nazari, F., Hoffmann, G., Gallei, M., Uhse, S., Darino, M. A., Olukayode, T., Reumann, D., Baggaley, L., & Djamei, A. (2019). Systematic Y2H Screening Reveals Extensive Effector-Complex Formation. *Frontiers in Plant Science*, *10*. <https://doi.org/10.3389/fpls.2019.01437>
- Arora, S., Steuernagel, B., Gaurav, K., Chandramohan, S., Long, Y., Matny, O., Johnson, R., Enk, J., Periyannan, S., Singh, N., Asyraf Md Hatta, M., Athiyannan, N., Cheema, J., Yu, G., Kangara, N., Ghosh, S., Szabo, L. J., Poland, J., Bariana, H., ... Wulff, B. B. H. (2019). Resistance gene cloning from a wild crop relative by sequence capture and association genetics. *Nature Biotechnology*, *37*(2), 139–143. <https://doi.org/10.1038/s41587-018-0007-9>
- Avni, R., Nave, M., Barad, O., Baruch, K., Twardziok, S. O., Gundlach, H., Hale, I., Mascher, M., Spannagl, M., Wiebe, K., Jordan, K. W., Golan, G., Deek, J., Ben-Zvi, B., Ben-Zvi, G., Himmelbach, A., MacLachlan, R. P., Sharpe, A. G., Fritz, A., ... Distelfeld, A. (2017). Wild emmer genome architecture and diversity elucidate wheat evolution and domestication. *Science*, *357*(6346), 93–97. <https://doi.org/10.1126/science.aan0032>
- Balint-Kurti, P. (2019). The plant hypersensitive response: Concepts, control and consequences. *Molecular Plant Pathology*, *20*(8), 1163–1178. <https://doi.org/10.1111/mpp.12821>
- Barua, P., You, M. P., Bayliss, K. L., Lanoiselet, V., & Barbetti, M. J. (2018). Extended survival of *Puccinia graminis* f. sp. *tritici* urediniospores: Implications for biosecurity and on-farm management. *Plant Pathology*, *67*(4), 799–809. <https://doi.org/10.1111/ppa.12794>
- Beard, M., North, J. A., & Price, S. R. F. (1998). *Religions of Rome: A History* (Vol. 1). Cambridge University Press.
- Bigeard, J., Colcombet, J., & Hirt, H. (2015). Signaling Mechanisms in Pattern-Triggered Immunity (PTI). *Molecular Plant*, *8*(4), 521–539. <https://doi.org/10.1016/j.molp.2014.12.022>
- Boller, T., & Felix, G. (2009). A Renaissance of Elicitors: Perception of Microbe-Associated Molecular Patterns and Danger Signals by Pattern-Recognition Receptors. *Annual Review*

- of Plant Biology*, 60(1), 379–406.
<https://doi.org/10.1146/annurev.arplant.57.032905.105346>
- Bolton, M. D., Kolmer, J. A., & Garvin, D. F. (2008). Wheat leaf rust caused by *Puccinia triticina*. *Molecular Plant Pathology*, 9(5), 563–575. <https://doi.org/10.1111/j.1364-3703.2008.00487.x>
- Bolus, S., Akhunov, E., Coaker, G., & Dubcovsky, J. (2019). Dissection of cell death induction by wheat stem rust resistance protein Sr35 and its matching effector AvrSr35. *Molecular Plant-Microbe Interactions*, MPMI-08-19-0216-R. <https://doi.org/10.1094/MPMI-08-19-0216-R>
- Bushnell, W. R., & Roelfs, A. P. (Eds.). (1984). *The Cereal rusts: Vol. II*. Academic Press.
- Cavanagh, C. R., Chao, S., Wang, S., Huang, B. E., Stephen, S., Kiani, S., Forrest, K., Saintenac, C., Brown-Guedira, G. L., Akhunova, A., See, D., Bai, G., Pumphrey, M., Tomar, L., Wong, D., Kong, S., Reynolds, M., Silva, M. L. da, Bockelman, H., ... Akhunov, E. (2013). Genome-wide comparative diversity uncovers multiple targets of selection for improvement in hexaploid wheat landraces and cultivars. *Proceedings of the National Academy of Sciences*, 110(20), 8057–8062. <https://doi.org/10.1073/pnas.1217133110>
- Cereal Disease Lab: USDA ARS*. (n.d.). Retrieved September 13, 2020, from <https://www.ars.usda.gov/midwest-area/stpaul/cereal-disease-lab/>
- Cesari, S., Moore, J., Chen, C., Webb, D., Periyannan, S., Mago, R., Bernoux, M., Lagudah, E. S., & Dodds, P. N. (2016). Cytosolic activation of cell death and stem rust resistance by cereal MLA-family CC-NLR proteins. *Proceedings of the National Academy of Sciences of the United States of America*, 113(36), 10204–10209. <https://doi.org/10.1073/pnas.1605483113>
- Chen, E. C. H., Morin, E., Beaudet, D., Noel, J., Yildirim, G., Ndikumana, S., Charron, P., St-Onge, C., Giorgi, J., Krüger, M., Marton, T., Ropars, J., Grigoriev, I. V., Hainaut, M., Henrissat, B., Roux, C., Martin, F., & Corradi, N. (2018). High intraspecific genome diversity in the model arbuscular mycorrhizal symbiont *Rhizophagus irregularis*. *New Phytologist*, 220(4), 1161–1171. <https://doi.org/10.1111/nph.14989>
- Chen, J., Upadhyaya, N. M., Ortiz, D., Sperschneider, J., Li, F., Bouton, C., Breen, S., Dong, C., Xu, B., Zhang, X., Mago, R., Newell, K., Xia, X., Bernoux, M., Taylor, J. M., Steffenson, B., Jin, Y., Zhang, P., Kanyuka, K., ... Dodds, P. N. (2017). Loss of AvrSr50 by somatic exchange in stem rust leads to virulence for Sr50 resistance in wheat. *Science*, 358(6370), 1607–1610. <https://doi.org/10.1126/science.aao4810>
- Chen, X., & Line, R. (1992). Identification of stripe rust resistance genes in wheat genotypes used to differentiate North American races of *Puccinia striiformis*. *Phytopathology*, 82(12), 1428–1434. <https://doi.org/10.1094/phyto-82-1428>
- Choi, H. W., & Klessig, D. F. (2016). DAMPs, MAMPs, and NAMPs in plant innate immunity. *BMC Plant Biology*, 16. <https://doi.org/10.1186/s12870-016-0921-2>

- Cozzitorto, J. A., Jimbo, M., Chand, S., Blanco, F., Lal, S., Gilbert, M., Winter, J. M., Gorospe, M., & Brody, J. R. (2015). Studying RNA-Binding Protein Interactions with Target mRNAs in Eukaryotic Cells: Native Ribonucleoprotein Immunoprecipitation (RIP) Assays. In S. Nakagawa & T. Hirose (Eds.), *Nuclear Bodies and Noncoding RNAs: Methods and Protocols* (pp. 239–246). Springer. https://doi.org/10.1007/978-1-4939-2253-6_14
- Dodds, P. N., Lawrence, G. J., Catanzariti, A.-M., Teh, T., Wang, C.-I. A., Ayliffe, M. A., Kobe, B., & Ellis, J. G. (2006). Direct protein interaction underlies gene-for-gene specificity and coevolution of the flax resistance genes and flax rust avirulence genes. *Proceedings of the National Academy of Sciences*, *103*(23), 8888–8893. <https://doi.org/10.1073/pnas.0602577103>
- Duplessis, S., Cuomo, C. A., Lin, Y.-C., Aerts, A., Tisserant, E., Veneault-Fourrey, C., Joly, D. L., Hacquard, S., Amselem, J., Cantarel, B. L., Chiu, R., Coutinho, P. M., Feau, N., Field, M., Frey, P., Gelhaye, E., Goldberg, J., Grabherr, M. G., Kodira, C. D., ... Martin, F. (2011). Obligate biotrophy features unraveled by the genomic analysis of rust fungi. *Proceedings of the National Academy of Sciences of the United States of America*, *108*(22), 9166–9171. <https://doi.org/10.1073/pnas.1019315108>
- Elmansour, H., Singh, D., Dracatos, P. M., & Park, R. F. (2017). Identification and characterization of seedling and adult plant resistance to *Puccinia hordei* in selected African barley germplasm. *Euphytica*, *213*(6), 119. <https://doi.org/10.1007/s10681-017-1902-8>
- FAOSTAT. (n.d.). Retrieved July 16, 2020, from <http://www.fao.org/faostat/en/#search/hectares%20of%20wheat>
- Ferrari, S., Savatin, D. V., Sicilia, F., Gramegna, G., Cervone, F., & De Lorenzo, G. (2013). Oligogalacturonides: Plant damage-associated molecular patterns and regulators of growth and development. *Frontiers in Plant Science*, *4*. <https://doi.org/10.3389/fpls.2013.00049>
- Flor, H. H. (1942). Inheritance of pathogenicity in *Melampsora lini*. *Phytopathology*, *32*, 653–669.
- Gill, B. S., & Friebe, B. (n.d.). *Cytogenetics, phylogeny and evolution of cultivated wheats*. Retrieved August 6, 2020, from <http://www.fao.org/3/y4011e/y4011e07.htm>
- Glémin, S., Scornavacca, C., Dainat, J., Burgarella, C., Viader, V., Ardisson, M., Sarah, G., Santoni, S., David, J., & Ranwez, V. (2019). Pervasive hybridizations in the history of wheat relatives. *Science Advances*, *5*(5), eaav9188. <https://doi.org/10.1126/sciadv.aav9188>
- GlobalRust.org*. (2019). [Text]. GlobalRust.Org. <https://globalrust.org/>

- Gu, L., Si, W., Zhao, L., Yang, S., & Zhang, X. (2015). Dynamic evolution of NBS–LRR genes in bread wheat and its progenitors. *Molecular Genetics and Genomics*, 290(2), 727–738. <https://doi.org/10.1007/s00438-014-0948-8>
- Gustafson, P., Raskina, O., Ma, X., & Nevo, E. (2009). *Wheat Evolution, Domestication, and Improvement*. Wiley, Danvers.
- Hartman, G. L., Pawlowski, M. L., Chang, H.-X., & Hill, C. B. (2016). 3—Successful Technologies and Approaches Used to Develop and Manage Resistance against Crop Diseases and Pests. In C. Madramootoo (Ed.), *Emerging Technologies for Promoting Food Security* (pp. 43–66). Woodhead Publishing. <https://doi.org/10.1016/B978-1-78242-335-5.00003-2>
- Hassan, M. Q., Gordon, J. A. R., Lian, J. B., van Wijnen, A. J., Stein, J. L., & Stein, G. S. (2010). Ribonucleoprotein immunoprecipitation (RNP-IP): A direct in vivo analysis of microRNA-targets. *Journal of Cellular Biochemistry*, 110(4), 817–822. <https://doi.org/10.1002/jcb.22562>
- Hodson, D. (2019, December 2). *RustTracker.org | A Global Wheat Rust Monitoring System*. RustTracker.Org. <https://rusttracker.cimmyt.org/>
- Hoffmann, E. de. (2005). Mass Spectrometry. In *Kirk-Othmer Encyclopedia of Chemical Technology*. American Cancer Society. <https://doi.org/10.1002/0471238961.1301191913151518.a01.pub2>
- Hogenhout, S. A., Van der Hoorn, R. A. L., Terauchi, R., & Kamoun, S. (2009). Emerging concepts in effector biology of plant-associated organisms. *Molecular Plant-Microbe Interactions: MPMI*, 22(2), 115–122. <https://doi.org/10.1094/MPMI-22-2-0115>
- Igarashi, D., Bethke, G., Xu, Y., Tsuda, K., Glazebrook, J., & Katagiri, F. (2013). Pattern-Triggered Immunity Suppresses Programmed Cell Death Triggered by Fumonisin B1. *PLoS ONE*, 8(4). <https://doi.org/10.1371/journal.pone.0060769>
- Jin, Y., Szabo, L. J., Pretorius, Z. A., Singh, R. P., Ward, R., & Fetch, T. (2008). Detection of Virulence to Resistance Gene Sr24 Within Race TTKS of *Puccinia graminis* f. Sp. *Tritici*. *Plant Disease*, 92(6), 923–926. <https://doi.org/10.1094/PDIS-92-6-0923>
- Jin, Y., Szabo, L. J., Rouse, M. N., Fetch, T., Pretorius, Z. A., Wanyera, R., & Njau, P. (2009). Detection of Virulence to Resistance Gene Sr36 Within the TTKS Race Lineage of *Puccinia graminis* f. Sp. *Tritici*. *Plant Disease*, 93(4), 367–370. <https://doi.org/10.1094/PDIS-93-4-0367>
- Jones, J. D. G., & Dangl, J. L. (2006). The plant immune system. *Nature*, 444(7117), 323–329. <https://doi.org/10.1038/nature05286>
- Kaboord, B., & Perr, M. (2008). Isolation of Proteins and Protein Complexes by Immunoprecipitation. In A. Posch (Ed.), *2D PAGE: Sample Preparation and*

- Fractionation* (pp. 349–364). Humana Press. https://doi.org/10.1007/978-1-60327-064-9_27
- Keen, N. T. (1990). Gene-for-Gene Complementarity in Plant-Pathogen Interactions. *Annual Review of Genetics*, 24(1), 447–463. <https://doi.org/10.1146/annurev.ge.24.120190.002311>
- Kihara, H. (1994). Discovery of the DD-analyser, one of the ancestors of *Triticum vulgare*. *Agriculture and Horticulture*, 19, 889–890.
- Koehler, P., Wieser, H., & Konitzer, K. (2014). Chapter 2—Gluten—The Precipitating Factor. In P. Koehler, H. Wieser, & K. Konitzer (Eds.), *Celiac Disease and Gluten* (pp. 97–148). Academic Press. <https://doi.org/10.1016/B978-0-12-420220-7.00002-X>
- Kourelis, J., & van der Hoorn, R. A. L. (2018). Defended to the Nines: 25 Years of Resistance Gene Cloning Identifies Nine Mechanisms for R Protein Function [OPEN]. *The Plant Cell*, 30(2), 285–299. <https://doi.org/10.1105/tpc.17.00579>
- Krattinger, S. G., Lagudah, E. S., Spielmeier, W., Singh, R. P., Huerta-Espino, J., McFadden, H., Bossolini, E., Selter, L. L., & Keller, B. (2009). A Putative ABC Transporter Confers Durable Resistance to Multiple Fungal Pathogens in Wheat. *Science*, 323(5919), 1360–1363. <https://doi.org/10.1126/science.1166453>
- Krol, E., Mentzel, T., Chinchilla, D., Boller, T., Felix, G., Kemmerling, B., Postel, S., Arents, M., Jeworutzki, E., Al-Rasheid, K. A. S., Becker, D., & Hedrich, R. (2010). Perception of the Arabidopsis danger signal peptide 1 involves the pattern recognition receptor AtPEPR1 and its close homologue AtPEPR2. *The Journal of Biological Chemistry*, 285(18), 13471–13479. <https://doi.org/10.1074/jbc.M109.097394>
- Leonard, K. J., & Szabo, L. J. (2005). Stem rust of small grains and grasses caused by *Puccinia graminis*. *Molecular Plant Pathology*, 6(2), 99–111. <https://doi.org/10.1111/j.1364-3703.2005.00273.x>
- Li, F., Upadhyaya, N. M., Sperschneider, J., Matny, O., Nguyen-Phuc, H., Mago, R., Raley, C., Miller, M. E., Silverstein, K. A. T., Henningsen, E., Hirsch, C. D., Visser, B., Pretorius, Z. A., Steffenson, B. J., Schwessinger, B., Dodds, P. N., & Figueroa, M. (2019). Emergence of the Ug99 lineage of the wheat stem rust pathogen through somatic hybridisation. *Nature Communications*, 10(1), 1–15. <https://doi.org/10.1038/s41467-019-12927-7>
- Lin, X., N'Diaye, A., Walkowiak, S., Nilsen, K. T., Cory, A. T., Haile, J., Kutcher, H. R., Ammar, K., Loladze, A., Huerta-Espino, J., Clarke, J. M., Ruan, Y., Knox, R., Fobert, P., Sharpe, A. G., & Pozniak, C. J. (2018). Genetic analysis of resistance to stripe rust in durum wheat (*Triticum turgidum* L. var. Durum). *PLoS ONE*, 13(9). <https://doi.org/10.1371/journal.pone.0203283>
- Lu, X., Kracher, B., Saur, I. M. L., Bauer, S., Ellwood, S. R., Wise, R., Yaeno, T., Maekawa, T., & Schulze-Lefert, P. (2016). Allelic barley MLA immune receptors recognize sequence-

- unrelated avirulence effectors of the powdery mildew pathogen. *Proceedings of the National Academy of Sciences of the United States of America*, 113(42), E6486–E6495. <https://doi.org/10.1073/pnas.1612947113>
- Luderer, R., Rivas, S., Nürnberger, T., Mattei, B., Van den Hooven, H. W., Van der Hoorn, R. A. L., Romeis, T., Wehrfritz, J.-M., Blume, B., Nennstiel, D., Zuidema, D., Vervoort, J., De Lorenzo, G., Jones, J. D. G., De Wit, P. J. G. M., & Joosten, M. H. A. J. (2001). No Evidence for Binding Between Resistance Gene Product Cf-9 of Tomato and Avirulence Gene Product AVR9 of *Cladosporium fulvum*. *Molecular Plant-Microbe Interactions*®, 14(7), 867–876. <https://doi.org/10.1094/MPMI.2001.14.7.867>
- Ma, L., Lukasik, E., Gawehns, F., & Takken, F. L. W. (2012). The Use of Agroinfiltration for Transient Expression of Plant Resistance and Fungal Effector Proteins in *Nicotiana benthamiana* Leaves. In M. D. Bolton & B. P. H. J. Thomma (Eds.), *Plant Fungal Pathogens: Methods and Protocols* (pp. 61–74). Humana Press. https://doi.org/10.1007/978-1-61779-501-5_4
- Mago, R., Zhang, P., Vautrin, S., Šimková, H., Bansal, U., Luo, M.-C., Rouse, M., Karaoglu, H., Periyannan, S., Kolmer, J., Jin, Y., Ayliffe, M. A., Bariana, H., Park, R. F., McIntosh, R., Doležel, J., Bergès, H., Spielmeier, W., Lagudah, E. S., ... Dodds, P. N. (2015). The wheat Sr50 gene reveals rich diversity at a cereal disease resistance locus. *Nature Plants*, 1(12), 1–3. <https://doi.org/10.1038/nplants.2015.186>
- Marla, S. R., Chu, K., Chintamanani, S., Multani, D. S., Klempien, A., DeLeon, A., Bong-suk, K., Dunkle, L. D., Dilkes, B. P., & Johal, G. S. (2018). Adult plant resistance in maize to northern leaf spot is a feature of partial loss-of-function alleles of Hm1. *PLOS Pathogens*, 14(10), e1007356. <https://doi.org/10.1371/journal.ppat.1007356>
- Marmisolle, F. E., García, M. L., & Reyes, C. A. (2018). RNA-binding protein immunoprecipitation as a tool to investigate plant miRNA processing interference by regulatory proteins of diverse origin. *Plant Methods*, 14(1), 9. <https://doi.org/10.1186/s13007-018-0276-9>
- Marsalis, M. A., & Goldberg, N. P. (n.d.). *Leaf, Stem, and Stripe Rust Diseases of Wheat*. 8.
- McDonald, B. S. and M. (2017). *High quality DNA from Fungi for long read sequencing e.g. PacBio, Nanopore MinION*. <https://doi.org/10.17504/protocols.io.k6qczdw>
- McIntosh, R. A., Dyck, P. L., The, T. T., Cusick, J., & Milne, D. L. (1984). Cytogenetical studies in wheat. XIII. Sr35—A third gene from *Triticum monococcum* for resistance to *Puccinia graminis tritici*. *Zeitschrift Fur Pflanzenzuchtung*, 92, 1–14.
- McIntosh, R. A., Wellings, C. R., & Park, R. F. (Eds.). (1995). *Wheat Rusts: An Atlas of Resistance Genes*. Springer Netherlands. <https://www.springer.com/gp/book/9789401040419>
- McNally, K. E., Menardo, F., Lüthi, L., Praz, C. R., Müller, M. C., Kunz, L., Ben-David, R., Chandrasekhar, K., Dinoor, A., Cowger, C., Meyers, E., Xue, M., Zeng, F., Gong, S., Yu,

- D., Bourras, S., & Keller, B. (2018). Distinct domains of the AVRPM3^{A2/F2} avirulence protein from wheat powdery mildew are involved in immune receptor recognition and putative effector function. *New Phytologist*, *218*(2), 681–695. <https://doi.org/10.1111/nph.15026>
- Meadows, R. (2011). Why Biotrophs Can't Live Alone. *PLOS Biology*, *9*(7), e1001097. <https://doi.org/10.1371/journal.pbio.1001097>
- Middle East: Wheat—Producing countries (Tons)—2016*. (n.d.). Retrieved July 4, 2020, from <https://en.actualitix.com/country/moor/middle-east-wheat-production.php>
- Mishra, S. P., Mishra, C., Sahoo, S. S., Sethy, K., & Behera, K. (2017). Chromatin Immunoprecipitation (ChIP) Assay—A Tool for Functional Analysis of Gene Expression. *International Journal of Chemical Studies*, *7*.
- Moscou, M. J., & Esse, H. P. van. (2017). The quest for durable resistance. *Science*, *358*(6370), 1541–1542. <https://doi.org/10.1126/science.aar4797>
- Mundt, C. C. (2014). Durable resistance: A key to sustainable management of pathogens and pests. *Infection, Genetics and Evolution*, *27*, 446–455. <https://doi.org/10.1016/j.meegid.2014.01.011>
- Nissen, R. M., & Yamamoto, K. R. (2000). The glucocorticoid receptor inhibits NFκB by interfering with serine-2 phosphorylation of the RNA polymerase II carboxy-terminal domain. *Genes & Development*, *14*(18), 2314–2329.
- Nürnbergger, T., & Brunner, F. (2002). Innate immunity in plants and animals: Emerging parallels between the recognition of general elicitors and pathogen-associated molecular patterns. *Current Opinion in Plant Biology*, *5*(4), 318–324. [https://doi.org/10.1016/s1369-5266\(02\)00265-0](https://doi.org/10.1016/s1369-5266(02)00265-0)
- Operaña, T. N., & Tukey, R. H. (2007). Oligomerization of the UDP-glucuronosyltransferase 1A Proteins: HOMO- AND HETERODIMERIZATION ANALYSIS BY FLUORESCENCE RESONANCE ENERGY TRANSFER AND CO-IMMUNOPRECIPITATION. *Journal of Biological Chemistry*, *282*(7), 4821–4829. <https://doi.org/10.1074/jbc.M609417200>
- Ozeretskovskaya, O. L., Vasyukova, N. I., Perekhod, E. A., Chalenko, G. I., Il'inskaya, L. I., & Gerasimova, N. G. (2001). Plant Resistance Suppressors in the Pathosystem Formed by Potato and the Causal Agent of Late Blight. *Applied Biochemistry and Microbiology*, *37*(5), 506–511. <https://doi.org/10.1023/A:1010254225826>
- Ozkan, H., Levy, A. A., & Feldman, M. (2001). *Allopolyploidy-Induced Rapid Genome Evolution in the Wheat (Aegilops–Triticum) Group*. 14.
- Padliya, N. D., & Cooper, B. (2006). Mass spectrometry-based proteomics for the detection of plant pathogens. *PROTEOMICS*, *6*(14), 4069–4075. <https://doi.org/10.1002/pmic.200600146>

- Park, R. F. (2015). Wheat: Biotrophic Pathogen Resistance. In *Encyclopedia of Food Grains* (Second, Vols. 4–4, pp. 264–272). Elsevier Inc.
- Park, R. F., Poulsen, D., Barr, A. R., Cakir, M., Moody, D. B., Raman, H., & Read, B. J. (2003). Mapping genes for resistance to *Puccinia hordei* in barley. *Australian Journal of Agricultural Research*, *54*(12), 1323–1333. <https://doi.org/10.1071/ar02244>
- Patpour, M., Hovmøller, M. S., Shahin, A. A., Newcomb, M., Olivera, P., Jin, Y., Luster, D., Hodson, D., Nazari, K., & Azab, M. (2015). First Report of the Ug99 Race Group of Wheat Stem Rust, *Puccinia graminis* f. Sp. *Tritici*, in Egypt in 2014. *Plant Disease*, *100*(4), 863–863. <https://doi.org/10.1094/PDIS-08-15-0938-PDN>
- Periyannan, S., Milne, R. J., Figueroa, M., Lagudah, E. S., & Dodds, P. N. (2017). An overview of genetic rust resistance: From broad to specific mechanisms. *PLoS Pathogens*, *13*(7). <https://doi.org/10.1371/journal.ppat.1006380>
- Periyannan, S., Moore, J., Ayliffe, M., Bansal, U., Wang, X., Huang, L., Deal, K., Luo, M., Kong, X., Bariana, H., Mago, R., McIntosh, R., Dodds, P., Dvorak, J., & Lagudah, E. (2013). The Gene Sr33, an Ortholog of Barley Mla Genes, Encodes Resistance to Wheat Stem Rust Race Ug99. *Science*, *341*(6147), 786–788. <https://doi.org/10.1126/science.1239028>
- Phizicky, E. M., & Fields, S. (1995). Protein-protein interactions: Methods for detection and analysis. *Microbiological Reviews*, *59*(1), 94–123.
- Prentice, N., Cuendet, L. S., Geddes, W. F., & Smith, F. (2002, May 1). *The Constitution of a Glucomannan from Wheat Stem Rust (Puccinia graminis tritici) Urediospores I* (world). American Chemical Society. <https://doi.org/10.1021/ja01512a045>
- Pretorius, Z. A., Singh, R. P., Wagoire, W. W., & Payne, T. S. (2000). Detection of Virulence to Wheat Stem Rust Resistance Gene Sr31 in *Puccinia graminis* f. Sp. *Tritici* in Uganda. *Plant Disease*, *84*(2), 203–203. <https://doi.org/10.1094/PDIS.2000.84.2.203B>
- Rahmatov, M., Rouse, M. N., Steffenson, B. J., Andersson, S. C., Wanyera, R., Pretorius, Z. A., Houben, A., Kumarse, N., Bhavani, S., & Johansson, E. (2016). Sources of Stem Rust Resistance in Wheat-Alien Introgression Lines. *Plant Disease*, *100*(6), 1101–1109. <https://doi.org/10.1094/PDIS-12-15-1448-RE>
- Riaz, A., Periyannan, S., Aitken, E., & Hickey, L. (2016). A rapid phenotyping method for adult plant resistance to leaf rust in wheat. *Plant Methods*, *12*(1), 17. <https://doi.org/10.1186/s13007-016-0117-7>
- Robinson, R. A. (1977). Plant Pathosystems. *Annals of the New York Academy of Sciences*, *287*(1), 238–242. <https://doi.org/10.1111/j.1749-6632.1977.tb34243.x>
- Roser, M., & Ritchie, H. (2013). Hunger and Undernourishment. *Our World in Data*. <https://ourworldindata.org/hunger-and-undernourishment>

- Rouse, M. N., Nirmala, J., Jin, Y., Chao, S., Fetch, T. G., Pretorius, Z. A., & Hiebert, C. W. (2014). Characterization of Sr9h, a wheat stem rust resistance allele effective to Ug99. *Theoretical and Applied Genetics*, *127*(8), 1681–1688. <https://doi.org/10.1007/s00122-014-2330-y>
- Rust Diseases of Wheat*. (n.d.). Retrieved August 6, 2020, from <https://ohioline.osu.edu/factsheet/plpath-cer-12>
- Rutter, W. B., Salcedo, A., Akhunova, A., He, F., Wang, S., Liang, H., Bowden, R. L., & Akhunov, E. (2017). Divergent and convergent modes of interaction between wheat and *Puccinia graminis* f. Sp. *Triticum* isolates revealed by the comparative gene co-expression network and genome analyses. *BMC Genomics*, *18*(1), 291. <https://doi.org/10.1186/s12864-017-3678-6>
- Saintenac, C., Zhang, W., Salcedo, A., Rouse, M. N., Trick, H. N., Akhunov, E., & Dubcovsky, J. (2013). Identification of Wheat Gene Sr35 That Confers Resistance to Ug99 Stem Rust Race Group. *Science*, *341*(6147), 783–786. <https://doi.org/10.1126/science.1239022>
- Salcedo, A., Rutter, W., Wang, S., Akhunova, A., Bolus, S., Chao, S., Anderson, N., Soto, M. F. D., Rouse, M., Szabo, L., Bowden, R. L., Dubcovsky, J., & Akhunov, E. (2017). Variation in the AvrSr35 gene determines Sr35 resistance against wheat stem rust race Ug99. *Science*, *358*(6370), 1604–1606. <https://doi.org/10.1126/science.aao7294>
- Salim, K., Fenton, T., Bacha, J., Urien-Rodriguez, H., Bonnert, T., Skynner, H. A., Watts, E., Kerby, J., Heald, A., Beer, M., McAllister, G., & Guest, P. C. (2002). Oligomerization of G-protein-coupled Receptors Shown by Selective Co-immunoprecipitation. *Journal of Biological Chemistry*, *277*(18), 15482–15485. <https://doi.org/10.1074/jbc.M201539200>
- Sánchez-Martín, J., Steuernagel, B., Ghosh, S., Herren, G., Hurni, S., Adamski, N., Vrána, J., Kubaláková, M., Krattinger, S. G., Wicker, T., Doležel, J., Keller, B., & Wulff, B. B. H. (2016). Rapid gene isolation in barley and wheat by mutant chromosome sequencing. *Genome Biology*, *17*(1), 221. <https://doi.org/10.1186/s13059-016-1082-1>
- Saur, I. M. L., Bauer, S., Lu, X., & Schulze-Lefert, P. (2019). A cell death assay in barley and wheat protoplasts for identification and validation of matching pathogen AVR effector and plant NLR immune receptors. *Plant Methods*, *15*(1), 118. <https://doi.org/10.1186/s13007-019-0502-0>
- Savile, D. B. O. (1984). Taxonomy of the Cereal Rust Fungi. In W. Bushnell (Ed.), *The Cereal Rusts: Origins, Specificity, Structure, and Physiology* (Vol. 1, pp. 79–111). Academic Press, Inc.
- Schumann, G. L., & Leonard, K. J. (2000). *Stem rust of wheat (black rust)*. APS. <https://www.apsnet.org/edcenter/disandpath/fungalbasidio/pdlessons/Pages/StemRust.aspx>
- Schwessinger, B. (2017). Fundamental wheat stripe rust research in the 21st century. *New Phytologist*, *213*(4), 1625–1631. <https://doi.org/10.1111/nph.14159>

- Sharma, H. C., & Gill, B. S. (1983). Current status of wide hybridization in wheat. *Euphytica*, 32(1), 17–31. <https://doi.org/10.1007/BF00036860>
- Shewry, P. R. (2009). Wheat. *Journal of Experimental Botany*, 60(6), 1537–1553. <https://doi.org/10.1093/jxb/erp058>
- Shiraishi, T., Yamada, T., Saitoh, K., Kato, T., Toyoda, K., Yoshioka, H., Kim, H.-M., Ichinose, Y., Tahara, M., & Oku, H. (1994). Suppressors: Determinants of Specificity Produced by Plant Pathogens. *Plant and Cell Physiology*, 35(8), 1107–1119. <https://doi.org/10.1093/oxfordjournals.pcp.a078703>
- Simmonds, N. W. (Ed.). (1979). *Evolution of crop plants* (2nd ed.). Longman Group Limited.
- Singh, S., & Bowden, R. L. (2011). Molecular mapping of adult-plant race-specific leaf rust resistance gene Lr12 in bread wheat. *Molecular Breeding*, 28(2), 137–142. <https://doi.org/10.1007/s11032-010-9467-4>
- Singh, R. P., & Huerta-Espino, J. (2003). Effect of leaf rust resistance gene Lr34 on components of slow rusting at seven growth stages in wheat. *Euphytica*, 129(3), 371–376. <https://doi.org/10.1023/A:1022216327934>
- Singh, R. P., Hodson, D. P., Huerta-Espino, J., Jin, Y., Bhavani, S., Njau, P., Herrera-Foessel, S., Singh, P. K., Singh, S., & Govindan, V. (2011). The Emergence of Ug99 Races of the Stem Rust Fungus is a Threat to World Wheat Production. *Annual Review of Phytopathology*, 49(1), 465–481. <https://doi.org/10.1146/annurev-phyto-072910-095423>
- Singh, R. P., Hodson, D. P., Huerta-Espino, J., Jin, Y., Njau, P., Wanyera, R., Herrera-Foessel, S. A., & Ward, R. W. (2008). Will Stem Rust Destroy the World's Wheat Crop? In *Advances in Agronomy* (Vol. 98, pp. 271–309). Elsevier. [https://doi.org/10.1016/S0065-2113\(08\)00205-8](https://doi.org/10.1016/S0065-2113(08)00205-8)
- Singh, R. P., Hodson, D. P., Jin, Y., Lagudah, E. S., Ayliffe, M. A., Bhavani, S., Rouse, M. N., Pretorius, Z. A., Szabo, L. J., Huerta-Espino, J., Basnet, B. R., Lan, C., & Hovmøller, M. S. (2015). Emergence and Spread of New Races of Wheat Stem Rust Fungus: Continued Threat to Food Security and Prospects of Genetic Control. *Phytopathology*, 105(7), 872–884. <https://doi.org/10.1094/PHTO-01-15-0030-FI>
- Sissons, M. (2008). Role of Durum Wheat Composition on the Quality of Pasta and Bread. *Global Science Books*, 2(2), 75–90.
- Soria, M. (2019, July 27). *Rusts resistance gene Lr34-Yr18-Sr57, powdery mildew resistance gene Pm18*. MASWheat. <https://maswheat.ucdavis.edu/protocols/Lr34>
- Spatafora, J. W., Aime, M. C., Grigoriev, I. V., Martin, F., Stajich, J. E., & Blackwell, M. (2017). The Fungal Tree of Life: From Molecular Systematics to Genome-Scale Phylogenies. *The Fungal Kingdom*, 3–34. <https://doi.org/10.1128/microbiolspec.FUNK-0053-2016>

- Staskawicz, B. J., Dahlbeck, D., & Keen, N. T. (1984). Cloned avirulence gene of *Pseudomonas syringae* pv. *Glycinea* determines race-specific incompatibility on *Glycine max* (L.) Merr. *Proceedings of the National Academy of Sciences*, *81*(19), 6024–6028. <https://doi.org/10.1073/pnas.81.19.6024>
- Steuernagel, B., Periyannan, S. K., Hernández-Pinzón, I., Witek, K., Rouse, M. N., Yu, G., Hatta, A., Ayliffe, M., Bariana, H., Jones, J. D. G., Lagudah, E. S., & Wulff, B. B. H. (2016). Rapid cloning of disease-resistance genes in plants using mutagenesis and sequence capture. *Nature Biotechnology*, *34*(6), 652–655. <https://doi.org/10.1038/nbt.3543>
- Tabery, M., James, Piotrowska, & Darden, L. (2020). Molecular Biology. In E. N. Zalta (Ed.), *The Stanford Encyclopedia of Philosophy* (Summer 2020). Metaphysics Research Lab, Stanford University. <https://plato.stanford.edu/archives/sum2020/entries/molecular-biology/>
- Tadesse, W., Bishaw, Z., & Assefa, S. (2019). Wheat production and breeding in Sub-Saharan Africa: Challenges and opportunities in the face of climate change. *International Journal of Climate Change Strategies and Management*, *11*(5), 696–715. <https://doi.org/10.1108/IJCCSM-02-2018-0015>
- Terzi, L. C., & Simpson, G. G. (2009). Arabidopsis RNA immunoprecipitation. *The Plant Journal*, *59*(1), 163–168. <https://doi.org/10.1111/j.1365-313X.2009.03859.x>
- The International Wheat Genome Sequencing Consortium (IWGSC). (2014). A chromosome-based draft sequence of the hexaploid bread wheat (*Triticum aestivum*) genome. *Science*, *345*(6194). <https://doi.org/10.1126/science.1251788>
- The International Wheat Genome Sequencing Consortium (IWGSC), Appels, R., Eversole, K., Stein, N., Feuillet, C., Keller, B., Rogers, J., Pozniak, C. J., Choulet, F., Distelfeld, A., Poland, J., Ronen, G., Sharpe, A. G., Barad, O., Baruch, K., Keeble-Gagnère, G., Mascher, M., Ben-Zvi, G., Josselin, A.-A., ... Wang, L. (2018). Shifting the limits in wheat research and breeding using a fully annotated reference genome. *Science*, *361*(6403), eaar7191. <https://doi.org/10.1126/science.aar7191>
- Thind, A. K., Wicker, T., Šimková, H., Fossati, D., Moullet, O., Brabant, C., Vrána, J., Doležel, J., & Krattinger, S. G. (2017). Rapid cloning of genes in hexaploid wheat using cultivar-specific long-range chromosome assembly. *Nature Biotechnology*, *35*(8), 793–796. <https://doi.org/10.1038/nbt.3877>
- Upadhyaya, N. M., Garnica, D. P., Karaoglu, H., Sperschneider, J., Nemri, A., Xu, B., Mago, R., Cuomo, C. A., Rathjen, J. P., Park, R. F., Ellis, J. G., & Dodds, P. N. (2015). Comparative genomics of Australian isolates of the wheat stem rust pathogen *Puccinia graminis* f. Sp. *Tritici* reveals extensive polymorphism in candidate effector genes. *Frontiers in Plant Science*, *5*. <https://doi.org/10.3389/fpls.2014.00759>
- Van de Weyer, A.-L., Monteiro, F., Furzer, O. J., Nishimura, M. T., Cevik, V., Witek, K., Jones, J. D. G., Dangl, J. L., Weigel, D., & Bemm, F. (2019). A Species-Wide Inventory of

- NLR Genes and Alleles in *Arabidopsis thaliana*. *Cell*, 178(5), 1260-1272.e14.
<https://doi.org/10.1016/j.cell.2019.07.038>
- Venske, E., dos Santos, R. S., Busanello, C., Gustafson, P., & Costa de Oliveira, A. (2019). Bread wheat: A role model for plant domestication and breeding. *Hereditas*, 156(1), 16.
<https://doi.org/10.1186/s41065-019-0093-9>
- Wang, J.-C., Derynck, M. K., Nonaka, D. F., Khodabakhsh, D. B., Haqq, C., & Yamamoto, K. R. (2004). *Chromatin immunoprecipitation (ChIP) scanning identifies primary glucocorticoid receptor target genes*. 6.
- Wang, Z. L., Li, L. H., He, Z. H., Duan, X. Y., Zhou, Y. L., Chen, X. M., Lillemo, M., Singh, R. P., Wang, H., & Xia, X. C. (2005). Seedling and Adult Plant Resistance to Powdery Mildew in Chinese Bread Wheat Cultivars and Lines. *Plant Disease*, 89(5), 457–463.
<https://doi.org/10.1094/PD-89-0457>
- Webb, C. A., Szabo, L. J., Bakkeren, G., Garry, C., Staples, R. C., Eversmeyer, M., & Fellers, J. P. (2006). Transient expression and insertional mutagenesis of *Puccinia triticina* using biolistics. *Functional & Integrative Genomics*, 6(3), 250–260.
<https://doi.org/10.1007/s10142-005-0009-9>
- Weis, C., Pfeilmeier, S., Glawischnig, E., Isono, E., Pachel, F., Hahne, H., Kuster, B., Eichmann, R., & Hückelhoven, R. (2013). Co-immunoprecipitation-based identification of putative BAX INHIBITOR-1-interacting proteins involved in cell death regulation and plant–powdery mildew interactions. *Molecular Plant Pathology*, 14(8), 791–802.
<https://doi.org/10.1111/mpp.12050>
- WHEAT in the World* » CGIAR Research Program on WHEAT. (n.d.). Retrieved July 6, 2020, from <https://wheat.org/wheat-in-the-world/>
- Wheat leaf rust: USDA ARS*. (2017, April 10). USDA ARS. <https://www.ars.usda.gov/midwest-area/stpaul/cereal-disease-lab/docs/cereal-rusts/wheat-leaf-rust/>
- Wheat Nutrition. (n.d.). *National Association of Wheat Growers*. Retrieved August 6, 2020, from <https://www.wheatworld.org/wheat-101/wheat-industry/wheat-nutrition/>
- Wheat stem rust: USDA ARS*. (n.d.). Retrieved August 6, 2020, from <https://www.ars.usda.gov/midwest-area/stpaul/cereal-disease-lab/docs/cereal-rusts/wheat-stem-rust/>
- Wheat stripe rust: USDA ARS*. (n.d.). Retrieved August 6, 2020, from <https://www.ars.usda.gov/midwest-area/stpaul/cereal-disease-lab/docs/cereal-rusts/wheat-stripe-rust/>
- Whitlow, T. H., Bassuk, N. L., Ranney, T. G., & Reichert, D. L. (1992). An Improved Method for Using Electrolyte Leakage to Assess Membrane Competence in Plant Tissues. *Plant Physiology*, 98(1), 198–205.

- Willcox, G. (2005). The distribution, natural habitats and availability of wild cereals in relation to their domestication in the Near East: Multiple events, multiple centres. *Vegetation History and Archaeobotany*, *14*(4), 534–541. <https://doi.org/10.1007/s00334-005-0075-x>
- Woods Ignatoski, K. M. (2001). Immunoprecipitation and Western Blotting of Phosphotyrosine-Containing Proteins. In A. D. Reith (Ed.), *Protein Kinase Protocols* (pp. 39–48). Humana Press. <https://doi.org/10.1385/1-59259-059-4:39>
- Young, K. H. (1998). Yeast Two-hybrid: So Many Interactions, (in) So Little Time.... *Biology of Reproduction*, *58*(2), 302–311. <https://doi.org/10.1095/biolreprod58.2.302>
- Young, N. D. (1990). Potential applications of map-based cloning to plant pathology. *Physiological and Molecular Plant Pathology*, *37*(2), 81–94. [https://doi.org/10.1016/0885-5765\(90\)90001-E](https://doi.org/10.1016/0885-5765(90)90001-E)
- Zhang, J., Zhang, P., Dodds, P., & Lagudah, E. (2020). How Target-Sequence Enrichment and Sequencing (TESeq) Pipelines Have Catalyzed Resistance Gene Cloning in the Wheat-Rust Pathosystem. *Frontiers in Plant Science*, *11*. <https://doi.org/10.3389/fpls.2020.00678>
- Zhang, W., Chen, S., Abate, Z., Nirmala, J., Rouse, M. N., & Dubcovsky, J. (2017). Identification and characterization of Sr13, a tetraploid wheat gene that confers resistance to the Ug99 stem rust race group. *Proceedings of the National Academy of Sciences*, *114*(45), E9483–E9492. <https://doi.org/10.1073/pnas.1706277114>
- Zhang, W., Olson, E., Saintenac, C., Rouse, M., Abate, Z., Jin, Y., Akhunov, E., Pumphrey, M., & Dubcovsky, J. (2010). Genetic Maps of Stem Rust Resistance Gene Sr35 in Diploid and Hexaploid Wheat. *Crop Science*, *50*(6), 2464–2474. <https://doi.org/10.2135/cropsci2010.04.0202>

Chapter 2 - The effect of the allelic diversity in *AvrSr35* on *Sr35*-triggered hypersensitive response

2.1 Abstract

Ug99 is the most devastating race of *Puccinia graminis* f. sp. *tritici* (*Pgt*), causing wheat stem rust. This race was originally detected in Uganda in 1999, earning the name ‘Ug99’ (with the US nomenclature of TTKSK) (Pretorius et al., 2000; Jin et al., 2007). Ug99 has since rapidly evolved and spread in parts of Africa and the Middle East (Singh et al., 2015), causing significant yield loss and food insecurity. Currently, there are thirteen known virulent races within this group of *Pgt* (*GlobalRust.Org*, 2020). The expansion of the Ug99 lineage proves that this fungus is capable of evolving quickly and overcoming a large number of wheat resistance genes (*R*) used to develop varieties grown around the world. The emergence of the Ug99 race highlights the importance of studies aimed at understanding the evolutionary dynamic of *R* genes and their corresponding avirulence (*Avr*) factors in wheat-stem rust pathosystems. In this study, we used *in planta* transient expression assay in *Nicotiana benthamiana* to investigate interaction between the Ug99-effective *Sr35* resistance gene (Saintenac et al., 2013) and an allelic series that contains both heterozygous and homozygous alleles of *AvrSr35* avirulence factors (Salcedo et al., 2017) identified in a diverse set of *Pgt* isolates, including isolates from the Ug99 group. The analysis showed that the *Sr35* allele used in our study is capable of recognizing and triggering defense response upon interaction with nearly all *AvrSr35* variants, except one, found in the *Sr35*-virulent *Pgt* race QTHJC. This *AvrSr35* variant carries three critical amino acid changes that are conserved among *Sr35*-virulent isolates. These sites appear to affect the ability of *Sr35* to induce hypersensitive response (HR) in tobacco leaves. Combined with phylogenetic analysis, the tobacco assay results suggest that the origin of the QTHJC variant of *AvrSr35* likely preceded

the origin of more common virulent variants of *AvrSr35* carrying the transposable element insertion in the coding sequence. Based on our results, we propose a two-stage model of the *AvrSr35* gene evolution that starts with emergence of diverged gene variants showing reduced avirulence response upon recognition by *Sr35* followed by origin of the virulent loss-of-function *AvrSr35* variant. In addition, this study utilized transient expression in wheat protoplasts to validate the interactions between *Sr35* and the allelic series of *AvrSr35*. However, our preliminary results contradict results obtained using the transient expression assay in tobacco, which leads us to believe that there is an unknown factor expressed in wheat cells that affects this interaction and has yet to be studied.

2.2 Objectives of study

This study is aimed at advancing our knowledge of the wheat-rust pathosystem by characterizing the interaction between the *R* gene and multiple variants of the *Avr* gene identified in a diverse collection of *Pgt* isolates. Based on studies performed by Salcedo et al. (2017), I hypothesize that the origin of *Sr35*-virulence in *AvrSr35* could be driven by loss of function due to MITE insertion or due to the accumulation of amino acid changes. I hypothesize that virulence of the *AvrSr35* variant is associated with amino acid changes affecting the ability of *Sr35* to recognize *AvrSr35* and trigger immune response. By comparing sequences of the *Sr35*-virulent QTHJC *AvrSr35* variant with that of avirulent variants, critical regions of *AvrSr35* for recognition by *Sr35* can be identified. This study will lead to a better understanding of the evolutionary mechanisms leading to the origin of *Sr35*-virulent isolates.

2.3 Introduction

2.3.1 Stem rust group- Ug99

Wheat stem rust, caused by the fungal pathogen *Puccinia graminis* f. sp. *tritici* (*Pgt*), is one of the most damaging fungal pathogens in agriculture causing up to 70% yield losses (Beard et al., 2004). Since being a large threat in the U.S. during the 1950's, there are many control strategies in place to defend against *Pgt*. Stem rust resistance (*R*) genes, the use of fungicides, and the eradication of stem rust's alternate host of common barberry (*Berberis vulgaris*) have been used (McIntosh et al., 1995; Peterson, 2013). However in 1999, lines with a commonly used stem rust *R* gene, *Sr31*, were overcome with a new race of stem rust found in Uganda known as Ug99, and designated TTKSK (Jin et al., 2008; Pretorius et al., 2000). There has since been a rapid spread and evolution of Ug99, leading to the identification of thirteen new races within this group of stem rust: TTKSK (Ug99), TTKSF, TTKST (Ug99+Sr24), TTTSK (Ug99+Sr36), TTKSP, PTKSK, PTKST, TTKSF+, TTKTT, TTHSK, PTKTK, TTHST (Hodson, 2019). Research of various wheat lines and stem rust races has led to the identification more than 70 stem rust *R* genes for wheat (McIntosh et al., 1995). Of these 70 *R* genes, many are effective at some level against one or many isolates within the Ug99 race group (*Sr2*, *Sr13*, *Sr15*, *Sr21*, *Sr22*, *Sr24*, *Sr25*, *Sr26*, *Sr27*, *Sr28*, *Sr32*, *Sr33*, *Sr35*, *Sr36*, *Sr37*, *Sr39*, *Sr40*, *Sr42*, *Sr43*, *Sr44*, *Sr45*, *Sr46*, *Sr47*, *Sr48*, *Sr50*, *Sr51*, *Sr52*, *Sr53*, *Sr55*, *Sr57*, *Sr58*, *SrTA10171*, *SrTA10187*, *SrTA1662*, *SrTmp*, *SrWeb*, *Sr1RSAmigo* (Faris et al., 2008; Ghazvini et al., 2012; Hiebert et al., 2010; Jin et al., 2007; Jin & Singh, 2006; Kolmer et al., 2011; Liu, Jin, et al., 2011; Liu, Rouse, et al., 2011; Singh et al., 2011; Olson et al., 2013a, 2013b; Qi et al., 2011; Rouse & Jin, 2011; Rouse et al., 2011; Singh et al., 2013; Niu et al., 2014; Yu et al., 2014; Guerrero-Chavez et al., 2015; Gao et al., 2019)). *Sr35*, found in *Triticum monococcum* by McIntosh et al. in 1984, is one of the *R*

genes that demonstrated near immunity against the Ug99 race group effective at all stages of plant development. With the identification of the *Pgt* fungal avirulence (*Avr*) gene *AvrSr35* (Salcedo et al., 2017), the *AvrSr35-Sr35* gene pair provides a useful system for studying effector-triggered plant immunity pathogen interactions.

2.3.2 Wheat-stem rust pathosystem

A pathosystem describes a specific set of interactions between a pathogen and host that define the outcome of infection (Robinson, 1977). The host's effector-triggered immunity (ETI) pathways play important roles in pathogen perception and depend on interaction between fungal effectors and the host's resistance genes (Peterson, 2013). ETI is consistent with the gene-for-gene interaction concept proposed by Harold Flor (1942) while studying flax (*Linum usitatissimum*) and flax rust (*Melampsora lini*). This concept links plant resistance and susceptibility with the presence or absence of interacting *R* and *Avr* genes in pathosystem.

According to the gene-for-gene model, plant resistance only occurs when the plant host has an *R* gene that recognizes the fungal pathogen's *Avr* gene, leading to hypersensitive response (HR), or cell death at the site of infection. If the plant's genome does not encode the complementary *R* gene to the fungus's *Avr* gene or if there is a mutation present in the *R* or *Avr* gene sequence, then the plant will succumb to infection.

2.3.3 *Sr35* gene

The *Sr35* resistance gene was first identified in *Triticum monococcum*, a diploid wheat variety commonly known as cultivated einkorn (Koehler et al., 2014; McIntosh et al., 1984). Sequencing and positional cloning using *T. monococcum* DV92 bacterial artificial chromosomes (BAC) libraries identified *Sr35* as a coiled-coil, nucleotide-binding, leucine-rich repeat (NLR) intracellular receptor protein which was shown by Saintenac et al. (2013) to be required for

conferring resistance against Ug99 via EMS-induced random knockout mutations. Although this gene is from an ancestor of bread wheat (*T. aestivum*), it has demonstrated near immunity to the Ug99 lineage when transferred as a transgene into polyploid wheat (Saintenac et al., 2013). *Sr35* can provide early stage resistance by triggering an immune signal in response to early expression of *AvrSr35*, which results in halted growth of fungal infection hyphae and therefore inhibits the formation of haustoria (Salcedo et al., 2017). Characterization of NLR genes, such as *Sr35*, gives us a better understanding of how they function within a pathosystem and how effective they are against wheat pests and pathogens (Bulus et al., 2019). In addition, a larger arsenal of well-annotated NLR genes will allow scientists to practice proper gene stewardship by minimizing over-implementation of any single R gene and utilizing broad-spectrum resistance through gene pyramiding (Periyannan et al., 2017).

Alongside the agronomic benefits from cloning *R* genes, this also creates many more avenues for functional analysis and molecular research to further understand mechanisms of plant immunity. Currently, there are only seven *R* genes known to be effective against Ug99 that have been cloned: *Sr13* (Zhang et al., 2017), *Sr21* (Chen et al., 2018), *Sr22* (Steuernagel et al., 2016), *Sr33* (Periyannan et al., 2013), *Sr35* (Saintenac et al., 2013), *Sr45* (Steuernagel et al., 2016), and *Sr50* (Mago et al., 2015). These *R* genes provide an entry point for studying host-pathogen interaction and identification of corresponding fungal *Avr* genes. There are only two documented examples of *R-Avr* pairs for cereal rusts: *Sr35-AvrSr35* and *Sr50-AvrSr50* (Saintenac et al., 2013; Salcedo et al., 2017; Mago et al., 2015; Chen et al., 2017).

2.3.4 *AvrSr35* gene

One of the two *Avr* gene that has been identified in cereal rusts is *AvrSr35*, which upon recognition by *Sr35* triggers an immune response (Salcedo et al., 2017). Using a comparative

genomics approach, Salcedo et al. (2017) studied genome-wide sequence variation in a diverse panel of natural and EMS mutagenized *Pgt* isolates and identified the fungal *AvrSr35* gene that was responsible for *Sr35* avirulence (Salcedo et al., 2017). In addition to the identification of *AvrSr35*, Salcedo et al. (2017) also characterized its allelic diversity, which helped to reveal that the origin of *Sr35*-virulent isolates of *Pgt* is mostly associated with the insertion of a TE into the coding region of *AvrSr35*. However, this diversity analysis also helped to uncover a variant of *AvrSr35* without the TE insertion that came from the *Sr35*-virulent *Pgt* isolate, suggesting that other factors also played a role in the evolution of virulence to *Sr35*.

One study, conducted by McNally et al. (2018), investigated natural variations in the AVRPM^{a2/f2} protein sequence of wheat powdery mildew (*Blumeria graminis* f. sp. *tritici*) and the corresponding *R* genes in wheat. They accumulated a collection of powdery mildew isolates from around the world and characterized *AvrPm^{a2/f2}* sequence diversity. Despite the diversity in this panel of powdery mildew isolates, they found that the complete *AvrPm^{3a2/f2}* gene component that determines recognition was fixed among all isolates, showing no evidence of polymorphism; however, 12 new haplotypes were found that encode for unique proteins (Bourras et al., 2015; McNally et al., 2018). Using a transient expression assay in *N. benthamiana*, they found that none of the 12 haplotypes produced evidence of a hypersensitive response, suggesting that the new variants encode for inactive *Avr* genes and that AVRPM^{3A2/F2}-A is the only active protein variant found in natural isolates (McNally et al., 2018). They also found that isolates that encode for the AVRPM^{3A2/F2}-A variant could be associated with a fungal suppressor effector called SVRPM^{3A1/F1}, which suppresses the recognition of *AvrPm^{3a2/f2}* by the *Pm^{3a/f}* gene (McNally et al., 2018).

Recent studies detected suppressor effectors in other pathosystems as well, such as the tomato (*Solanum lycopersicum*)-*Fol* soil fungus (*Fusarium oxysporum* f.sp. *lycopersici*) pathosystem, as shown in Houterman et al. (2008). The *AVR1* gene has been found to be recognized by the *I* gene in tomato, while suppressing the disease resistance conferred by tomato genes *I-2* and *I-3* (Houterman et al., 2008; Petit-Houdenot & Fudal, 2017). Another example comes from a study done in the rapeseed (*Brassica napus*)-stem canker (*Leptosphaeria maculans*) pathosystem (Plissonneau et al., 2016). Plissonneau et al. (2016) demonstrated that *AvrLm4-7* could suppress the resistance signaling response of *Rlm3* recognizing *AvrLm3*, leading to stem canker infection (Petit-Houdenot & Fudal, 2017).

There are also several cases where a single *R* gene recognizes multiple *Avr* genes and *vice-versa*. Rooney et al. (2005) and Lozano-Torres et al. (2012, pp. 10119–10124) show such an interaction for tomato and tomato leaf mold (*Cladosporium fulvum*) and the yellow potato cyst nematode (*Globodera rostochiensis*), respectively. They found that the tomato *Cf2* gene recognizes the leaf mold *Avr2-Rcr3* gene complex and the nematode *Gr-VAPI-Rcr3* gene complex, thus maintaining resistance to both pathogens (Lozano-Torres et al., 2012; Petit-Houdenot & Fudal, 2017; Rooney et al., 2005). On the other hand, there are also cases where a single *Avr* gene can be recognized by multiple *R* genes. One such case is depicted in studies done by Rouxel et al. (2003) and Gout et al. (2006, 2007), investigating the rapeseed-stem canker pathosystem. They find that the stem canker *AvrLm1* gene is recognized by the two rapeseed *R* genes *Rlm1* and *LepR3* (Gout et al., 2006, 2007; Petit-Houdenot & Fudal, 2017; Rouxel et al., 2003).

Different models of *R-Avr* interaction have been proposed based on these and other studies, including the guard model (Van der Biezen & Jones, 1998), decoy model (Zhou & Chai, 2008; Zipfel & Rathjen, 2008), and elicitor-suppressor model (Bushnell & Roelfs, 1984). By expanding

the set of characterized *R-Avr* pairs, scientists can better understand the applicability of these models to different cases or can develop improved models that more adequately capture a broad range of possible *R-Avr* gene interactions. These interaction models along with *R-Avr* complex characterizations will lead to a better knowledge of plant-pathogen coevolution, *R* gene specificity and viability, and eventually lead to the conception of better plant protection strategies and plant performance.

2.4 Materials and Methods

2.4.1 Allelic diversity analyses of *AvrSr35* variants

Nucleotide sequences compiled by Salcedo et al. (2017) were aligned using the MUSCLE program (version 3.8.31, Edgar, 2004; Madeira et al., 2019) with default settings. The EMBOSS Transeq program (version 6.6.0, Rice et al., 2000; Madeira et al., 2019) with default settings was used to translate the nucleic acid sequences into the corresponding peptide sequences, followed by an amino acid alignment using MUSCLE with default settings. Alignments were used to construct phylogenetic trees using the CLC Sequence Viewer 7 program (<https://digitalinsights.qiagen.com>) using the tree construction default settings of Neighbor-Joining method and Jukes-Cantor nucleotide distance measure. Newick tree formats were exported and uploaded to the iTOL program Version 5.6.3 (Letunic & Bork, 2019) to edit the phylogenetic trees and root them to the RKQQC v2 isolate.

2.4.2 *Agrobacterium* transformation

Transformation of plasmid DNA into *E. coli* (DH5 α ; NEB, C2989K) and *Agrobacterium tumefaciens* strain C5851 cells were performed by electroporation and heat shock treatment (modification of Miller & Nickoloff, 1995 and Sambrook & Russell, 1989 hereafter referenced).

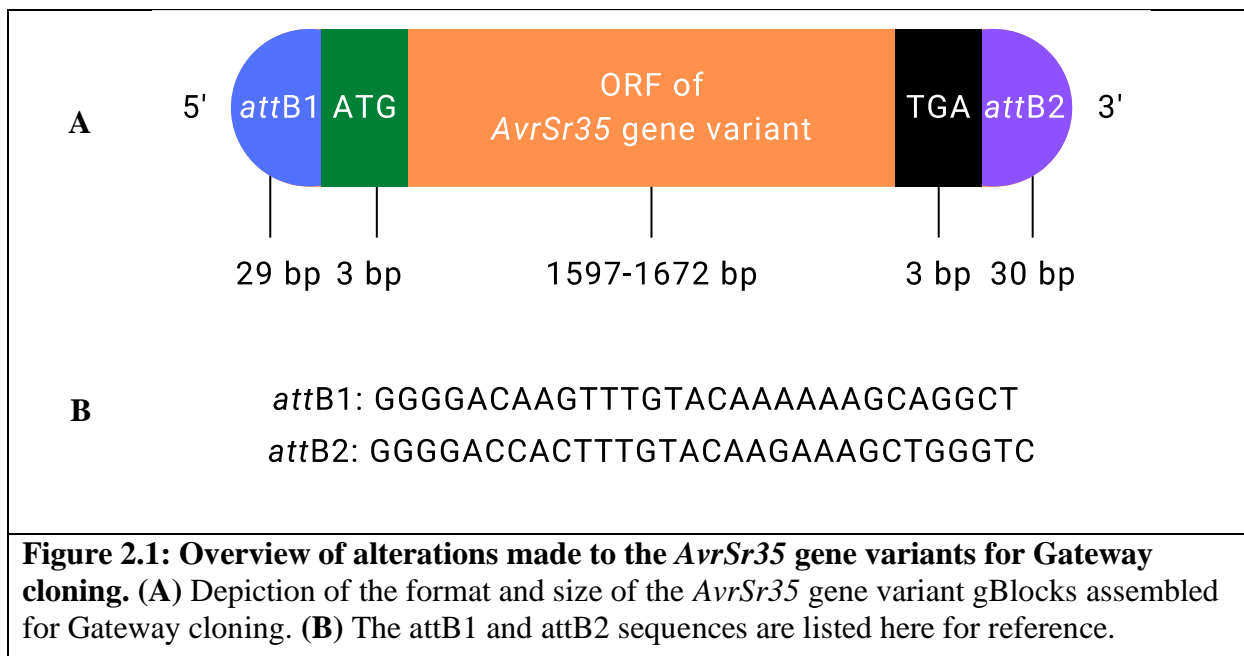
Electroporation was performed using 20 μ l of competent DH5 α cells mix with 1 μ l of 100 ng/ μ l plasmid containing the target gene. An Electroporator 2510 (Eppendorf) with voltage set to 1,500 volts and the mixture was set to pulse two times. The cells are then placed on ice to recover, followed by adding 500 μ l of SOC media and agitating at 250 rpm while incubating at 37°C for one hour. Cells were plated on lysogeny broth (LB) media plates with Zeocin (50 μ g/ml) or Spectinomycin (50 μ g/ml).

For *E. coli* heat shock transformation (modifications of Sambrook & Russell, 1989 hereafter referenced), 1 μ l of 100 ng/ μ l plasmid DNA and 20 μ l of DH5 α competent cells are mixed together, placed on ice for 30 minutes, incubated at 42°C for 30 seconds to 1 minute, and placed on ice for ~1 minute to recover. The cells are then added to 1 ml of LB media and agitated at 250 rpm while incubating at 37°C for one hour. For *Agrobacterium* heat shock transformation, 150 μ l of competent cells are placed on ice for 30 minutes. The cells are then mixed with 5 μ l of 100 ng/ μ l plasmid DNA and place on ice for 5 minutes. The sample mixture is then flash frozen using liquid nitrogen (N₂) and incubated at 37°C for 5 minutes. The cells are then added to 1 ml of LB media and agitated at 250 rpm while incubating at 28°C for 3-4 hours. Cells were pelleted using centrifuge at 5,000 g for 30 seconds and resuspending the cells in 200 μ l of LB media. These resuspended cells are then plated on LB media plates with Spectinomycin (50 μ g/ml) and Rifampicin (10 μ g/ml) and incubated at 28°C for 1-2 days.

2.4.3 Gateway cloning

Sequences for the *AvrSr35* (MF474174.1) gene variants and *Sr35* were altered for Gateway Cloning. For this cloning project the open reading frame (ORF) for each variant is used (ranging from 1,597-1,672 bp). We opted to remove the signal peptide sequence (75 bp) from the 5' end and the ATG start codon were added to the 5' end followed by the sequence for the *attB1*

recombination site (29 bp) (Figure 2.1). The TGA stop codon and the sequence for the reverse complement of the *attB2* recombination site (30 bp) were added to the 3' end (Figure 2.1).



Modified sequences of the *AvrSr35* variants and *Sr35* were synthesized as g-block gene fragments by Integrated DNA Technologies (IDT). G-block fragment cloning was performed using Gateway BP and LR Clonase™ technologies (Invitrogen). 2 µl of 50 ng/µl of the g-blocks, 1 µl of 150 ng/µl of pDONOR vector, and 5 µl Tris-EDTA (1 x TE) buffer with 2 µl of BP Clonase™ II enzyme mix and incubated at room temperature (25°C) overnight. Following the incubation, 1 µl of Proteinase K is added to stop the reaction, samples are then incubated at 37°C for 10 minutes. Transform 1 µl of plasmid into *E. coli* strain DH5α is conducted through electroporation as detailed above. To validate the BP Clonase™ reaction, single colony PCR was performed using specific PCR primers (Table 1) with the conditions of 94°C for 5 minutes, 10 cycles of 94°C for 30 seconds, 58°C for 30 seconds, and 72°C for 45 seconds, followed by 18 cycles of 94°C for 30 seconds, 52°C for 30 seconds, and 72°C for 45 seconds, followed by 72°C

for 7 minutes. Agarose gel validation was done using 1.8-2% gels and a 100-2000 bp ladder (ThermoFisher Scientific, SM0403 or SM1191) were completed to ensure expected lengths. Following BP Clonase™ recombination, the LR Clonase™ reaction starts by adding 1 µl of 50 ng/µl of the BP Clonase™ product, referred to as the entry clone, 1 µl of 150 ng/µl of pIPKb004, and 8 µl of 1 x TE buffer were mixed together. 2 µl of LR Clonase™ II enzyme mix was added, and mix was incubated at 25°C overnight. Reaction was stopped by adding 1 µl of Proteinase K and incubating at 37°C for 10 minutes. Five µl of LR Clonase reaction mix was then transformed into the *Agrobacterium tumefaciens* strain C5851 using the 37°C heat shock method detailed above.

2.4.4 Transient expression in *Nicotiana benthamiana*

Initial screening of susceptible versus resistant variants of *AvrSr35* was performed using the *N. benthamiana* *Agrobacterium* infiltration assay (Li, 2011). Healthy tobacco plants are grown from seedlings and fertilized after 2 weeks with 1 tablespoon of Miracle-Gro per liter of water, repeating fertilization every two days. *N. benthamiana* was grown in a growth chamber under the following growth conditions: 25°C, 50% humidity, 16 hours light, and 8 hours dark. After 4 weeks the tobacco was at the third and fourth leaf growth stage. To ensure an accurate infiltration, single *Agrobacterium* colonies containing the gene of interest were obtained for each *AvrSr35* variant. The single colonies were increased in 5 ml of LB media with Spectinomycin (50 µg/ml) and Rifampicin (10 µg/ml) and incubated overnight at 28°C. One ml of the overnight culture is transferred to 25 ml fresh LB media with Spectinomycin (50 µg/ml), Rifampicin (10 µg/ml), and Acetosyringone (20 µM) and agitated at 250 rpm while incubating at 28°C overnight. The cells are then pelleted by centrifuging at 5,000 g for 15 minutes and resuspended in resuspension solution (1 M MgCl₂, 0.5 M MES-K (pH 5.6), and Acetosyringone (20 µM)).

Cell count is measured using a liquid chromatography/mass spectrometry (LC-MA) BioSpec reader (Shimadzu) to obtain the A_{600} value of ~ 0.4 . Cells are incubated in resuspension solution at 25°C overnight and the concentration is measured again the following morning to ensure sufficient cell count (A_{600} value of ~ 0.4). Mixtures of each *AvrSr35* variant with *Sr35* were co-infiltrated into tobacco leaves making a 2 cm diameter circle of infection (typically uses 1-2 ml of *Agrobacterium* mixture). As a positive control we used *AvrSr35* variant identified by Salcedo et al. (2017) co-infiltrated with *Sr35* construct. A negative control included a truncated version of *AvrSr35* (*AvrSr35*Q72*) co-infiltrated with *Sr35*. As a blank control we used a resuspension buffer. Infiltration is performed using a needleless 5 ml syringe by applying light pressure on the underside of the third and fourth leaves from the bottom of the plant with the mouth of the syringe. While holding the leaf in place with a finger on the opposite side, there is a slight break in the tissue and we simultaneously released cells from the syringe at a slow rate. Infiltration is immediately visualized by a darker wet circle around the infiltration site on the leaf surface that has ~ 20 mm radius. Over the time intervals of 12, 20, 24, 36, and 48 hours photos were taken of the leaves to visually record hypersensitive response (HR).

2.4.5 RNA isolation and gene expression (RT-PCR and qPCR)

To test expression of constructs in the infiltrated tobacco leaves, 0.1 g of leaf tissue was sampled 12 hours after infiltration. Total RNA was isolated from each of the *AvrSr35* variants and controls (RNeasy Kit, Qiagen, Hilden, Germany). From the infected tobacco RNA, cDNA was synthesized by performing RT-PCR (Invitrogen, SuperScript® III First-Strand Synthesis SuperMix for qRT-PCR). Starting with a concentration of 250 ng/ μl of RNA with a total volume of 1.6 μl per sample, the RNA was denatured by incubating at 65°C for 10 minutes. To stop the reaction, samples were put on ice for 2 minutes while 2 μl of the reverse transcription (RT)

reaction mix (includes oligo(dT)₂₀ (2.5 μM), random hexamers (2.5 ng/μl), 10 mM MgCl₂, and dNTPs), 0.4 μl of the RT enzyme mixes (includes SuperScript® III RT and RNaseOUT™, and 1 μl of specific PCR primers (Table 1) were added. The remainder of the RT-PCR conditions of 25°C for 10 minutes, 50°C for 30 minutes, 85°C for 5 minutes, and 4°C hold commenced after the solutions were added. 25 μl of cDNA was then diluted in 12 μl of ddH₂O. PCR was performed using the following conditions of 94°C for 5 minutes, 10 cycles of 94°C for 30 seconds, 58°C for 30 seconds and 72°C for 45 seconds, followed by 18 cycles of 94°C for 30 seconds, 52°C for 30 seconds, and 72°C for 45 seconds, followed by 4°C hold. Agarose gel electrophoresis using a 1% gel and a 400-8000 bp ladder (ThermoFisher Scientific, SM1283) was performed to ensure the integrity and quality of the cDNA. To quantify gene expression, qPCR was performed using the synthesized cDNA (Applied Biosystems, PowerUp SYBR Green Master Mix). For each sample we used three primer sets to detect expression of the always present Protein Phosphate 2A housekeeping gene in tobacco, “NbPP2A gene,” (Genebank TC21939) (NbPP2A_F and NbPP2A_R), the *Sr35* resistance gene (Sr35_qPCR_F1 and Sr35_qPCR_R1), and the *AvrSr35* variants (AllAvrSr35Variant_F2 and AllAvrSr35Variant_R2) (Table 2.1). All reactions were run on the BioRad CFX with PCR conditions of 50°C for 2 minutes, 95°C for 2 minutes, 40 cycles of 95°C for 15 seconds and 60°C for 1 minute, followed by 65°C for 5 seconds, and 95°C for 5 seconds. The relative gene expression levels were calculated using the $2^{-\Delta\Delta CT}$ method (Livak & Schmittgen, 2001). The standard deviation was calculated across the five biological replicates for samples and, due to malfunction in the RNA isolation, only two replicates for controls and are included as error bars in the expression plots (Figure 2.4).

2.4.6 Create Sr35 + YFP vector

To visually observe the interaction of *Sr35* and each of the *AvrSr35* variants in protoplasts, *Sr35* was attached to a yellow fluorescent protein (YFP). Using 0.5 μ l of the restriction enzyme HindIII (NEB), we subcloned the pIPKb004-*Sr35* target gene from the plasmid DNA that was obtained as the original product of Gateway Cloning and obtained a purified sample by means of gel extraction (QIAquick Gel Extraction Kit, Qiagen, Hilden, Germany). This *Sr35* region taken from pIPKb004 is the coding sequence of the entire gene and contains its original promoter (35S) and terminator (NOS). We then used 0.5 μ l of the same restriction enzyme (HindIII) to create an opening in our backbone, the pA9eYFP donor vector. One μ l of T4 DNA ligase (NEB) was then used to attach the *Sr35* target gene to the pA9eYFP backbone to create this pA9eYFP-*Sr35* vector that was now refer to as 9YS (construct is in pUC19, p35S::*Sr35*::NOS+pzUbi::YFP::NOS). To ensure the length of DNA was the same as what we expected of a successfully cloned plasmid, PCR and Sanger validation were performed. Using PCR conditions of 98°C for 1 minute, 5 cycles of 98°C for 10 seconds, 65°C for 20 seconds, and 72°C for 2 minutes, followed by 5 cycles of 98°C for 10 seconds, 60°C for 20 seconds, and 72°C for 2 minutes, proceeded by 25 cycles of 98°C for 10 seconds, 55°C for 20 seconds, and 72°C for 2 minutes, and finished with 72°C for 5 minutes. Our samples were then treated and cleaned using 0.5 μ l Exonuclease I (ExoI) and 1 μ l Shrimp Alkaline Phosphatase (SAP) into 2.5 μ l of the PCR product and incubated at 37°C for 15 minutes to remove excess dNTPs and primers. The enzymes were then inactivated by incubating at 80°C for 15 minutes. The PCR products were then diluted in 15 μ l of molecular grade water. Using BigDye® (Life Science) sequencing kit, with 2 μ l of 100 ng/ μ l of plasmids, 1.5 μ l 5x sequencing buffer, 2 μ l sequencing primer, 1 μ l freshly made 50% dimethyl sulfoxide (DMSO), 1 μ l BigDye®, and 2.5 μ l of water. Plasmids

were then amplified using PCR conditions of 98°C for 5 minutes, 40 cycles of 96°C for 10 seconds, 50°C for 5 seconds, and 60°C for 4 minutes, followed by a 4°C hold to obtain a sufficient amount of DNA for sequencing. Samples were purified using 5 µl of 25mM EDTA, 36 µl of ethanol/sodium acetate, and 60 µl 70% ethanol then resuspended in 20 µl of Hi-Di (Thermo Fisher). By performing the above preparations and utilizing Sanger sequencing, we were able to validate vector that the 9YS vector contained all of the necessary parts to function as the fluorescent resistance gene used during the transformation of wheat protoplasts.

2.4.7 Isolation and transformation of wheat protoplasts

Wheat protoplast refers to wheat cells without the cell wall, which were used in several studies to assess *R-Avr* interaction (Saur et al., 2019; Miao & Jiang, 2007; Rehman et al., 2016). To observe this we utilized wheat protoplasts, which are plant cells without the cell wall; this makes it easier to transform cells with plasmid DNA. About 150 seedlings of the wheat cultivar “BobWhite” were stored in darkness at 25°C for two to three weeks to isolate protoplasts. These conditions make it so that the plant cell wall is less durable due to the lack of light to make cellulose. The seedlings are finely minced, placed in 15 ml of W5 solution (0.1% glucose, 0.08% KCl, 0.9% NaCl, 1.84% CaCl₂·2H₂O, 2 mM MES-KOH (pH 5.7)), and vacuumed at -600 mbar for 30 minutes, releasing the pressure every 10 minutes. The W5 was then removed and replaced by 40 ml of enzyme solution (0.5% cellulase, 0.25% macerozyme, 0.6 M mannitol, 10 mM MES-KOH (pH 5.7), 10 mM CaCl₂, and 0.1% BSA) and digested at 25°C for 2 hours in the dark while agitating at 30 rpm. The protoplasts were collected by filtering through a 40 µm nylon mesh and distributed equally into two 50 ml tubes. The remaining tissue was washed with 20 ml of W5 and filtered a second time and distributed equally into the two 50 ml tubes. Adding the W5 solution to the sample mixture dilutes the enzymes and protects the cells from mannitol

damage. Protoplasts are collected by centrifuging at 100 g for 7 minutes with an acceleration level of 6 and deceleration level of 4. Pelleted cells are washed by slowly adding 10 ml of W5 at a 90° angle and collected again by centrifuging at 50 g for 5 minutes. This step is then repeated and followed by re-suspending the protoplasts in 3 ml of W5 and incubating on ice for 30 minutes. During this incubation, cells are counted under a microscope in order to calculate the number of protoplasts that can be transformed. If the protoplast isolation has been successful, there should be approximately 2×10^6 cells. Cells are then pelleted by centrifuging at 50 g for 2 minutes and resuspended in about 2 ml MMG solution (0.4 M mannitol, 15 mM $MgCl_2$, and 4 mM MES-KOH (pH 5.7)). The amount of MMG may vary depending on how many cells are isolated. Co-transformation is completed by gently mixing 100 μ l of the isolated protoplasts with >30 μ l of each plasmid (3 μ g/ml) and 130 μ l of PEG solution (0.2 M mannitol, 40% PEG, and 0.1 M $CaCl_2$) in 2 ml round bottom tubes (Eppendorf). The protoplasts are then incubated in the darkness at 25°C for 30 minutes to ensure that the plasmids are accepted into the protoplasts. 500 μ l of W5 buffer is added to the solution to stop the transformation reaction. Cells are pelleted by centrifuging at 100 g for 2 minutes and washed with 1 ml of W5. Cells are then collected by centrifuging at 100 g for 2 minutes. To condense the volume of the samples, roughly 750 μ l are removed from each tube leaving about 200 μ l per sample. All samples are then transferred to a black Nunclon™ Delta Surface 96 well plate (Shan et al., 2013) and the absorbance is read using Synergy H1 Hybrid Reader and the Gen5 software (BioTek) with the method of detecting the fluorescence of samples by measuring the wavelengths of excitation at 485 nm and emission at 530 nm. In between plate readings, the samples are stored in the darkness at 25°C. Initial readings were measured by the Gen5 plate reader after 30 minutes followed by measurements taken at 0.5, 12, 16, 20, 24, 36, 48, and 60 hours after completing protoplast transformation to

visualize the intensity of fluorescence of each of the *AvrSr35* variants paired with 9YS. Due to the protein-protein interactions leading to hypersensitive response, we are able to infer which variants have a positive, negative, and intermediate interaction with *Sr35*.

2.4.8 Statistical analyses for wheat protoplast transformation

We compared fluorescence intensity values of the wheat protoplasts that were co-transformed with plasmids containing *AvrSr35* variants and the 9YS construct using statistical routines implemented in R (version 3.6.1; R Core Team, 2019). The wheat protoplast protocol was run in two separate experiments, one on September 24, 2019 and the other in October 1, 2019. To combine the two data sets without introducing temporal bias, each data set was normalized using the ‘scale’ function from the base distribution of R. Z-scores of absorbance values between the two data sets were combined into a single dataset for analysis. The combined dataset was subset into individual time points, then linear models were fit for each time point with analysis of variance (ANOVA) using the ‘aov’ function from the base distribution of R. In each model the normalized absorbance values were the dependent variables and the *AvrSr35* variant identity of each sample (the independent variable) was included as a fixed factor. Because the *AvrSr35* variant identity factor has 14 levels, the ANOVA was only able to determine if at least one of the variants was different from all other variants. To get a more nuanced understanding of the relationship between each variant at each time point, Tukey’s *post hoc* tests were utilized with the ‘HSD.test’ function from the agricolae package in R (version 1.3-1; de Mendiburu, 2019) to perform pairwise comparisons of normalized absorbance values between variants. For each pairwise comparison, an adjusted p-value of 0.05 was used as a threshold for statistical significance.

2.5 Results

2.5.1 *AvrSr35* allelic diversity in *Pgt* population

Using nucleotide and amino acid sequences of homozygous and heterozygous *AvrSr35* alleles from the population of diverse *Pgt* isolates from the U.S. (77%) and Africa (33%) (Salcedo et al., 2017), phylogenetic trees were constructed (Figure 2.2). As shown in Figure 2.2, this population of *Pgt* races has undergone sequence divergence and can be divided into two clades: an avirulent clade (Figure 2.2, B, blue section) and a virulent clade (Figure 2.2, B, red section); this is expanded upon from work done by Salcedo et al. (2017). According to the phylogenetic tree in Figure 2.2, there is a monophyletic group of isolates, where all virulent isolates descend from a single common ancestor, that have non-functional *AvrSr35* genes, making them virulent against *Sr35*. These isolates, shown in red in Figure 2.2, B, all have a miniature inverted transposable element (MITE) insertion causing the *Avr* gene to be non-functional, except an isolate from Minnesota, USA, QTHJC, which is the only virulent isolate tested that does not have a MITE insertion. The position of the QTHJC gene variant sequence on the phylogenetic tree suggests that its origin predates the origin of the *AvrSr35* variants with the MITE insertion. The virulence of QTHJC towards *Sr35* suggests that it might carry DNA sequence changes that either affect sites involved in interaction with *Sr35* or these particular isolates have other genetic factors suppressing *Sr35*-mediated resistance response. We have identified unique variable sites differentiating the *Sr35*-virulent group (Figure 2.2, B) isolates. In total, three unique amino acid changes can be found only in the virulent isolates at sites E240K, K559D-N, and R569H (Figure 2.2, B), including the QTHJC variant.

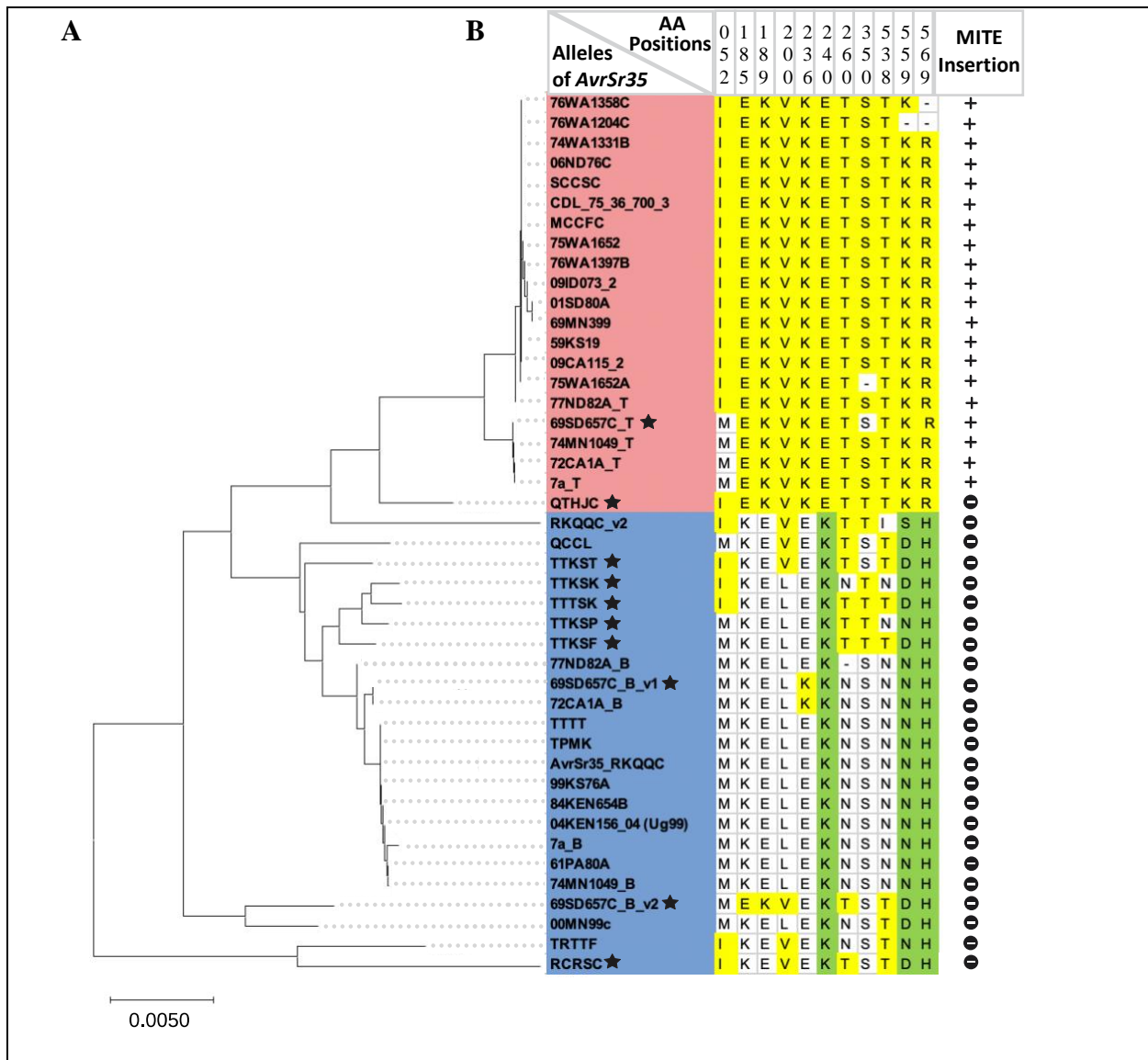


Figure 2.2: *AvrSr35* amino acid sequence diversity. This figure is originally from Salcedo et al. (2017) and has been expounded on in this study. (A) Neighbor-Joining phylogenetic tree based on amino acid sequences of homozygous and heterozygous *AvrSr35* alleles from multiple isolates. For many of the U.S. isolates, the names will indicate the year (last two digits) and location (state abbreviation) from which they came. The scale represents the number of amino acid substitutions per amino acid site. (B) Amino acid variable sites sequence alignment identifying amino acids that cause specific changes to the *Sr35* virulent isolate QTHJC. The stars next to isolate names indicate which isolates were tested in this study. *AvrSr35* alleles containing miniature inverted transposable elements (MITE) insertion, which disrupts the avirulence coding sequence by causing a premature stop codon are marked +, while isolates without the MITE insertion are marked with a circled -. The red details nonfunctional *AvrSr35* alleles making them virulent isolates. The blue coloring details isolates containing functional *AvrSr35* alleles making them avirulent isolates. Yellow coloring indicates amino acids that are consistent in QTHJC at the specified site. Green coloring identifies unique variable sites that are specific to QTHJC and other nonfunctional *AvrSr35* alleles.

2.5.2 Evaluating interaction between *Sr35* and *AvrSr35* variants using the *N. benthamiana* transient expression system

To investigate the ability of the *AvrSr35* gene variants from different isolates to interact with *Sr35* and trigger HR, we transiently co-expressed *Sr35* with the *AvrSr35* variants in tobacco leaves. The initial screening of *Sr35*-*AvrSr35* variant interaction included controls of *AvrSr35_{wr}*-*Sr35* (positive), *AvrSr35_{Q72}*-*Sr35* (negative), and clean resuspension buffer (blank) (Figure 2.3). Of the chosen *AvrSr35* variants, five were selected from the Ug99 lineage (TTKSK, TTKSF, TTKST, TTTSK, and TTKSP), while the remaining five were from US isolates and races (69SD657C-V1, 69SD657C-V2, 69SD657C-V3, QTHJC, and RCRSC). Agroinfiltrated tobacco leaves were visually evaluated for HR over the timeframe of 24, 36, 48, and 60 hours post infection (HPI) for all *Sr35*-*AvrSr35* pairings studied and can be seen in Figure 2.3- 24 HPI. Compared to positive control, out of the ten tested *AvrSr35* variants, the QTHJC variant showed the slowest rate of HR development in the *N. benthamiana* assay, with first visible signs of HR detected at 36 HPI. The other *AvrSr35* variants manifested clear HR within 24 HPI, most showing the levels of HR equal to that observed for the positive control. At the final measured time point of 60 HPI, all *Sr35*-*AvrSr35* variant pairings displayed HR. This result is consistent with the earlier study that demonstrated that the *Sr35* construct alone transiently expressed in tobacco leaves over time also develops HR symptoms (Bolus et al., 2019).

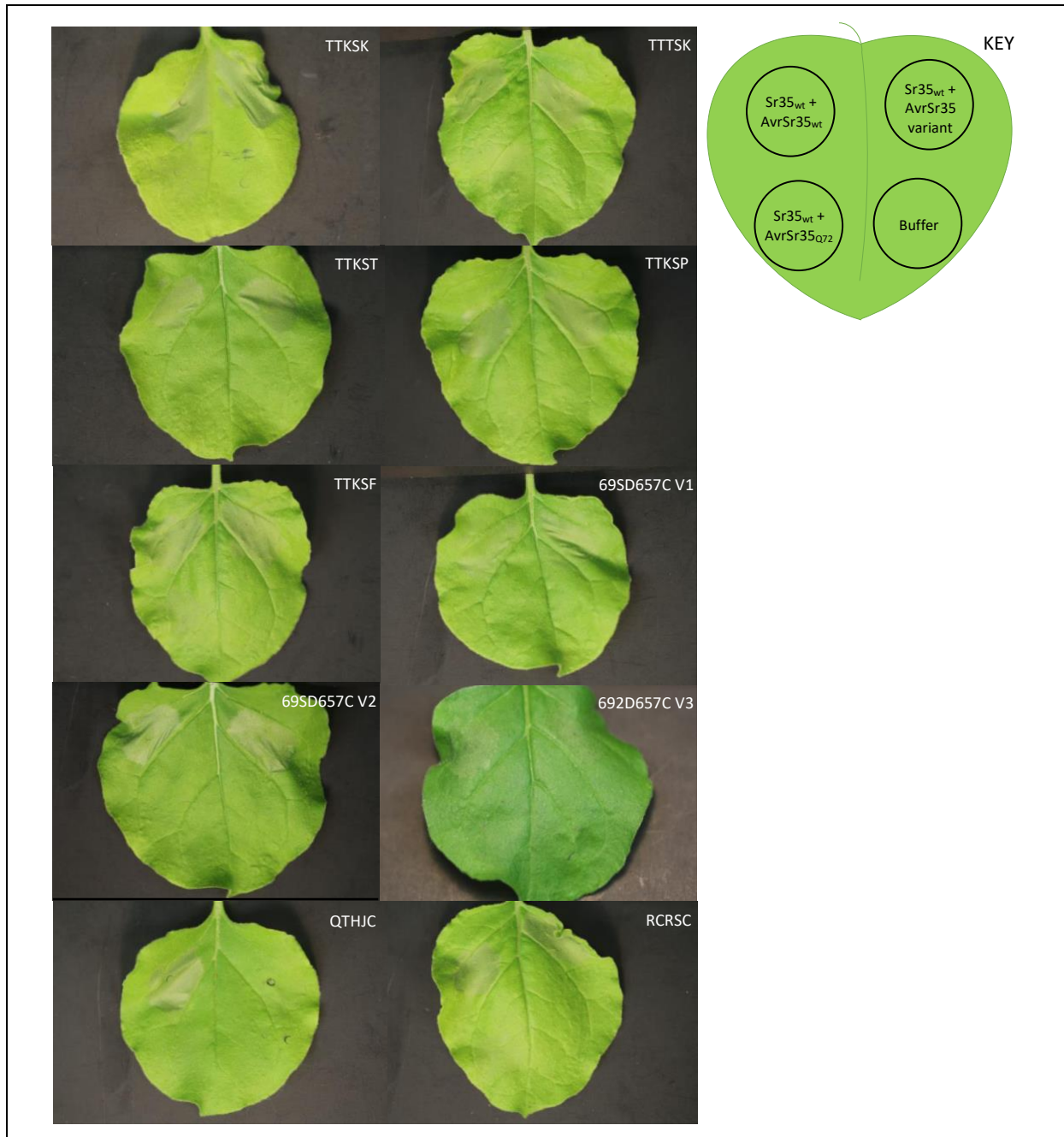


Figure 2.3: Evaluation of interactions between allelic variants of *AvrSr35* and *Sr35* using *N. benthamiana* infiltration system. Each tobacco leaf was co-infiltrated with *Agrobacterium* samples containing *Sr35*+*AvrSr35* (positive control), *Sr35*+*AvrSr35* variant (test), *Sr35*+*AvrSr35***Q72* (negative control), and an injection of the resuspension buffer without any form of *Agrobacterium* (blank control).

To ensure that reduced HR in tobacco leaves co-infiltrated with the QTHJC variant of the *AvrSr35* gene are not affected by the lack of construct expression, quantitative RT-PCR was

performed to measure the expression levels of *AvrSr35* and *Sr35* constructs. qRT-PCR was executed on total RNA isolated from *Agrobacterium*-infiltrated leaf tissue from *N. benthamiana* (Figure 2.4). As previously described (Salcedo et al., 2017; Liu et al., 2012), *NbP22A* gene showing low cross-tissue variation in expression was used as a reference for estimating the relative expression levels of target genes (Figure 2.4, A). We used *AvrSr35* and *Sr35*-specific primers to detect transcripts of the transiently expressed genes (Table 2.1).

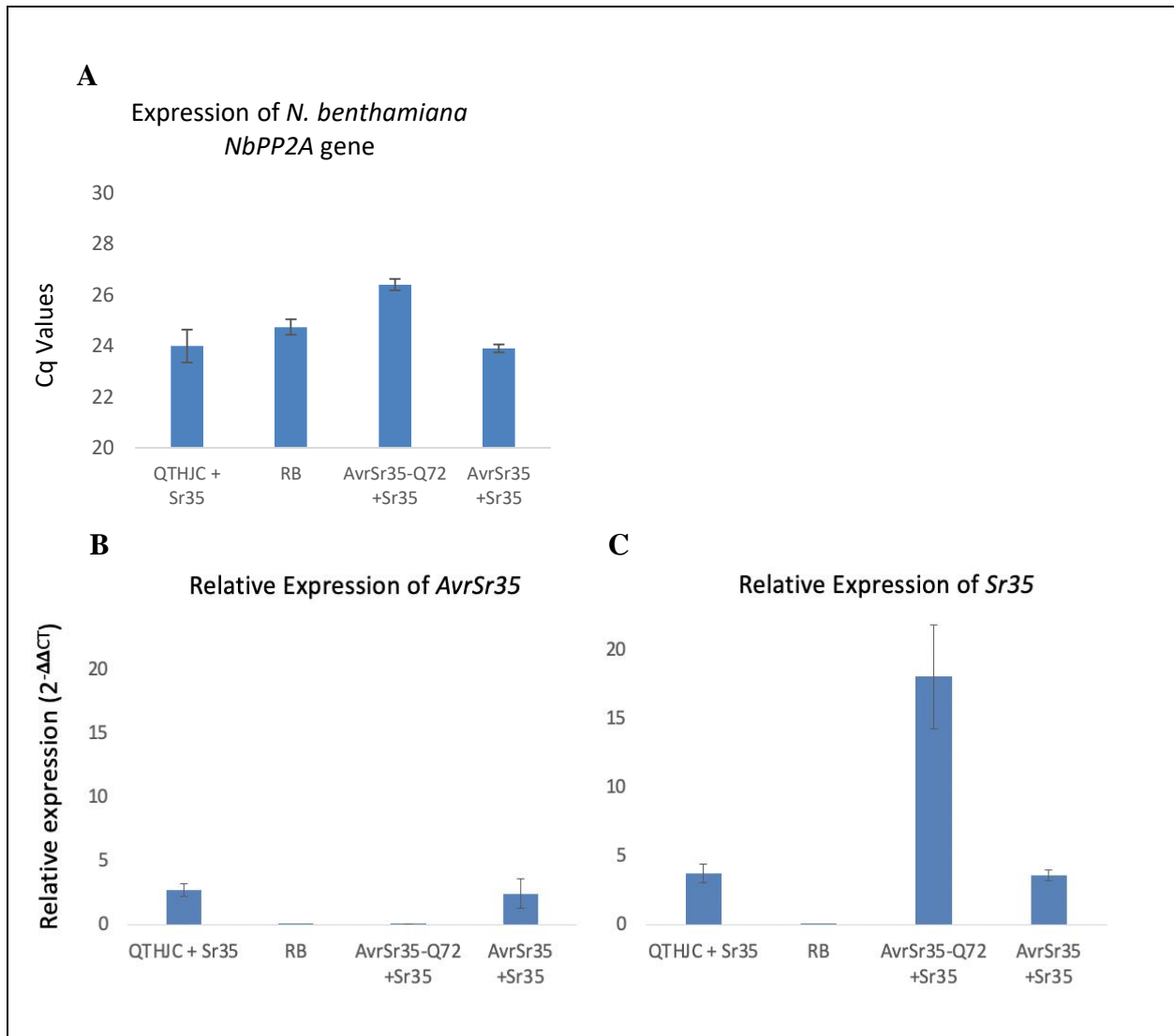


Figure 2.4: qRT-PCR Ct values demonstrating the expression of QTHJC and control gene constructs in the *Agrobacterium* infiltrated tobacco leaves. (A) Shows average expression of the *N. benthamiana* housekeeping gene *NbPP2A* in infected leaves. (B) Shows relative expression of the fungal *AvrSr35* gene and variants measured relative to the tobacco *NbPP2A* (*N. benthamiana* housekeeping gene). Due to *AvrSr35Q72 being a truncated version of the *AvrSr35**wt, there is no relative expression observed for *AvrSr35**Q72. (C) Shows expression of the wheat *Sr35* gene relative to the tobacco *NbPP2A* gene in infected leaves.**

Table 2.1: Primer Sequences used throughout this study. Colony PCR and vector design primers used to validate presence of *AvrSr35* variants throughout the cloning process. Sanger Sequencing primers used to validate correct *AvrSr35* variant sequencing after the cloning process. RT-PCR and qPCR primers used to target specific genes to track expression.

Name	Sequence	Notes
s2351_1508F2	ATGGCCATGAGGAACCTTTGCTGC	Colony PCR
2055R	TTTTGTTGTATGTGACCGGTCTTG	Colony PCR
s2351_2057F	AAGATCCTAAAAGAGATTGAAGAACAAG	Colony PCR, Sanger Sequencing
3766R	TCACAATTTGCCTTCATGAACAT	Colony PCR
AvrSr35_RT_for1	CCATGAGGAACCTTTGCTGCA	RT-PCR/cDNA PCR
AvrSr35_RT_rev1	GAATCTACCAAATCAGATGTGTCTGG	RT-PCR/cDNA PCR
Sr35_qPCR_F1	GCCGTGGAGTGTTGTTCAAC	qPCR
Sr35_qPCR_R1	GGTTGCCTATCCCAGATGGC	qPCR
AllAvrSr35Variant_F2	GCAACACCAAAAATTTCCCCTGA	qPCR, Sanger Sequencing
AllAvrSr35Variant_R2	TGACTGTAAAGCTTGGATGTTGATG	qPCR
NbPP2A_F	GACCCTGATGTTGATGTTGCT	qPCR
NbPP2A_R	GAGGGATTTGAAGAGAGATTTTC	qPCR
NOS-R2	AGATCGCTCGACGCGCATGCGCGTCGAGCGATCTAGTAACA	Vector design/validation PCR
35S-F2	CGGGTCACGCTGCACTGCAGCATGCACATACAAA TGGACGAA	Vector design/validation PCR
AllAvrSr35Variant_R3	CCAAGATGGAAGAAAATATGCTG	Sanger Sequencing
AllAvrSr35Variant_R4	CAACTTTGCCTTGACCCATT	Sanger Sequencing
AllAvrSr35Variant_R5	TGGAAATCAAACTGGCAAA	Sanger Sequencing
RCRSC_R	TCATTTCTGGGTCCAAGAGC	Sanger Sequencing
AllAvrSr35Variant_F3	CAATGAACCGGTGAATGTTG	Sanger Sequencing
AllAvrSr35Variant_F4	TTCCCATTTTTGATGCTGAA	Sanger Sequencing
AllAvrSr35Variant_F5	TCAAAAGGAAATGTGCTTGC	Sanger Sequencing
NOS F	TTGCGCGCTATATTTTGT	Sanger Sequencing
NOS R	GAATCCTGTTGCCGGTCTT	Sanger Sequencing
35S F	TTTGTAGAGAGAGACTGGTGATTTTC	Sanger Sequencing
35S R	CACTGACGTAAGGGATGACG	Sanger Sequencing
attR1 F	TGACTGGATATGTTGTGTTTTACA	Sanger Sequencing
attR1 R	AAAAAGCTGAACGAGAAACG	Sanger Sequencing
attR2 F	AAGAAAGCTGAACGAGAAACG	Sanger Sequencing
attR2 R	TGACTGGATATGTTGTGTTTTACA	Sanger Sequencing

2.5.3 Evaluating interaction between *Sr35* and *AvrSr35* variants by transient expression in the wheat protoplasts

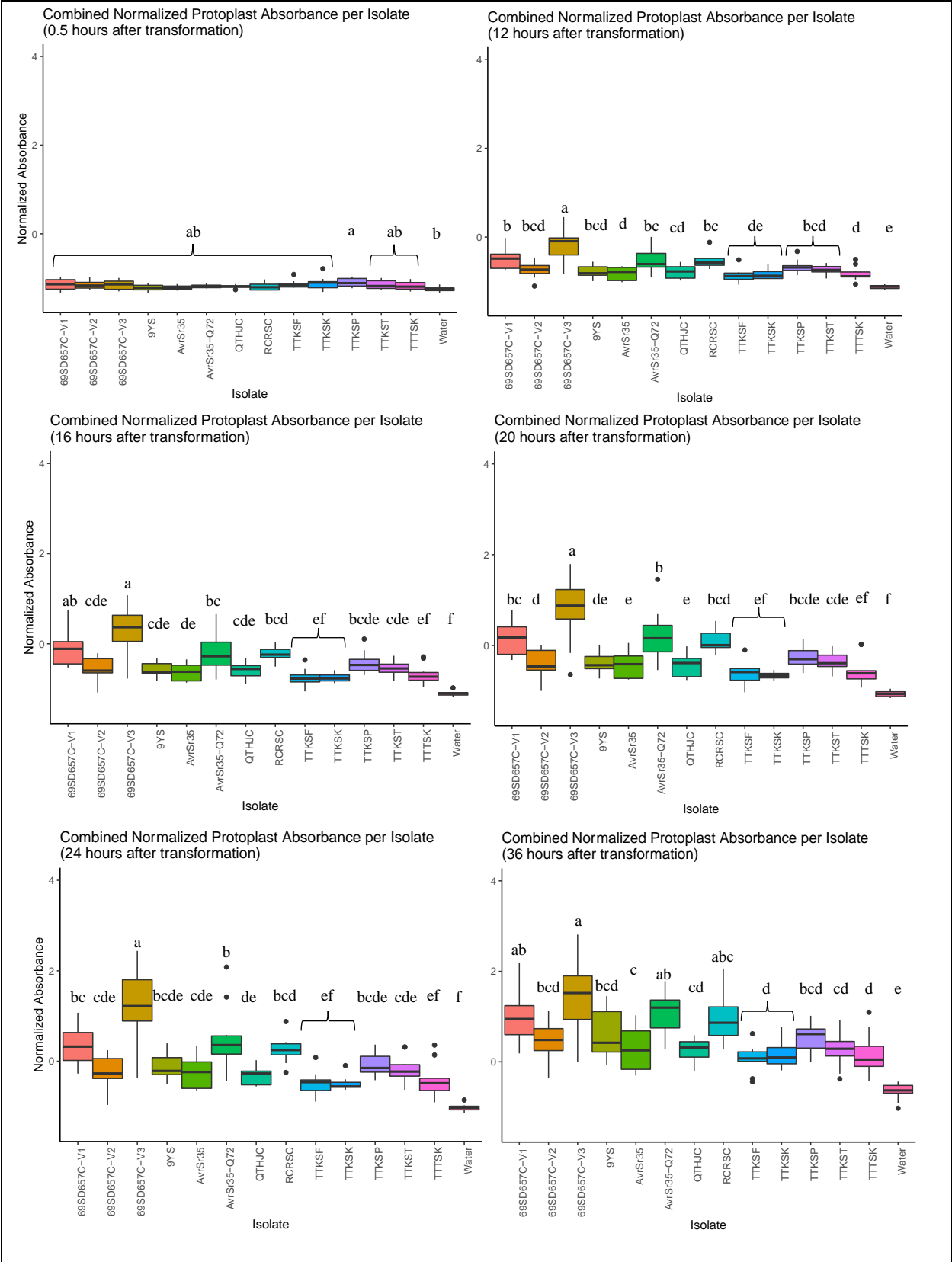
The transient expression assay in *N. benthamiana* provides an easy and fast biological assay to assess interaction between matching resistance genes and effectors (Kamoun, 2006). However, whether interactions confirmed by this assay accurately reflect interactions occurring in wheat remain unclear. Here, we explored the possibility of using transient expression in the suspension of wheat protoplast cells to validate interactions detected in tobacco leaves (Shan et al., 2013). For this purpose, we used protoplasts isolated from the leaves of wheat cultivar “BobWhite” to transiently co-express various versions of the *AvrSr35* gene with the cloned variant of *Sr35* co-located on the same plasmid with the gene encoding the yellow fluorescent protein (YFP) (will henceforth be referred to as 9YS) (Figure 2.5). The HR was monitored using a plate-reader based on the intensity of fluorescence emitted by the YFP expressed from the 9YS construct.

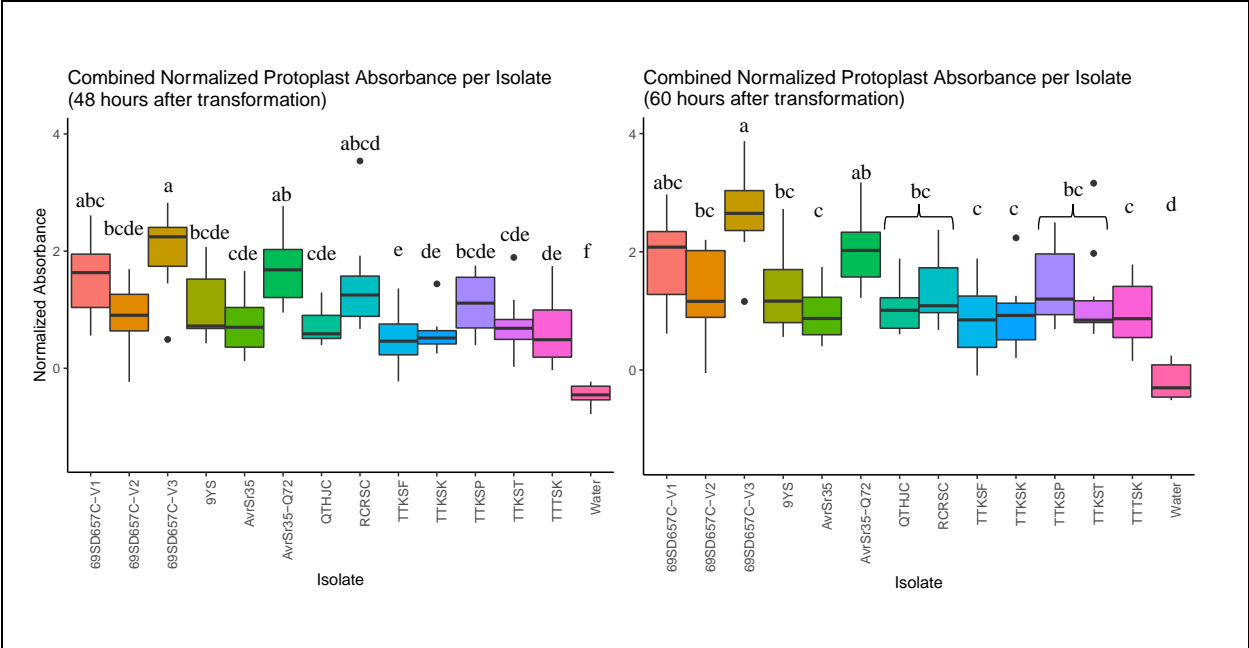
*AvrSr35***Q72* co-transformed with 9YS was used as a negative control and therefore shows a higher fluorescence, verifying that the lack on interaction keeps the protoplasts intact. *AvrSr35* co-transformed with 9YS is the positive control, which has lower absorbance levels due to cell death caused by interaction. Unexpectedly, we observed reduction of fluorescence signal in the protoplast assay transformed with 9YS construct, which carries the *Sr35* and YFP genes.

Analysis of fluorescence signal intensity from 0.5 hours post infection (HPI) to 16 HPI showed no significant differences among samples (Figure 2.5, Appendix A). Starting at 20 HPI the *AvrSr35* alleles 69SD657C-V1, 69SD657C-V3 and RCRSC showed a higher fluorescence level, comparable to that produced by negative control transformed with the *AvrSr35***Q72* construct, suggesting that these variants of the *AvrSr35* gene induce lower hypersensitive response (Figure 2.5, Appendix A). The *AvrSr35* alleles 69SD657C-V2, QTHJC, TTKSF, TTKSK, TTKST, and

TTTSK showed reduction in fluorescence signal comparable to that of the controls at 20 HPI, consistent with stronger HR (Figure 2.5, Appendix A). Throughout all of the remaining time points, we see the same trends of fluorescence signal intensity as at 20 HPI (Figure 2.5). Across all variants, the fluorescence signal intensity increases as time progresses (Figure 2.5).

Throughout these time points, the QTHJC allele of *AvrSr35* showed signals comparable to positive control (*AvrSr35*) [Appendix A: 95 % confidence interval of mean difference between QTHJC and *AvrSr35* at 20 HPI: (-0.832, 0.825), adjusted *P*-value = 1; at 24 HPI: (-0.897, 0.759), adjusted *P*-value = 1; at 36 HPI: (-0.833, 0.822), adjusted *P*-value = 1; at 48 HPI: (-0.862, 0.795), adjusted *P*-value = 1; at 60 HPI: (-0.769, 0.887), adjusted *P*-value = 1].





Isolates

- 69SD657C-V1
- 69SD657C-V2
- 69SD657C-V3
- 9YS
- AvrSr35
- AvrSr35-Q72
- QTHJC
- RCRSC
- TTKSF
- TTKSK
- TTKSP
- TTKST
- TTTSK
- Water

Figure 2.5: Combined normalized protoplast absorbance per isolate at various hours post infection (HPI). Wheat protoplasts were transformed with pUC19+YFP+Sr35 (9YS) alongside the test isolates. If positive interactions occur, we would visualize a lower normalized absorbance level due to cell death whereas if negative interactions occur, we would visualize a higher normalized absorbance level indicating the cells are still intact. Water, without 9YS, is one of the negative controls showing low absorbance indicating the lack of yellow fluorescent protein (YFP). *AvrSr35-Q72* is the other negative control, however, it shows a higher absorbance alongside test isolates 69SD657C-V1, 69SD657C-V3, RCRSC, and TTKSP. 9YS and *AvrSr35* are the positive controls, which have lower absorbance levels alongside test isolates 69SD657C-V2, QTHJC, TTKSF, TTKSK, TTKST, and TTTSK.

Table 2.2: Summary of presence or absence of hypersensitive response (HR) seen in *N. benthamiana* infiltration system alongside the wheat protoplast system at 24 Hours Post Infection (HPI) between allelic variants of *AvrSr35* and *Sr35*. Tobacco leaves were co-infiltrated with *Agrobacterium* samples containing *Sr35* and *AvrSR35* variants. Wheat protoplasts were co-transformed with plasmids containing *Sr35* and *AvrSr35* variants.

Allele	Tobacco	Protoplast
<i>Sr35</i> (alone)	+	+
<i>AvrSr35</i>	+	+
<i>AvrSr35-Q72</i>	-	-
TTKSK	+	+
TTTSK	+	+
TTKST	+	+
TTKSP	+	+
TTKSF	+	+
69SD657C V1	+	+
69SD657C V2	+	+
69SD657C V3	+	-
QTHJC	-	+
RCRSC	+	+

2.6 Discussion

This study was conducted to understand the effects of allelic diversity in *AvrSr35* on *Sr35*-based resistance in wheat. Previously, we observed the loss of avirulence to *Sr35* in these group of *Pgt* isolates associated with the insertion of MITE (Salcedo et al., 2017). However, our results demonstrated that although the levels of sequence divergence among avirulent gene variants can be high, as for example for the RCRSC and QTHJC *AvrSr35* variants used in this study, *Avr-R* based recognition could be determined by specific amino acids within the avirulence protein. The set of *AvrSr35* variants that were tested in this study included sequences showing 1-20 amino acid differences from the original RKQQC variant of AVRSR35 (Salcedo et al., 2017). The results presented in this study suggest that only three amino acid changes are potentially linked

with transition of *Pgt* isolates from the *Sr35*-avirulent to the *Sr35*-virulent forms. Using comparative phylogenetic analysis and the *N. benthamiana* transient expression system we show that the variant of *AvrSr35* found in the QTHJC *Pgt* race carries amino acid changes at three sites that are likely responsible for reduced recognition of *AvrSr35* by the *Sr35* resistance gene. The attenuated HR in tobacco leaves co-infiltrated with the QTHJC variant of *AvrSr35* suggest that evolution of the virulent variants of the *AvrSr35* gene likely first occurred via accumulation of amino acid changes at these three critical sites. Finding of the QTHJC variant of *AvrSr35* without MITE insertion, that clusters with isolates carrying *AvrSr35* with MITE insertion suggests the possibility that this lineage of *Pgt* isolates acquired the ability to overcome *Sr35*-mediated resistance even before MITE insertion. The insertion of MITE into the coding sequence was likely a secondary event that resulted in the complete loss of the *AvrSr35* coding potential. Similar cases of avirulence factor divergence leading to the origin of virulent strains of pathogens have been documented for many pathosystems such as virulence of the bacterial pathogen *Xyella fastidiosa* in alfalfa (*Medicago sativa*) (Lopes et al., 2010) and gain of virulence in the rice blast fungus, *Magnaporthe grisea* (Kang et al., 2001) (see Sacristán & García-Arenal, 2008 for more information). This “sequence divergence” mode of avirulence gene evolution is likely associated with the necessity to maintain its function, which might be critical for compatible interaction between host and pathogen. In this scenario, insertion of transposable element into avirulence gene, as was observed for *AvrSr35* and other effectors (Salcedo et al., 2017), will likely have a negative impact on fitness (other examples can be seen in Grandaubert et al., 2014; Soyer et al., 2014; Fedoroff, 2012). Although, in earlier studies no visible differences in the growth rate between the *Pgt* isolates with and without functional variants of the *AvrSr35* gene were detected (Salcedo et al., 2017), it does not mean that *AvrSr35* function

loss has no effect on fitness. In natural populations, fitness is defined by ability of a pathogen to establish compatible interaction with the susceptible hosts and evade recognition by the host's resistance genes (van der Plank, 1968, p. 206). The frequency of resistant hosts in a population will, therefore, have a strong effect on the evolution of matching avirulence factors. In populations with low frequency of matching resistance genes, selection would benefit maintenance of avirulence factors if it promotes compatible interaction. In host populations with high frequency of matching resistance genes, the cost of maintaining the avirulence factors might become too high and retention of the loss-of-function variants of the avirulence factor might become more beneficial. This evolutionary dynamic likely underlies the origin of the allelic series of the *AvrSr35* gene in *Pgt*.

Determining the model in which *Sr35* and *AvrSr35* interact is also pertinent to how allelic diversity of *AvrSr35* will affect *Sr35*-based resistance. Based on the available data, we can propose several possible models to describe *Sr35*-*AvrSr35* interaction (Figure 2.6). Direct interaction between the avirulent variants of *AvrSr35* with *Sr35* triggers hypersensitive reaction in infected leaf tissues (Figure 2.6, Model 1). Disruption of coding sequence by MITE insertion results in loss of avirulence and inability of *Sr35* to trigger defense response in the presence of pathogen (Figure 2.6, Model 2). The discovery of the QTHJC variant of *AvrSr35* suggest that other modes of *R-Avr* gene interaction are also possible. Amino-acid sequence changes at three sites (Figure 2.2, B) in the QTHJC lineage also shared by other virulent isolates could have reduced the affinity between *AvrSr35* and *Sr35* reducing or completely halting avirulence response (Figure 2.6, Model 3). Other possibilities include the presence of another secreted effector protein in the QTHJC race of *Pgt* that can either block the *Sr35*-*AvrSr35* interaction or

interfere with downstream signaling triggered by *Sr35* upon recognition of *AvrSr35* (Figure 2.6, Model 4).

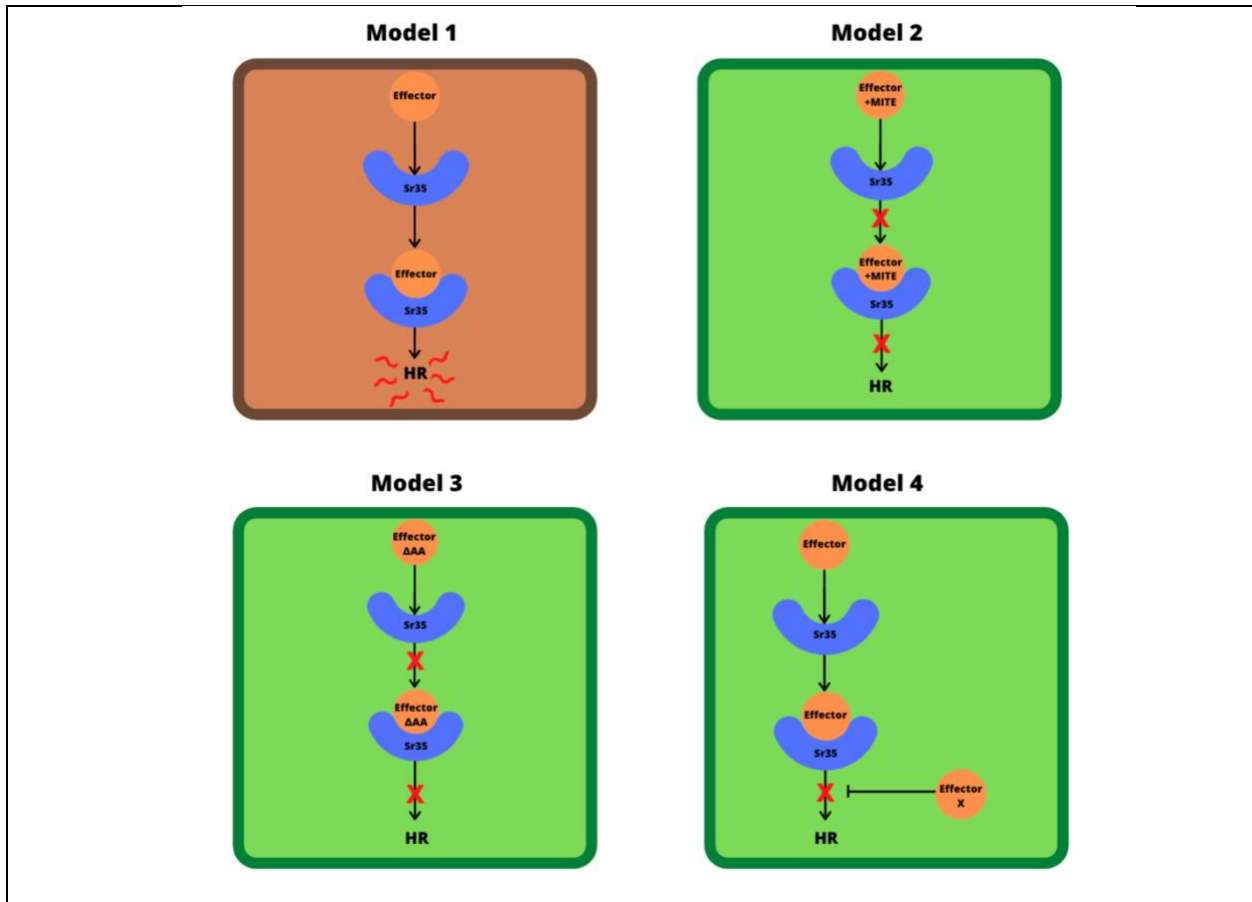


Figure 2.6: Models of Host-Pathogen interaction. (Model 1) Positive gene-for-gene model, where the effector or *Avr* gene is recognized by the corresponding *R* gene (i.e. *Sr35*) resulting in hypersensitive response (HR), (Model 2) Effector is no longer recognized by the *R* gene due to a miniature inverted transposable element (MITE) insertion resulting pathogen viability, (Model 3) Effector is no longer recognized by the *R* gene due to a critical change in its amino acid (Δ AA) resulting in pathogen viability, (Model 4) Effector is recognized by the *R* gene; however, a suppressor effector (Effector X) is present and therefore blocks the *R* gene's signaling for immune response resulting in pathogen viability.

In this project, we aimed to understand which of the models, model 3 or model 4, is consistent with the mode of interaction between *Pgt* race QTHJC and wheat. For this purpose, we opted to use agroinfiltration into the leaves of *N. benthamiana* to transiently co-express different variants of the *AvrSr35* gene along with the *Sr35* gene. We expect that if model 3 (Figure 2.6) is correct,

HR should not be seen or reduced in the infiltrated *N. benthamiana* leaves. However, strong HR response would be more consistent with model 4 (Figure 2.6), where HR is triggered in *N. benthamiana* leaves due to the lack of *AvrSr35* suppressor in the system.

The obtained results of the *N. benthamiana* assay confirmed expression of the avirulence gene in the leaves co-infiltrated with the *AvrSr35* variants from QTHJC, RCRSC, and RKQQC (*AvrSr35_{wt}*) isolates (Figure 2.3, B). Likewise, our analysis confirmed expression of the *Sr35* gene constructs in same samples (Figure 2.3, C). The relative levels of the *AvrSr35* and *Sr35* construct expression in the tissues co-infiltrated with the QTHJC variant of *AvrSr35* were comparable to those obtained for the positive control (Figure 2.3, B and C) suggesting that reduced HR elicited by the QTHJC variant is not due to lack of construct expression. The results of *N. benthamiana* screening are compatible with model 3 of the *Sr35*-*AvrSr35* interaction (Figure 2.6) and indicate that virulence of the QTHJC *AvrSr35* variant on *Sr35* is unlikely associated with the presence of a suppressor interfering with *Sr35*-mediated immune response. These results also suggest that QTHJC may have the variant of *AvrSr35* with amino acid changes that affect recognition by *Sr35*. This finding complements the results found in our sequence comparison analysis that *Sr35* virulent isolates may have essential amino acid deviations that are critical for *Sr35*-based recognition.

Preliminary results were obtained through the transformation of wheat protoplast cells to validate interactions detected in tobacco leaves (Shan et al., 2013). The fluorescence for the positive control (*AvrSr35* + 9YS) produced a lower absorbance level due to cell death caused by interaction and the negative control (*AvrSr35_{*Q72}* + 9YS) showed a higher fluorescence, verifying that the lack on interaction keeps the protoplasts intact. The reduction of fluorescence signal in the protoplast transformed with the 9YS construct is likely caused by HR triggered by

Sr35 itself, which was observed previously in tobacco leaves agroinfiltrated by the *Sr35* construct alone (Bolus et al., 2019). However, when *Sr35* was co-expressed along with the truncated version of the *AvrSr35* construct (*AvrSr35*Q72*), there was a reduced HR consistent with the results obtained in the tobacco transient expression assay (Table 2.2). It appears that interaction with a non-functional *AvrSr35* variant somehow interferes with downstream signaling resulting in cell death. The overall trend across significant time points for the *AvrSr35* alleles from 69SD657C-V1, 69SD657C-V3 and RCRSC showed a higher fluorescence level, suggesting that these gene variants induce lower hypersensitive response (Figure 2.5). In contrast, the overall trends for the *AvrSr35* alleles from 69SD657C-V2, QTHJC, TTKSF, TTKSK, TTKST, and TTTSK showed reduction in fluorescence signal, indicative of stronger HR (Figure 2.5). The QTHJC allele of *AvrSr35* showed signals comparable to positive control (*AvrSr35*) throughout all of the observed time points, which suggests that *Sr35* recognizes the QTHJC allele at a rate that is equivalent to that of the wildtype *AvrSr35* gene. These preliminary results contradict those obtained in the transient expression experiments performed using *N. benthamiana* on two accounts, the QTHJC and 69SD657C-V3 alleles of *AvrSr35* (Table 2.2). This contradiction could mean that additional factors are present in the homologous expression system (wheat protoplasts), but absent in the heterologous expression system (tobacco cells) that could have contributed to the observed discrepancy. In addition, untested alleles in other *Pgt* genomes could perform differently than the alleles tested in this study. Therefore, additional experiments are required to better understand the biological nature of different responses observed in the wheat protoplast and tobacco leaves as well as the diversity within the entire *Pgt* population. This research, including the prospect for future experiments, has provided a better understanding of the origin of new virulence specificities in wheat stem rust, has helped to evaluate the range of

Sr35 recognition specificity, and identified potentially significant amino acid changes affecting *AvrSr35-Sr35* interaction. I believe that the knowledge from this research coupled with additional research on the *AvrSr35* avirulence factor and its targets and the *Sr35* resistance gene will aid in adopting the elements of the *Sr35-AvrSr35* interaction system for advancing plant protection by means of biotechnology and gene editing.

2.7 References

- Beard, C., Jayasena, K., Thomas, G., & Loughman, R. (2004). Managing stem rust of wheat. *Plant Pathology, Department of Agriculture, Western Australia*, 8, 23-34.
- Bolus, S., Akhunov, E., Coaker, G., & Dubcovsky, J. (2019). Dissection of cell death induction by wheat stem rust resistance protein *Sr35* and its matching effector *AvrSr35*. *Molecular Plant-Microbe Interactions*, MPMI-08-19-0216-R. <https://doi.org/10.1094/MPMI-08-19-0216-R>
- Bourras, S., McNally, K. E., Ben-David, R., Parlange, F., Roffler, S., Praz, C. R., Oberhaensli, S., Menardo, F., Stirnweis, D., Frenkel, Z., Schaefer, L. K., Flückiger, S., Treier, G., Herren, G., Korol, A. B., Wicker, T., & Keller, B. (2015). Multiple Avirulence Loci and Allele-Specific Effector Recognition Control the *Pm3* Race-Specific Resistance of Wheat to Powdery Mildew. *The Plant Cell*, tpc.15.00171. <https://doi.org/10.1105/tpc.15.00171>
- Bushnell, W. R., & Roelfs, A. P. (Eds.). (1984). *The Cereal rusts: Vol. II*. Academic Press.
- Chen, E. C. H., Morin, E., Beaudet, D., Noel, J., Yildirim, G., Ndikumana, S., Charron, P., St-Onge, C., Giorgi, J., Krüger, M., Marton, T., Ropars, J., Grigoriev, I. V., Hainaut, M., Henrissat, B., Roux, C., Martin, F., & Corradi, N. (2018). High intraspecific genome diversity in the model arbuscular mycorrhizal symbiont *Rhizophagus irregularis*. *New Phytologist*, 220(4), 1161–1171. <https://doi.org/10.1111/nph.14989>
- Chen, J., Upadhyaya, N. M., Ortiz, D., Sperschneider, J., Li, F., Bouton, C., Breen, S., Dong, C., Xu, B., Zhang, X., Mago, R., Newell, K., Xia, X., Bernoux, M., Taylor, J. M., Steffenson, B., Jin, Y., Zhang, P., Kanyuka, K., ... Dodds, P. N. (2017). Loss of *AvrSr50* by somatic exchange in stem rust leads to virulence for *Sr50* resistance in wheat. *Science*, 358(6370), 1607–1610. <https://doi.org/10.1126/science.aao4810>
- CLC Sequence Viewer. Get the software safe and easy.* (n.d.). Software Informer. Retrieved July 16, 2020, from <https://clc-sequence-viewer.software.informer.com/7.0/>

- Dagvadorj, B., Ozketen, A. C., Andac, A., Duggan, C., Bozkurt, T. O., & Akkaya, M. S. (2017). A *Puccinia striiformis* f. Sp. *Tritici* secreted protein activates plant immunity at the cell surface. *Scientific Reports*, 7(1), 1141. <https://doi.org/10.1038/s41598-017-01100-z>
- Edgar, R. C. (2004). MUSCLE: Multiple sequence alignment with high accuracy and high throughput. *Nucleic Acids Research*, 32(5), 1792–1797. <https://doi.org/10.1093/nar/gkh340>
- Ellis, J. G., Dodds, P. N., & Lawrence, G. J. (2007). The role of secreted proteins in diseases of plants caused by rust, powdery mildew and smut fungi. *Current Opinion in Microbiology*, 10(4), 326–331. <https://doi.org/10.1016/j.mib.2007.05.015>
- F, M., Ym, P., J, L., N, B., T, G., N, M., P, B., Arn, T., Sc, P., Rd, F., & R, L. (2019). The EMBL-EBI search and sequence analysis tools APIs in 2019. *Nucleic Acids Research*, 47(W1), W636–W641. <https://doi.org/10.1093/nar/gkz268>
- Faris, J. D., Xu, S. S., Cai, X., Friesen, T. L., & Jin, Y. (2008). Molecular and cytogenetic characterization of a durum wheat–*Aegilops speltoides* chromosome translocation conferring resistance to stem rust. *Chromosome Research*, 16(8), 1097–1105. <https://doi.org/10.1007/s10577-008-1261-3>
- Fedoroff, N. V. (2012). Transposable Elements, Epigenetics, and Genome Evolution. *Science*, 338(6108), 758–767. JSTOR.
- Flor, H. H. (1942). Inheritance of pathogenicity in *Melampsora lini*. *Phytopathology*, 32, 653–669.
- Gao, L., Babiker, E. M., Nava, I. C., Nirmala, J., Bedo, Z., Lang, L., Chao, S., Gale, S., Jin, Y., Anderson, J. A., Bansal, U., Park, R. F., Rouse, M. N., Bonman, J. M., & Bariana, H. (2019). Temperature-sensitive wheat stem rust resistance gene Sr15 is effective against *Puccinia graminis* f. Sp. *Tritici* race TTKSK. *Plant Pathology*, 68(1), 143–151. <https://doi.org/10.1111/ppa.12928>
- Ghazvini, H., Hiebert, C. W., Zegeye, T., Liu, S., Dilawari, M., Tsilo, T., Anderson, J. A., Rouse, M. N., Jin, Y., & Fetch, T. (2012). Inheritance of resistance to Ug99 stem rust in wheat cultivar Norin 40 and genetic mapping of Sr42. *Theoretical and Applied Genetics*, 125(4), 817–824. <https://doi.org/10.1007/s00122-012-1874-y>
- GlobalRust.org*. (2019). [Text]. GlobalRust.Org. <https://globalrust.org/>
- Gout, L., Fudal, I., Kuhn, M.-L., Blaise, F., Eckert, M., Cattolico, L., Balesdent, M.-H., & Rouxel, T. (2006). Lost in the middle of nowhere: The AvrLm1 avirulence gene of the Dothideomycete *Leptosphaeria maculans*. *Molecular Microbiology*, 60(1), 67–80. <https://doi.org/10.1111/j.1365-2958.2006.05076.x>
- Gout, L., Kuhn, M. L., Vincenot, L., Bernard-Samain, S., Cattolico, L., Barbetti, M., Moreno-Rico, O., Balesdent, M.-H., & Rouxel, T. (2007). Genome structure impacts molecular evolution at the AvrLm1 avirulence locus of the plant pathogen *Leptosphaeria maculans*.

Environmental Microbiology, 9(12), 2978–2992. <https://doi.org/10.1111/j.1462-2920.2007.01408.x>

- Grandaubert, J., Lowe, R. G., Soyer, J. L., Schoch, C. L., Van de Wouw, A. P., Fudal, I., Robbertse, B., Lapalu, N., Links, M. G., Ollivier, B., Linglin, J., Barbe, V., Mangenot, S., Cruaud, C., Borhan, H., Howlett, B. J., Balesdent, M.-H., & Rouxel, T. (2014). Transposable element-assisted evolution and adaptation to host plant within the *Leptosphaeria maculans*-*Leptosphaeria biglobosa* species complex of fungal pathogens. *BMC Genomics*, 15(1), 891. <https://doi.org/10.1186/1471-2164-15-891>
- Gu, L., Si, W., Zhao, L., Yang, S., & Zhang, X. (2015). Dynamic evolution of NBS–LRR genes in bread wheat and its progenitors. *Molecular Genetics and Genomics*, 290(2), 727–738. <https://doi.org/10.1007/s00438-014-0948-8>
- Guerrero-Chavez, R., Glover, K. D., Rouse, M. N., & Gonzalez-Hernandez, J. L. (2015). Mapping of two loci conferring resistance to wheat stem rust pathogen races TTKSK (Ug99) and TRTTF in the elite hard red spring wheat line SD4279. *Molecular Breeding*, 35(1), 8. <https://doi.org/10.1007/s11032-015-0198-4>
- Hiebert, C. W., Fetch, T. G., & Zegeye, T. (2010). Genetics and mapping of stem rust resistance to Ug99 in the wheat cultivar Webster. *Theoretical and Applied Genetics*, 121(1), 65–69. <https://doi.org/10.1007/s00122-010-1291-z>
- Hodson, D. (2019, December 2). *RustTracker.org | A Global Wheat Rust Monitoring System*. RustTracker.Org. <https://rusttracker.cimmyt.org/>
- Hogenhout, S. A., Van der Hoorn, R. A. L., Terauchi, R., & Kamoun, S. (2009). Emerging concepts in effector biology of plant-associated organisms. *Molecular Plant-Microbe Interactions: MPMI*, 22(2), 115–122. <https://doi.org/10.1094/MPMI-22-2-0115>
- Houterman, P. M., Cornelissen, B. J. C., & Rep, M. (2008). Suppression of Plant Resistance Gene-Based Immunity by a Fungal Effector. *PLOS Pathogens*, 4(5), e1000061. <https://doi.org/10.1371/journal.ppat.1000061>
- Jin, Y., & Singh, R. P. (2006). Resistance in U.S. Wheat to Recent Eastern African Isolates of *Puccinia graminis* f. Sp. *Tritici* with Virulence to Resistance Gene Sr31. *Plant Disease*, 90(4), 476–480. <https://doi.org/10.1094/PD-90-0476>
- Jin, Y., Singh, R. P., Ward, R. W., Wanyera, R., Kinyua, M., Njau, P., Fetch, T., Pretorius, Z. A., & Yahyaoui, A. (2007). Characterization of Seedling Infection Types and Adult Plant Infection Responses of Monogenic Sr Gene Lines to Race TTKS of *Puccinia graminis* f. Sp. *Tritici*. *Plant Disease*, 91(9), 1096–1099. <https://doi.org/10.1094/PDIS-91-9-1096>
- Jin, Y., Szabo, L. J., Pretorius, Z. A., Singh, R. P., Ward, R., & Fetch, T. (2008). Detection of Virulence to Resistance Gene Sr24 Within Race TTKS of *Puccinia graminis* f. Sp. *Tritici*. *Plant Disease*, 92(6), 923–926. <https://doi.org/10.1094/PDIS-92-6-0923>

- Jones, J. D. G., & Dangl, J. L. (2006). The plant immune system. *Nature*, *444*(7117), 323–329. <https://doi.org/10.1038/nature05286>
- Kamoun, S. (2006). A Catalogue of the Effector Secretome of Plant Pathogenic Oomycetes. *Annual Review of Phytopathology*, *44*(1), 41–60. <https://doi.org/10.1146/annurev.phyto.44.070505.143436>
- Kang, S., Lebrun, M. H., Farrall, L., & Valent, B. (2001). Gain of virulence caused by insertion of a Pot3 transposon in a Magnaporthe grisea avirulence gene. *Molecular Plant-Microbe Interactions: MPMI*, *14*(5), 671–674. <https://doi.org/10.1094/MPMI.2001.14.5.671>
- Koehler, P., Wieser, H., & Konitzer, K. (2014). Chapter 2—Gluten—The Precipitating Factor. In P. Koehler, H. Wieser, & K. Konitzer (Eds.), *Celiac Disease and Gluten* (pp. 97–148). Academic Press. <https://doi.org/10.1016/B978-0-12-420220-7.00002-X>
- Kolmer, J. A., Garvin, D. F., & Jin, Y. (2011). Expression of a Thatcher Wheat Adult Plant Stem Rust Resistance QTL on Chromosome Arm 2BL is Enhanced by Lr34. *Crop Science*, *51*(2), 526–533. <https://doi.org/10.2135/cropsci2010.06.0381>
- Letunic, I., & Bork, P. (2019). Interactive Tree Of Life (iTOL) v4: Recent updates and new developments. *Nucleic Acids Research*, *47*(W1), W256–W259. <https://doi.org/10.1093/nar/gkz239>
- Li, X. (2011). Infiltration of Nicotiana benthamiana Protocol for Transient Expression via Agrobacterium. *BIO-PROTOCOL*, *1*. <https://doi.org/10.21769/BioProtoc.95>
- Liu, D., Shi, L., Han, C., Yu, J., Li, D., & Zhang, Y. (2012). Validation of Reference Genes for Gene Expression Studies in Virus-Infected Nicotiana benthamiana Using Quantitative Real-Time PCR. *PLoS ONE*, *7*(9). <https://doi.org/10.1371/journal.pone.0046451>
- Liu, L., Wang, M. N., Feng, J. Y., See, D. R., Chao, S. M., & Chen, X. M. (2018). Combination of all-stage and high-temperature adult-plant resistance QTL confers high-level, durable resistance to stripe rust in winter wheat cultivar Madsen. *Theoretical and Applied Genetics*, *131*(9), 1835–1849. <https://doi.org/10.1007/s00122-018-3116-4>
- Liu, W., Jin, Y., Rouse, M., Friebe, B., Gill, B., & Pumphrey, M. O. (2011). Development and characterization of wheat-Ae. Searsii Robertsonian translocations and a recombinant chromosome conferring resistance to stem rust. *Theoretical and Applied Genetics*, *122*(8), 1537–1545. <https://doi.org/10.1007/s00122-011-1553-4>
- Liu, W., Rouse, M., Friebe, B., Jin, Y., Gill, B., & Pumphrey, M. O. (2011). Discovery and molecular mapping of a new gene conferring resistance to stem rust, Sr53, derived from Aegilops geniculata and characterization of spontaneous translocation stocks with reduced alien chromatin. *Chromosome Research*, *19*(5), 669–682. <https://doi.org/10.1007/s10577-011-9226-3>
- Niu, Z., Klindworth, D. L., Yu, G., L Friesen, T., Chao, S., Jin, Y., Cai, X., Ohm, J.-B., Rasmussen, J. B., & Xu, S. S. (2014). Development and characterization of wheat lines carrying stem rust resistance gene Sr43

- derived from *Thinopyrum ponticum*. *Theoretical and Applied Genetics*, 127(4), 969–980. <https://doi.org/10.1007/s00122-014-2272-4>
- Lopes, J. R. S., Daugherty, M. P., & Almeida, R. P. P. (2010). Strain origin drives virulence and persistence of *Xylella fastidiosa* in alfalfa. *Plant Pathology*, 59(5), 963–971. <https://doi.org/10.1111/j.1365-3059.2010.02325.x>
- Lozano-Torres, J. L., Wilbers, R. H. P., Gawronski, P., Boshoven, J. C., Finkers-Tomczak, A., Cordewener, J. H. G., America, A. H. P., Overmars, H. A., Van 't Klooster, J. W., Baranowski, L., Sobczak, M., Ilyas, M., van der Hoorn, R. A. L., Schots, A., de Wit, P. J. G. M., Bakker, J., Goverse, A., & Smant, G. (2012). Dual disease resistance mediated by the immune receptor Cf-2 in tomato requires a common virulence target of a fungus and a nematode. *Proceedings of the National Academy of Sciences of the United States of America*, 109(25), 10119–10124. <https://doi.org/10.1073/pnas.1202867109>
- Mago, R., Zhang, P., Vautrin, S., Šimková, H., Bansal, U., Luo, M.-C., Rouse, M., Karaoglu, H., Periyannan, S., Kolmer, J., Jin, Y., Ayliffe, M. A., Bariana, H., Park, R. F., McIntosh, R., Doležel, J., Bergès, H., Spielmeyer, W., Lagudah, E. S., ... Dodds, P. N. (2015). The wheat Sr50 gene reveals rich diversity at a cereal disease resistance locus. *Nature Plants*, 1(12), 1–3. <https://doi.org/10.1038/nplants.2015.186>
- McIntosh, R. A., Dyck, P. L., The, T. T., Cusick, J., & Milne, D. L. (1984). Cytogenetical studies in wheat. XIII. Sr35—A third gene from *Triticum monococcum* for resistance to *Puccinia graminis tritici*. *Zeitschrift Fur Pflanzenzuchtung*, 92, 1–14.
- McIntosh, R. A., Wellings, C. R., & Park, R. F. (Eds.). (1995). *Wheat Rusts: An Atlas of Resistance Genes*. Springer Netherlands. <https://www.springer.com/gp/book/9789401040419>
- McNally, K. E., Menardo, F., Lüthi, L., Praz, C. R., Müller, M. C., Kunz, L., Ben-David, R., Chandrasekhar, K., Dinooor, A., Cowger, C., Meyers, E., Xue, M., Zeng, F., Gong, S., Yu, D., Bourras, S., & Keller, B. (2018). Distinct domains of the AVRPM3^{A2/F2} avirulence protein from wheat powdery mildew are involved in immune receptor recognition and putative effector function. *New Phytologist*, 218(2), 681–695. <https://doi.org/10.1111/nph.15026>
- Miller, E. M., & Nickoloff, J. A. (1995). *Escherichia coli* Electrotransformation. In J. A. Nickoloff (Ed.), *Electroporation Protocols for Microorganisms* (pp. 105–113). Humana Press. <https://doi.org/10.1385/0-89603-310-4:105>
- Norkunas, K., Harding, R., Dale, J., & Dugdale, B. (2018). Improving agroinfiltration-based transient gene expression in *Nicotiana benthamiana*. *Plant Methods*, 14(1), 71. <https://doi.org/10.1186/s13007-018-0343-2>
- Olson, E. L., Rouse, M. N., Pumphrey, M. O., Bowden, R. L., Gill, B. S., & Poland, J. A. (2013a). Simultaneous transfer, introgression, and genomic localization of genes for resistance to stem rust race TTKSK (Ug99) from *Aegilops tauschii* to wheat. *Theoretical and Applied Genetics*, 126(5), 1179–1188. <https://doi.org/10.1007/s00122-013-2045-5>

- Olson, E. L., Rouse, M. N., Pumphrey, M. O., Bowden, R. L., Gill, B. S., & Poland, J. A. (2013b). Introgression of stem rust resistance genes SrTA10187 and SrTA10171 from *Aegilops tauschii* to wheat. *Theoretical and Applied Genetics*, *126*(10), 2477–2484. <https://doi.org/10.1007/s00122-013-2148-z>
- Periyannan, S., Milne, R. J., Figueroa, M., Lagudah, E. S., & Dodds, P. N. (2017). An overview of genetic rust resistance: From broad to specific mechanisms. *PLoS Pathogens*, *13*(7). <https://doi.org/10.1371/journal.ppat.1006380>
- Periyannan, S., Moore, J., Ayliffe, M., Bansal, U., Wang, X., Huang, L., Deal, K., Luo, M., Kong, X., Bariana, H., Mago, R., McIntosh, R., Dodds, P., Dvorak, J., & Lagudah, E. (2013). The Gene Sr33, an Ortholog of Barley Mla Genes, Encodes Resistance to Wheat Stem Rust Race Ug99. *Science*, *341*(6147), 786–788. <https://doi.org/10.1126/science.1239028>
- Peterson, P. D. (2013, August). “*The Barberry or Bread*”: *The Public Campaign to Eradicate Common Barberry in the United States in the Early 20th Century*. <https://www.apsnet.org/edcenter/apsnetfeatures/Pages/Barberry.aspx>
- Petit-Houdenot, Y., & Fudal, I. (2017). Complex Interactions between Fungal Avirulence Genes and Their Corresponding Plant Resistance Genes and Consequences for Disease Resistance Management. *Frontiers in Plant Science*, *8*. <https://doi.org/10.3389/fpls.2017.01072>
- Plissonneau, C., Daverdin, G., Ollivier, B., Blaise, F., Degrave, A., Fudal, I., Rouxel, T., & Balesdent, M.-H. (2016). A game of hide and seek between avirulence genes AvrLm4-7 and AvrLm3 in *Leptosphaeria maculans*. *The New Phytologist*, *209*(4), 1613–1624. <https://doi.org/10.1111/nph.13736>
- Pretorius, Z. A., Singh, R. P., Wagoire, W. W., & Payne, T. S. (2000). Detection of Virulence to Wheat Stem Rust Resistance Gene Sr31 in *Puccinia graminis*. F. Sp. *Tritici* in Uganda. *Plant Disease*, *84*(2), 203–203. <https://doi.org/10.1094/PDIS.2000.84.2.203B>
- Qi, L. L., Pumphrey, M. O., Friebe, B., Zhang, P., Qian, C., Bowden, R. L., Rouse, M. N., Jin, Y., & Gill, B. S. (2011). A novel Robertsonian translocation event leads to transfer of a stem rust resistance gene (Sr52) effective against race Ug99 from *Dasypyrum villosum* into bread wheat. *Theoretical and Applied Genetics*, *123*(1), 159–167. <https://doi.org/10.1007/s00122-011-1574-z>
- Rahmatov, M., Otambekova, M., Muminjanov, H., Rouse, M. N., Hovmøller, M. S., Nazari, K., Steffenson, B. J., & Johansson, E. (2019). Characterization of stem, stripe and leaf rust resistance in Tajik bread wheat accessions. *Euphytica*, *215*(3), 55. <https://doi.org/10.1007/s10681-019-2377-6>
- Rice, P., Longden, I., & Bleasby, A. (2000). EMBOSS: The European Molecular Biology Open Software Suite. *Trends in Genetics: TIG*, *16*(6), 276–277. [https://doi.org/10.1016/s0168-9525\(00\)02024-2](https://doi.org/10.1016/s0168-9525(00)02024-2)

- Robinson, R. A. (1977). Plant Pathosystems. *Annals of the New York Academy of Sciences*, 287(1), 238–242. <https://doi.org/10.1111/j.1749-6632.1977.tb34243.x>
- Rooney, H. C. E., Klooster, J. W. van't, Hoorn, R. A. L. van der, Joosten, M. H. A. J., Jones, J. D. G., & Wit, P. J. G. M. de. (2005). Cladosporium Avr2 Inhibits Tomato Rcr3 Protease Required for Cf-2-Dependent Disease Resistance. *Science*, 308(5729), 1783–1786. <https://doi.org/10.1126/science.1111404>
- Rouse, M. N., & Jin, Y. (2011). Stem Rust Resistance in A-Genome Diploid Relatives of Wheat. *Plant Disease*, 95(8), 941–944. <https://doi.org/10.1094/PDIS-04-10-0260>
- Rouse, Matthew N., Olson, E. L., Gill, B. S., Pumphrey, M. O., & Jin, Y. (2011). Stem Rust Resistance in *Aegilops tauschii* Germplasm. *Crop Science*, 51(5), 2074–2078. <https://doi.org/10.2135/cropsci2010.12.0719>
- Rouxel, T., Penaud, A., Pinochet, X., Brun, H., Gout, L., Delourme, R., Schmit, J., & Balesdent, M.-H. (2003). A 10-year Survey of Populations of *Leptosphaeria maculans* in France Indicates a Rapid Adaptation Towards the Rlm1 Resistance Gene of Oilseed Rape. *European Journal of Plant Pathology*, 109(8), 871–881. <https://doi.org/10.1023/A:1026189225466>
- Rust Spore- A Global Wheat Rust Monitoring System*. (2019, December 4). Food and Agriculture Organization of the United Nations. <http://www.fao.org/agriculture/crops/rust/stem/rust-report/stem-ug99racettksk/en/>
- Sacristan, S., & Garcia-Arenal, F. (2008). The evolution of virulence and pathogenicity in plant pathogen populations. *Molecular Plant Pathology*, 9(3), 369–384. <https://doi.org/10.1111/j.1364-3703.2007.00460.x>
- Saintenac, C., Zhang, W., Salcedo, A., Rouse, M. N., Trick, H. N., Akhunov, E., & Dubcovsky, J. (2013). Identification of Wheat Gene Sr35 That Confers Resistance to Ug99 Stem Rust Race Group. *Science*, 341(6147), 783–786. <https://doi.org/10.1126/science.1239022>
- Salcedo, A., Rutter, W., Wang, S., Akhunova, A., Bolus, S., Chao, S., Anderson, N., Soto, M. F. D., Rouse, M., Szabo, L., Bowden, R. L., Dubcovsky, J., & Akhunov, E. (2017). Variation in the AvrSr35 gene determines Sr35 resistance against wheat stem rust race Ug99. *Science*, 358(6370), 1604–1606. <https://doi.org/10.1126/science.aao7294>
- Sambrook, J., & Russell, D. W. (1989). *Molecular Cloning A Laboratory Manual* (3rd Edition, Vol. 3). Cold Spring Harbor Laboratory Press. www.MolecularCloning.com
- Shan, Q., Wang, Y., Li, J., Zhang, Y., Chen, K., Liang, Z., Zhang, K., Liu, J., Xi, J. J., Qiu, J.-L., & Gao, C. (2013). Targeted genome modification of crop plants using a CRISPR-Cas system. *Nature Biotechnology*, 31(8), 686–688. <https://doi.org/10.1038/nbt.2650>
- Singh, R. P., Huerta-Espino, J., Bhavani, S., Herrera-Foessel, S. A., Singh, D., Singh, P. K., Velu, G., Mason, R. E., Jin, Y., Njau, P., & Crossa, J. (2011). Race non-specific

- resistance to rust diseases in CIMMYT spring wheats. *Euphytica*, 179(1), 175–186.
<https://doi.org/10.1007/s10681-010-0322-9>
- Singh, S., Singh, R. P., Bhavani, S., Huerta-Espino, J., & Eugenio, L.-V. E. (2013). QTL mapping of slow-rusting, adult plant resistance to race Ug99 of stem rust fungus in PBW343/Muu RIL population. *Theoretical and Applied Genetics*, 126(5), 1367–1375.
<https://doi.org/10.1007/s00122-013-2058-0>
- Singh, R. P., Hodson, D. P., Jin, Y., Lagudah, E. S., Ayliffe, M. A., Bhavani, S., Rouse, M. N., Pretorius, Z. A., Szabo, L. J., Huerta-Espino, J., Basnet, B. R., Lan, C., & Hovmøller, M. S. (2015). Emergence and Spread of New Races of Wheat Stem Rust Fungus: Continued Threat to Food Security and Prospects of Genetic Control. *Phytopathology*, 105(7), 872–884. <https://doi.org/10.1094/PHYTO-01-15-0030-FI>
- Soyer, J. L., Ghalid, M. E., Glaser, N., Ollivier, B., Linglin, J., Grandaubert, J., Balesdent, M.-H., Connolly, L. R., Freitag, M., Rouxel, T., & Fudal, I. (2014). Epigenetic Control of Effector Gene Expression in the Plant Pathogenic Fungus *Leptosphaeria maculans*. *PLOS Genetics*, 10(3), e1004227. <https://doi.org/10.1371/journal.pgen.1004227>
- Steuernagel, B., Periyannan, S. K., Hernández-Pinzón, I., Witek, K., Rouse, M. N., Yu, G., Hatta, A., Ayliffe, M., Bariana, H., Jones, J. D. G., Lagudah, E. S., & Wulff, B. B. H. (2016). Rapid cloning of disease-resistance genes in plants using mutagenesis and sequence capture. *Nature Biotechnology*, 34(6), 652–655.
<https://doi.org/10.1038/nbt.3543>
- Van der Biezen, E. A., & Jones, J. D. (1998). Plant disease-resistance proteins and the gene-for-gene concept. *Trends in Biochemical Sciences*, 23(12), 454–456.
[https://doi.org/10.1016/s0968-0004\(98\)01311-5](https://doi.org/10.1016/s0968-0004(98)01311-5)
- van der Plank, J. E. (1968). *Disease resistance in plants*. (1st ed.). Academic Press.
- Yu, L.-X., Barbier, H., Rouse, M. N., Singh, S., Singh, R. P., Bhavani, S., Huerta-Espino, J., & Sorrells, M. E. (2014). A consensus map for Ug99 stem rust resistance loci in wheat. *Theoretical and Applied Genetics*, 127(7), 1561–1581. <https://doi.org/10.1007/s00122-014-2326-7>
- Zhang, W., Chen, S., Abate, Z., Nirmala, J., Rouse, M. N., & Dubcovsky, J. (2017). Identification and characterization of Sr13, a tetraploid wheat gene that confers resistance to the Ug99 stem rust race group. *Proceedings of the National Academy of Sciences*, 114(45), E9483–E9492. <https://doi.org/10.1073/pnas.1706277114>
- Zhou, J.-M., & Chai, J. (2008). Plant pathogenic bacterial type III effectors subdue host responses. *Current Opinion in Microbiology*, 11(2), 179–185.
<https://doi.org/10.1016/j.mib.2008.02.004>
- Zipfel, C., & Rathjen, J. P. (2008). Plant immunity: AvrPto targets the frontline. *Current Biology: CB*, 18(5), R218–220. <https://doi.org/10.1016/j.cub.2008.01.016>

Chapter 3 - High-quality genome assembly and annotation of the

Puccinia graminis f. sp. *tritici* isolate RKQQC

Bliss Betzen¹, Yuanwen Guo¹, John Fellers^{1,2}, Katherine Jordan^{1,2}, Robert Bowden^{1,2}, Eduard Akhunov¹

¹ Department of Plant Pathology, Kansas State University, Manhattan, KS 66506, USA.

² USDA-ARS, Manhattan, KS 66506, USA.

3.1 Abstract

Recent advances in long-read sequencing technologies substantially reduced the cost and improved the quality of genome assemblies of the agriculturally-relevant pathogens, including the complex genomes of cereal rusts. The assembly of the dikaryotic *Puccinia graminis* f. sp. *tritici* (*Pgt*) genome is challenged by the presence of two haplotypes in the dikaryon. Recently, the PacBio sequencing platform was used to create the haplotype resolved assembly of the Ug99 race of *Pgt* (Li et al., 2019). Here, we tested the utility of Oxford Nanopore combined with short-read Illumina technology for creating a haplotype-resolved assembly of an American isolate of *Pgt* 99KS76A-1. The final assembly produced by Canu assembler and polished with Pilon included 1162 contigs with total length of 178.4 Mb and N50 of 1.35 Mb. The completeness of the genome assembly was confirmed by using benchmarking universal single-copy orthologs (BUSCOs) of basidiomycota. This analysis also showed the high level of gene duplication in the assembly consistent with the presence of two resolved haplotypes in assembly.

3.2 Objectives of study

Develop an updated, high-quality fungal reference genome to facilitate effector discovery and the development of protection strategies against wheat stem rust.

- Sequence the genome of *Pgt* race RKQQC using the Illumina and Oxford Nanopore technologies.
- Evaluate the quality of genome assembly and the feasibility of separating the haplotypes of two nuclei using data from the Oxford Nanopore technology.

3.3 Introduction

Recent studies demonstrated that multiple reference genomes (pan-genome) are required to adequately capture structural diversity (copy number variation, presence/absence variation) present in populations (De Maayer et al., 2014; Glasner et al., 2008; Mann et al., 2013). Pan-genomes provide a much more powerful resource for mapping genes and pathways underlying variation in important phenotypic traits than single reference genomes (De Maayer et al., 2014; Mann et al., 2013). In cereal rusts, with large highly repetitive genomes, effectors encoding genes represent one of the most important classes of genes, which also show high levels of intra-species presence/absence variation. Creating a detailed catalogue of effector gene diversity in *Pgt* will therefore require sequencing and assembling multiple *Pgt* genomes.

From short-read (2 X 300 base pairs (bp)) sequencing provided by Illumina (MiSeq, NextSeq, HiSeq), to medium length (300-500 bp) sequencing provided by Proton (Ion Torrent; ThermoFisher), to long-read (>70 kilobases and >1Megabases) sequencing provided by PacBio and Oxford Nanopore Technology (ONT) (Chaisson et al., 2015; Huddleston et al., 2014), there have been significant increases in the quality of genome assemblies. Many genome sequencing projects use a combination of several technologies (Kiran et al., 2016; Quainoo et al., 2017; Hacquard et al., 2013; Faino et al., 2015 to name a few). Long read length offered by PacBio and ONT is critical for assembling the highly repetitive regions of genomes composed of transposable elements or microsatellite repeats and generating more contiguous and longer assemblies. At the same time, the higher accuracy of Illumina short reads with an error rate of

less than 0.005% (Schirmer et al., 2016) helps to compensate for higher error rate inherent in PacBio, which is now as low as 0.2% (Wenger et al., 2019), and Oxford Nanopore technologies with error rates as low as 5% (Kono & Arakawa, 2019; Rang et al., 2018), though recent advance in sequencing chemistry have brought the error rate down to <1% (Hu et al., 2020). Although PacBio and Oxford Nanopore are comparable sequencing technologies, ONT is portable and is more cost-efficient than PacBio (Weirather et al., 2017; Quick et al., 2014). The hybrid method of assembling genomes has already been applied to several rust pathogens. For example, reference genomes have already been built or partially completed for leaf rust (*Puccinia triticina*) (Kiran et al., 2016), stripe rust (*Puccinia striiformis* f. sp. *tritici*) (Li et al., 2020), stem rust (*Puccinia graminis* f. sp. *tritici*) (Duplessis et al., 2011; Li et al., 2020), and flax rust (*Melampsora lini*) (Nemri et al., 2014).

Rust fungi have dikaryotic spores containing two haploid nuclei that significantly complicates genome assembly (Spatafora et al., 2017). Although the nuclei within each spore are genetically similar, they might have differences that are sufficient for allocating long sequence reads from different nuclei into separate contig assemblies (Li et al., 2020). With the use of long-read sequencing through Oxford Nanopore coupled with short-read Illumina sequencing for error correction, haplotype-resolved contigs are likely to be assembled to account for the presence of two nuclei. The goal of our study is to test the utility of Oxford Nanopore technology for creating a high-quality haplotype-resolved stem rust reference genome assembly for the *Pgt* race RKQQC.

3.4 Materials and Methods

3.4.1 Spore grow-up, collection, and spore mat formation

Wheat cultivar “Morocco” was grown in a growth chamber under the following growth conditions: 22°C, 40% humidity with 16 hours of light and 8 hours of dark in 9-inch by 9-inch pans. Planted seeds were then treated with cytosol (CytoCulture, 1 tbs per liter of water) chemical to stunt growth by disrupting cell division. Once plants reached the second leaf stage (10-12 days after planting), spores of *Pgt* race 0.5 g of RKQQC race spores were sprayed onto the plants. Atomizers (Tallgrass Solutions, Manhattan, KS) containing soltrol 170 oil (Chevron Phillips) and a small amount of sample spores (99:1) were prepared in a controlled greenhouse environment. Soltrol oil is used to help the spores adhere to the leaf surface for a better infection outcome. An air compressor is then attached to the sprayer head and spores are sprayed over the plant leaf tip at a pressure of 20 PSI. Plants were allowed to dry for 30 minutes and then were moved to dew chambers at the settings of 9°C wall, 43°C water, and 18-22°C air temperature. Plants are left in the dew chambers for 12-16 hours and immediately transferred to a controlled growth chamber setting and treated with Miracle-Gro (Home Depot) fertilizer.

Spore collection is typically done 2 weeks after infection and can be completed again in multiple rounds 2-3 days following the last collection until the plants die. A small shop vacuum is attached to the Spore Collector (Tallgrass Solutions, Manhattan, KS), a funnel-like suction head, and new vials are attached to the bottom of the head. Spores were collected with a vacuum and were separated from debris using a 40 µm sieve. The spores were then dried in a desiccator at room temperature containing drierite (Sigma-Aldrich) overnight. Dried spores are then divided 0.5 g per 1.7 ml tubes and stored in a -80°C freezer.

Due to the thick outer wall of urediniospores, it is difficult to obtain both high quality and high quantities of fungal DNA. Spores were germinated according to Webb et al. (2006). A 1x germination solution of nonyl alcohol (Sigma-Aldrich, 9 μ l), Tween 20 (Thermo Fisher, 65.2 μ l), ethanol (Thermo Fisher, 1.25 ml), and Milli Q water (Sigma-Aldrich, 1.25 ml) is diluted 500x and used as the basis for spore germination. Fresh urediniospores (roughly 0.4 g), collected as stated above, are then dusted in a fine layer over the top of the diluted germination solution using a 40 μ m metal sieve. Spore mats were collected 16 hours after the start, washed three times in a buchner funnel with double distilled water, then flash frozen.

3.4.2 Fungal DNA isolation

We used a high quality fungal DNA isolation protocol for long read sequencing from Schwessinger & McDonald (2017), with the following minor modifications from Fellers (unpublished). In brief, we started by making the lysis buffer as directed (5 ml Buffer A: 0.35 M sorbitol, 0.1 M Tris-HCl (pH 8.0), 5 mM EDTA (pH 8.0)- autoclaved to sterilize; 5 ml Buffer B: 0.2 M Tris-HCl (pH 8.0), 50 mM EDTA (pH 8.0), 2 M NaCl, 2% CTAB- autoclave to sterilize; 2 ml Buffer C: 5% Sarkosyl N-lauroylsarcosine sodium salt (Sigma L5125)- filter to sterilize; 1 ml of 10% PVP 40, 1 ml of sterile ddH₂O) and heat to 50 degrees after mixing and allow to cool to room temperature (Schwessinger & McDonald, 2017 hereafter referenced). The samples, either dried spore or spore mats, were ground as directed and added to the lysis buffer prior to adding 50 μ l of RNase A (10 mg/ml). The tubes were inverted using a Rotator Genie and rotating at the slowest speed for 1 hour at room temperature. 200 μ l of Proteinase K was added to the mixture and inversion continued as stated above for 1-2 hours at room temperature. The sample is then incubated for 5 minutes on ice followed by the addition of 2.8 ml potassium acetate (5M), mixing, and incubating on ice for 5 additional minutes as directed by the original protocol.

Samples are then centrifuged at 5000 xg for 12 minutes at 4°C as directed. The supernatant was removed using a big bore 10 ml pipette and placed into a new 50 ml tube followed by the addition of 15 ml of phenol/chloroform/isoamyl alcohol (P/C/I, 25:24:1) at room temperature and inverted on the Rotator Genie at the slowest speed for 5 minutes at room temperature. The mixture was centrifuged at 4000 xg for 10 minutes at 4°C and the supernatant was removed using a big bore pipette followed by an additional 15 ml P/C/I step. After the additional P/C/I step, the supernatant is transferred to a new 50 ml tube using a big bore pipette. The steps including sodium acetate, isopropanol, mixing, and 5-10-minute incubation at room temperature were all done as directed in the original protocol. The mixture was centrifuged at 8000 xg for 30 minutes at 4°C and the supernatant is slowly poured off, leaving a pellet at the bottom. The wash steps were completed as directed in the original protocol, following the wash steps, 5 µl of the sample were taken to run an agarose gel for a quality control check. Another round of wash steps were completed and samples were eluted as was done in the original protocol. The KSU Integrated Genomics Facility performed the Tape Station method to estimate the quality of samples. Following validation of quality, 80 µl of MagPure beads (ABP Biosciences) were added to the fungal DNA to clean up samples. The mixture was placed on the Rotator Genie for 5 minutes on the slowest speed at room temperature then placed over a magnetic bar to aid in separation of MagPure beads. The liquid was removed, and the beads were then washed twice with 70% ethanol without disturbing the pellet of beads. The liquid was removed once more, and the samples were left to air dry. Once dry, the fungal DNA was resuspended in 50 µl of the elution buffer (EB, Qiagen, Hilden, Germany).

3.4.3 Oxford Nanopore library prep and sequencing technology

This study utilized SMRT PacBio long reads from Salcedo et al. (2017) and long reads generated with Oxford Nanopore Technologies (ONT) MinION. ONT library creation of sample DNA is prepared using the MinION library preparation protocol provided by Oxford Nanopore. The purified fungal DNA was then sheared by performing 50 cycles of aspiration utilizing a P200 pipette. End repair is done by adding 6.5 μ l of FFPE Repair buffer and 2 μ l FFPE Enzyme mix (NEB, E7180S) and mixing followed by incubation at 20°C for 30 minutes. Samples were then cleaned using 100 μ l of AMPureXP beads (Beckman-Coulter) and inverting the sample mixture for 5 minutes on a Rotator Genie. Samples were then placed on a magnet; the liquid was removed, and the beads were washed twice using 200 μ l of 70% ethanol. After removing the ethanol, 60 μ l of nuclease free water was added to the beads and incubated for 2 minutes at room temperature. The liquid was then transferred to a clean tube and the DNA concentration was measured for each sample with a Qubit fluorometer (Invitrogen) at the KSU Integrated Genomic Facility to ensure quality of DNA extraction and library preparation steps so far. Samples were then treated with 7 μ l of NEBNext Ultra II End Prep buffer and 3 μ l of NEBNext Ultra II End Prep Enzyme mix (NEB, E7180S) to perform dA-tailing. Samples were mixed, then incubated at 20°C for 30 minutes, 65°C for 5 minutes, and briefly cooled on ice. Enriched DNA libraries were then purified with 60 μ l of AMPureXP beads, inverted for 5 minutes, placed on a magnet, and the liquid was removed. Beads were washed twice with 200 μ l of 70% ethanol, the ethanol was removed, and the beads were allowed to air dry at room temperature. 31 μ l of nuclease free water was mixed with the beads and samples incubated for 2 minutes at room temperature. Liquid was transferred to a new tube and DNA concentrations were again measured with a Qubit fluorometer for quality control. Adapters were ligated to the blunt ends of the sample DNA using

20 µl of the Adapter Mix (AMX 1D) and 50 µl of New England BioLabs Blunt and TA Ligase Master Mix (NEB, M0367S). The sample was mixed and incubated at 23°C for 15 minutes. Samples were treated with 40 µl of AMPureXP beads, inverted for 5 minutes, and placed on a magnet. The liquid was removed, and the beads were washed twice with 140 µl of ABB (MinION kit: SQK-LSK109). Samples were placed back on the magnet, the liquid was removed and replaced with 15 µl of ELB, the pre-sequencing mix provided (MinION kit: SQK-LSK109) and incubated at room temperature for 10 minutes. Samples were placed on a magnet and the liquid was then transferred to a new tube. DNA was analyzed with QuBit technology for a final quality control step. Samples were then applied to the MinION flowcell (sequencing kit: SQK-LSK109, R 9.4 version D). Sequencing was initiated by tethering the sample DNA to the outer surface of the flowcell and guiding through the pore. This method of sequencing requires no amplification and has moderate sequencing throughput for very long read data (> 1 mega-bases) with a high error rate as low as 5% (Kono & Arakawa, 2019; Rang et al., 2018). Oxford Nanopore is an affordable way to perform long read sequencing and pairs well with the short-read data accumulated from Illumina sequencing making it easy to map repeat regions, assemble large contigs, perform error correction, and complete a quality reference genome.

3.4.4 Illumina library prep and sequencing technology

The development of new genomic technologies allows for affordable and quick assembly of even the most complex genomes. One very useful technology is Illumina sequencing used for short reads between 200 and 600 base pairs. We utilized the Illumina MiSeq Personal Sequencing System at the Kansas State University Integrated Genomics Facility. Illumina is one of many next-generation sequencing platforms that leverages massively parallel sequencing of DNA molecules that are clonally amplified on a flowcell. Sample DNA is isolated, fragmented into

desired sequencing sizes, and adaptors are ligated to the fragments and then made single stranded. Sample DNA is then applied to Illumina flowcells which have oligonucleotide primers on the surface that bind to the adapters attached to the fragmented DNA. The DNA is then replicated using bridge PCR amplification to form about 1000 copies of DNA with the same sequence. Once amplified, enzymes find complimenting nucleotides to make fragments double stranded. The fragments are then denatured leaving single stranded templates for further amplification creating millions of dense double stranded DNA clusters. These clusters of DNA copies are sequenced by emitting a signal from each fluorescently labeled dNTP which is detected by a camera and records the nucleotide as the PCR cycles continue. This is the overall basis of Illumina sequencing. Illumina is very high throughput and can generate a large amount of short read data (roughly 2 x 300 base pairs) at an extremely low error rate of less than 0.005% (Schirmer et al., 2016). Due to this low rate of error, short read Illumina sequencing is often paired with long read sequencing and serves as a means of error correction.

3.4.5 Programs and pipelines: Canu, Pilon

We utilized established bioinformatic pipelines to trim, assemble, and edit our input reads from Oxford Nanopore and Illumina sequencing, as well as the PacBio reads from Salcedo et al. (2017). In brief, we used the Canu pipeline (version 1.7; Koren et al., 2017), with default setting and corrected Error Rate = 0.13, to overlap our raw reads to form consensus reads, trim portions of reads with low coverage, and then assemble the high-quality trimmed reads into contigs. Illumina Miseq reads were mapped to the Canu established assembly with BWA (version 0.7.17) with default settings. Following assembly, we used the Pilon pipeline (version 1.22; Walker et al., 2014) to polish the inherently error-prone input data from PacBio and Oxford Nanopore sequencing by aligning the Illumina MiSeq short mapping results to our assembly from Canu.

Pilon identified mismatches between the assembly and Illumina reads and filled gaps in the assembly, improving its overall quality.

3.4.6 Comparison of the completeness of 99KS76A-1 (race RKQQC) and CDL75-36–700-3 (race SCCL) genome assemblies using BUSCO.

Since there are other references and parts of *Pgt* isolates that have been sequenced, we are able to compare our assembly using Oxford Nanopore to others that have previously been completed.

The SCCL *Pgt* isolate was the first stem rust isolate to get sequenced using shotgun sequencing and Sanger sequencing chemistry (Duplessis et al., 2011). We compared the N50 value and the number of contigs between the SCCL genome assembly and our assembly after error correction with Pilon. However, we were also interested in determining whether our assembly had better haplotype-resolution compared to the SCCL genome. To understand whether our assembly was haplotype-resolved, we utilized the Benchmarking Universal Single-Copy Orthologs program (BUSCO; version 4 Simão et al., 2015). In BUSCO we set basidiomycota as the fungal lineage, which allowed us to compare our assembly with 1,764 phylogenetically related genes that are conserved throughout all of the currently sequenced fungal genomes. BUSCO identifies the sequences of these conserved orthologs in the assembly and computes the fraction that are conserved single gene copies, conserved duplicated gene copies, fragmented genes or missing genes that are not present in the basidiomycota fungal lineage in BUSCO.

3.5 Results and Discussion

The RKQQC reference genome was assembled using long-reads produced by Oxford Nanopore MinION and PacBio SMRT (Salcedo et al., 2017) sequencing technologies followed by error correction using Illumina MiSeq short-reads. The summary of sequence data used for genome

assembly is shown in Table 3.1. The average read lengths generated by MinION, SMRT, and MiSeq instruments were 4,258 bp/read, 2,350 bp/read, and 594 bp/paired-end read (2 x 300 bp), respectively (Table 3.1).

Table 3.1: Sequencing data statistics. Details the number of reads and the number of base pairs from Oxford Nanopore MinION, PacBio SMRT, and Illumina MiSeq that were used for this study.

	Number of reads	Number of bases
Oxford Nanopore MinION	4,175,267	17,778,854,332
PacBio SMRT	264,532	621,668,569
Illumina MiSeq	31,390,809 * 2	18,660,663,652

In total, 1,162 contigs ranging from 1,020 bp to 5,440,655 bp were assembled. The total length of the Canu haplotype-resolved contig assembly was 178,353,835 bp with an N50 value of 1,329,390 bp (Table 3.2). Following the Canu assembly step, error correction was performed by aligning MiSeq reads to the assembled contigs using Pilon (Walker et al., 2014). The correction generated 1,166 contigs ranging from 1,020 bp to 5,536,814 bp and were a total length of 180,987,563 bp with an N50 value of 1,345,248 bp (Table 3.2).

Table 3.2: *Pgt* genome assembly statistics generated by Canu and error correction using Pilon.

	Canu	Pilon
Number of contigs	1162	1166
Largest contig	5,440,655	5,536,814
Smallest contig	1,020	1,020
Total length	178,353,835	180,987,563
N50	1,329,390	1,345,248

Further, we assessed the completeness of the RKQQC race genome assembly using BUSCO (Simão et al., 2015) and compared completeness of its assembly with the completeness of assembly produced for the SCCL race (Duplessis et al., 2011). This particular assembly was generated using Sanger sequence data with the total length of the genome assembly being 89 Mb, which is nearly two times shorter than the total length of our assembly. These results indicate that the SCCL assembly is likely comprised of contigs assembled from reads coming from different *Pgt* nuclei, and unlikely that this assembly is haplotype resolved. According to the BUSCO analysis, out of 1,764 phylogenetically conserved genes, 1620 (92%) were completely assembled compared to 87% in the SCCL race genome (Figure 3.1). The RKQQC and SCCL genomes had 8% and 13% of these genes, respectively, partially assembled or missing in the assembly. However, the major difference between these two assemblies is the proportion of completely assembled genes that were present as single or duplicated copies. In the RKQQC race genome assembly, out of 1620 completely assembled genes, 1,276 (79%) were duplicated, whereas in SCCL genome assembly out of 1542 completely assembled genes only 103 (0.1%)

were duplicated (Figure 3.1, A and B). The drastic increase in the number of duplicated genes is indicative of successful separation of haplotypes from different nuclei from the *Pgt* dikaryon.

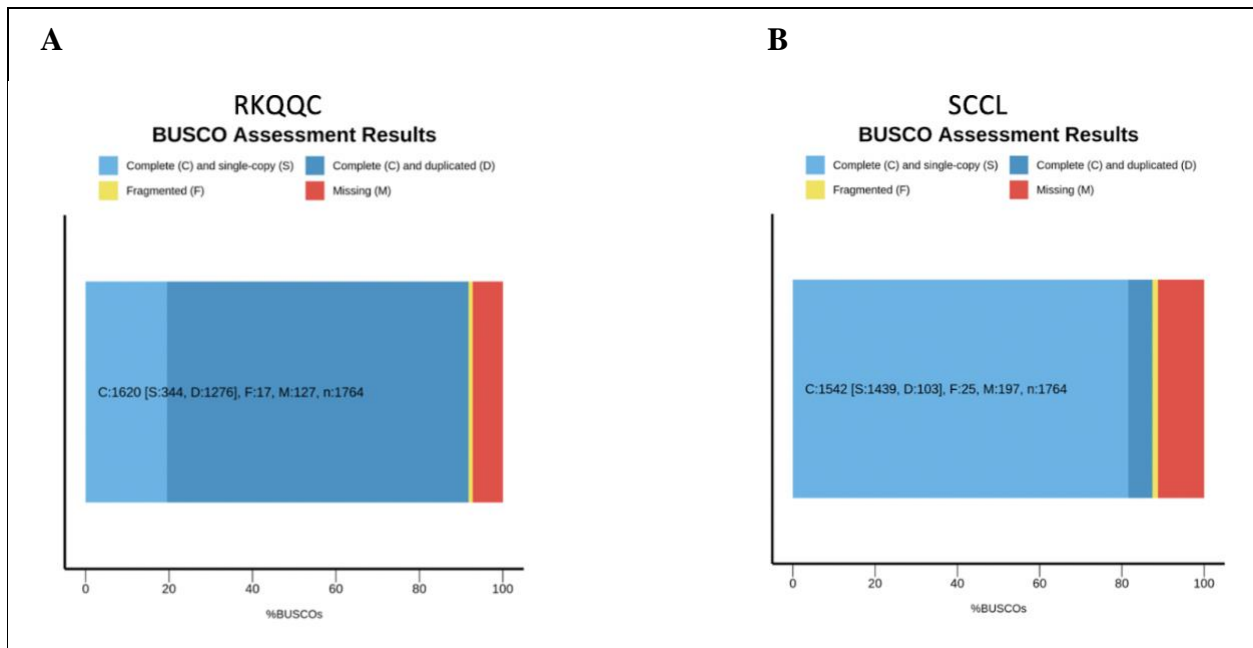


Figure 3.1: BUSCO comparison of RKQQC and SCCL assemblies. (A) The RKQQC assembly has 344 complete single gene copies, 1,276 complete duplicated gene copies, 17 fragmented genes, and 127 missing genes, while (B) the SCCL assembly has 1,439 complete single gene copies, 103 complete duplicated gene copies, 25 fragmented genes, and 197 missing genes.

The main purpose of this study to generate an improved, haplotype resolved RKQQC reference genome utilizing the Oxford Nanopore sequencing technology. Further analyses using this reference genome are forthcoming (unpublished). This study confirms that the combination of Oxford Nanopore sequencing technology with Illumina reads could produce high quality haplotype-resolved assembly of the rust genomes. This updated RKQQC assembly will be further improved using other genome-sequence finishing technologies, such as Hi-C and Chicago methods (van Steensel & Dekker, 2010; Dekker et al., 2013; Cairns et al., 2016). The new RKQQC assembly will be used to identify new avirulence genes and study evolution of new virulence specificities in the *Pgt* isolates.

3.6 References

- Cairns, J., Freire-Pritchett, P., Wingett, S. W., Várnai, C., Dimond, A., Plagnol, V., Zerbino, D., Schoenfelder, S., Javierre, B.-M., Osborne, C., Fraser, P., & Spivakov, M. (2016). CHiCAGO: Robust detection of DNA looping interactions in Capture Hi-C data. *Genome Biology*, *17*(1), 127. <https://doi.org/10.1186/s13059-016-0992-2>
- Chaisson, M. J. P., Huddleston, J., Dennis, M. Y., Sudmant, P. H., Malig, M., Hormozdiari, F., Antonacci, F., Surti, U., Sandstrom, R., Boitano, M., Landolin, J. M., Stamatoyannopoulos, J. A., Hunkapiller, M. W., Korlach, J., & Eichler, E. E. (2015). Resolving the complexity of the human genome using single-molecule sequencing. *Nature*, *517*(7536), 608–611. <https://doi.org/10.1038/nature13907>
- Dekker, J., Marti-Renom, M. A., & Mirny, L. A. (2013). Exploring the three-dimensional organization of genomes: Interpreting chromatin interaction data. *Nature Reviews. Genetics*, *14*(6), 390–403. <https://doi.org/10.1038/nrg3454>
- De Maayer, P., Chan, W. Y., Rubagotti, E., Venter, S. N., Toth, I. K., Birch, P. R. J., & Coutinho, T. A. (2014). Analysis of the *Pantoea ananatis* pan-genome reveals factors underlying its ability to colonize and interact with plant, insect and vertebrate hosts. *BMC Genomics*, *15*(1), 404. <https://doi.org/10.1186/1471-2164-15-404>
- Duplessis, S., Cuomo, C. A., Lin, Y.-C., Aerts, A., Tisserant, E., Veneault-Fourrey, C., Joly, D. L., Hacquard, S., Amselem, J., Cantarel, B. L., Chiu, R., Coutinho, P. M., Feau, N., Field, M., Frey, P., Gelhaye, E., Goldberg, J., Grabherr, M. G., Kodira, C. D., ... Martin, F. (2011). Obligate biotrophy features unraveled by the genomic analysis of rust fungi. *Proceedings of the National Academy of Sciences of the United States of America*, *108*(22), 9166–9171. <https://doi.org/10.1073/pnas.1019315108>
- Faino, L., Seidl, M. F., Datema, E., Berg, G. C. M. van den, Janssen, A., Wittenberg, A. H. J., & Thomma, B. P. H. J. (2015). Single-Molecule Real-Time Sequencing Combined with Optical Mapping Yields Completely Finished Fungal Genome. *MBio*, *6*(4). <https://doi.org/10.1128/mBio.00936-15>
- Glasner, J. D., Marquez-Villavicencio, M., Kim, H.-S., Jahn, C. E., Ma, B., Biehl, B. S., Rissman, A. I., Mole, B., Yi, X., Yang, C.-H., Dangl, J. L., Grant, S. R., Perna, N. T., & Charkowski, A. O. (2008). Niche-Specificity and the Variable Fraction of the *Pectobacterium* Pan-Genome. *Molecular Plant-Microbe Interactions*®, *21*(12), 1549–1560. <https://doi.org/10.1094/MPMI-21-12-1549>
- Hacquard, S., Kracher, B., Maekawa, T., Vernaldi, S., Schulze-Lefert, P., & Ver Loren van Themaat, E. (2013). Mosaic genome structure of the barley powdery mildew pathogen and conservation of transcriptional programs in divergent hosts. *Proceedings of the National Academy of Sciences of the United States of America*, *110*(24), E2219–E2228. <https://doi.org/10.1073/pnas.1306807110>

- Hu, Y., Fang, L., Nicholson, C., & Wang, K. (2020). *Implications of error-prone long-read whole-genome shotgun sequencing on characterizing reference microbiomes* [Preprint]. Genomics. <https://doi.org/10.1101/2020.03.05.978866>
- Huddleston, J., Ranade, S., Malig, M., Antonacci, F., Chaisson, M., Hon, L., Sudmant, P. H., Graves, T. A., Alkan, C., Dennis, M. Y., Wilson, R. K., Turner, S. W., Korlach, J., & Eichler, E. E. (2014). Reconstructing complex regions of genomes using long-read sequencing technology. *Genome Research*, *24*(4), 688–696. <https://doi.org/10.1101/gr.168450.113>
- Kiran, K., Rawal, H. C., Dubey, H., Jaswal, R., Devanna, B. N., Gupta, D. K., Bhardwaj, S. C., Prasad, P., Pal, D., Chhuneja, P., Balasubramanian, P., Kumar, J., Swami, M., Solanke, A. U., Gaikwad, K., Singh, N. K., & Sharma, T. R. (2016). Draft Genome of the Wheat Rust Pathogen (*Puccinia triticina*) Unravels Genome-Wide Structural Variations during Evolution. *Genome Biology and Evolution*, *8*(9), 2702–2721. <https://doi.org/10.1093/gbe/evw197>
- Kono, N., & Arakawa, K. (2019). Nanopore sequencing: Review of potential applications in functional genomics. *Development, Growth & Differentiation*, *61*(5), 316–326. <https://doi.org/10.1111/dgd.12608>
- Koren, S., Walenz, B. P., Berlin, K., Miller, J. R., Bergman, N. H., & Phillippy, A. M. (2017). Canu: Scalable and accurate long-read assembly via adaptive *k*-mer weighting and repeat separation. *Genome Research*, *27*(5), 722–736. <https://doi.org/10.1101/gr.215087.116>
- Li, Y., Xia, C., Wang, M., Yin, C., & Chen, X. (2020). Whole-genome sequencing of *Puccinia striiformis* f. sp. *Tritici* mutant isolates identifies avirulence gene candidates. *BMC Genomics*, *21*(1), 247. <https://doi.org/10.1186/s12864-020-6677-y>
- Li, F., Upadhyaya, N. M., Sperschneider, J., Matny, O., Nguyen-Phuc, H., Mago, R., Raley, C., Miller, M. E., Silverstein, K. A. T., Henningsen, E., Hirsch, C. D., Visser, B., Pretorius, Z. A., Steffenson, B. J., Schwessinger, B., Dodds, P. N., & Figueroa, M. (2019). Emergence of the Ug99 lineage of the wheat stem rust pathogen through somatic hybridisation. *Nature Communications*, *10*(1), 1–15. <https://doi.org/10.1038/s41467-019-12927-7>
- Macko, V., & Staples, R. C. (1973). Regulation of Uredospore Germination and Germ Tube Development. *Bulletin of the Torrey Botanical Club*, *100*(4), 223–229. JSTOR. <https://doi.org/10.2307/2484800>
- Mann, R. A., Smits, T. H. M., Bühlmann, A., Blom, J., Goesmann, A., Frey, J. E., Plummer, K. M., Beer, S. V., Luck, J., Duffy, B., & Rodoni, B. (2013). Comparative Genomics of 12 Strains of *Erwinia amylovora* Identifies a Pan-Genome with a Large Conserved Core. *PLOS ONE*, *8*(2), e55644. <https://doi.org/10.1371/journal.pone.0055644>
- Nemri, A., Saunders, D. G. O., Anderson, C., Upadhyaya, N. M., Win, J., Lawrence, G., Jones, D., Kamoun, S., Ellis, J., & Dodds, P. (2014). The genome sequence and effector

- complement of the flax rust pathogen *Melampsora lini*. *Frontiers in Plant Science*, 5. <https://doi.org/10.3389/fpls.2014.00098>
- Quainoo, S., Coolen, J. P. M., Hijum, S. A. F. T. van, Huynen, M. A., Melchers, W. J. G., Schaik, W. van, & Wertheim, H. F. L. (2017). Whole-Genome Sequencing of Bacterial Pathogens: The Future of Nosocomial Outbreak Analysis. *Clinical Microbiology Reviews*, 30(4), 1015–1063. <https://doi.org/10.1128/CMR.00016-17>
- Quick, J., Quinlan, A. R., & Loman, N. J. (2014). A reference bacterial genome dataset generated on the MinION™ portable single-molecule nanopore sequencer. *GigaScience*, 3, 22. <https://doi.org/10.1186/2047-217X-3-22>
- Rang, F. J., Kloosterman, W. P., & de Ridder, J. (2018). From squiggle to basepair: Computational approaches for improving nanopore sequencing read accuracy. *Genome Biology*, 19(1), 90. <https://doi.org/10.1186/s13059-018-1462-9>
- Rhoads, A., & Au, K. F. (2015). PacBio Sequencing and Its Applications. *Genomics, Proteomics & Bioinformatics*, 13(5), 278–289. <https://doi.org/10.1016/j.gpb.2015.08.002>
- Salcedo, A., Rutter, W., Wang, S., Akhunova, A., Bolus, S., Chao, S., Anderson, N., Soto, M. F. D., Rouse, M., Szabo, L., Bowden, R. L., Dubcovsky, J., & Akhunov, E. (2017). Variation in the AvrSr35 gene determines Sr35 resistance against wheat stem rust race Ug99. *Science*, 358(6370), 1604–1606. <https://doi.org/10.1126/science.aao7294>
- Schwessinger, B., & McDonald, M. (2017). *High quality DNA from Fungi for long read sequencing e.g. PacBio, Nanopore MinION*. <https://doi.org/10.17504/protocols.io.k6qczdww>
- Simão, F. A., Waterhouse, R. M., Ioannidis, P., Kriventseva, E. V., & Zdobnov, E. M. (2015). BUSCO: Assessing genome assembly and annotation completeness with single-copy orthologs. *Bioinformatics (Oxford, England)*, 31(19), 3210–3212. <https://doi.org/10.1093/bioinformatics/btv351>
- Spatafora, J. W., Aime, M. C., Grigoriev, I. V., Martin, F., Stajich, J. E., & Blackwell, M. (2017). The Fungal Tree of Life: From Molecular Systematics to Genome-Scale Phylogenies. *The Fungal Kingdom*, 3–34. <https://doi.org/10.1128/microbiolspec.FUNK-0053-2016>
- van Steensel, B., & Dekker, J. (2010). Genomics tools for unraveling chromosome architecture. *Nature Biotechnology*, 28(10), 1089–1095. <https://doi.org/10.1038/nbt.1680>
- Walker, B. J., Abeel, T., Shea, T., Priest, M., Abouelliel, A., Sakthikumar, S., Cuomo, C. A., Zeng, Q., Wortman, J., Young, S. K., & Earl, A. M. (2014). Pilon: An Integrated Tool for Comprehensive Microbial Variant Detection and Genome Assembly Improvement. *PLoS ONE*, 9(11), e112963. <https://doi.org/10.1371/journal.pone.0112963>
- Webb, C. A., Szabo, L. J., Bakkeren, G., Garry, C., Staples, R. C., Eversmeyer, M., & Fellers, J. P. (2006). Transient expression and insertional mutagenesis of *Puccinia triticina* using

biolistics. *Functional & Integrative Genomics*, 6(3), 250–260.
<https://doi.org/10.1007/s10142-005-0009-9>

- Wenger, A. M., Peluso, P., Rowell, W. J., Chang, P.-C., Hall, R. J., Concepcion, G. T., Ebler, J., Fungtammasan, A., Kolesnikov, A., Olson, N. D., Töpfer, A., Alonge, M., Mahmoud, M., Qian, Y., Chin, C.-S., Phillippy, A. M., Schatz, M. C., Myers, G., DePristo, M. A., ... Hunkapiller, M. W. (2019). Accurate circular consensus long-read sequencing improves variant detection and assembly of a human genome. *Nature Biotechnology*, 37(10), 1155–1162. <https://doi.org/10.1038/s41587-019-0217-9>
- Weirather, J. L., de Cesare, M., Wang, Y., Piazza, P., Sebastiano, V., Wang, X.-J., Buck, D., & Au, K. F. (2017). Comprehensive comparison of Pacific Biosciences and Oxford Nanopore Technologies and their applications to transcriptome analysis. *F1000Research*, 6. <https://doi.org/10.12688/f1000research.10571.2>
- Zhang, A., Li, S., Apone, L., Sun, X., Chen, L., Ettwiller, L. M., Langhorst, B. W., Noren, C. J., & Xu, M.-Q. (2018). Solid-phase enzyme catalysis of DNA end repair and 3' A-tailing reduces GC-bias in next-generation sequencing of human genomic DNA. *Scientific Reports*, 8(1), 15887. <https://doi.org/10.1038/s41598-018-34079-2>

Chapter 4 - Conclusions

This work provides better understanding of the evolutionary processes involved in the origin of *Sr35*-virulent *Pgt* isolates. Using the allelic variants of the *AvrSr35* gene from *Sr35*-virulent and *Sr35*-avirulent *Pgt* isolates (Salcedo et al., 2017), we showed that amino acid changes at a limited number of sites could also contribute to the origin of *Pgt* isolates virulent of *Sr35*. By comparing amino acid sequences of virulent and avirulent isolates we identified three amino acid changes sites (E240K, K559D-N, and R569H in the race QTHJC (Figure 2.2, B)) that are likely linked with *Sr35*-virulence. We speculate that these three variable sites are likely involved in interaction between *AvrSr35* and *Sr35*. Further studies are warranted to validate the effects of mutations at these sites on *AvrSr35*-*Sr35* interaction.

The ability of *Sr35* gene variants from *T. monococcum* to recognize different allelic variants of *AvrSr35* and trigger immune response (cell death) was studied *in planta* using homologous and heterologous transient expression systems: (1) agroinfiltration into *N. benthamiana* leaves, and (2) the transformation of the wheat protoplasts. The *N. benthamiana* transient expression assay supported our hypothesis that *Sr35*-virulence of the QTHJC race of *Pgt* is likely associated with the reduced ability of *Sr35* to trigger HR. However, the transformation of wheat protoplasts showed contradicting results, where the QTHJC race variant of *AvrSr35* showed HR response similar to that induced by the RKQQC race variant of *AvrSr35* used as a positive control (Table 2.2). There are several hypotheses that could explain these results. One possibility is associated with the presence of some factors in the homologous expression system (wheat protoplasts) that affect recognition by *Sr35*, whereas no such factors are present in *N. benthamiana* (Figure 2.6, Model 1). An alternative explanation is associated with the inability of the transient expression assay in the wheat protoplasts to effectively separate true HR response from the background

noise due to high levels of variation in fluorescence signal intensity from sample to sample. There could also be a paralog in QTHJC for the *AvrSr35* variant that causes it to act differently than we've observed in this study. One way to improve the wheat protoplast experiment would be to create new constructs utilizing the luciferase complementation imaging assay (Chen et al., 2008; Fujikawa & Kato, 2007; Li et al., 2011). Another way to develop this experiment would be to utilize wheat protoplasts that naturally contain *Sr35* and use constructs with only *AvrSr35* alleles for transformation. The effect of mutations in the *AvrSr35* variant from the QTHJC race on its interaction with *Sr35* could be also studied by co-immunoprecipitation of the *Sr35-AvrSr35* protein complexes, utilizing the yeast two-hybrid system or applying bi-molecular complementation assay (Section 1.10).

In addition to studying *Sr35-AvrSr35* interaction, another goal of this thesis was to develop a high-quality reference genome of an American isolate of *Pgt*. We completed the assembly of the RKQQC race's reference genome using data produced by ONT and Illumina technologies. Our assembly contained 1,166 contigs ranging from 1,020 bp to 5,536,814 bp with the total length of 180,987,563 bp and an N50 value of 1,345,248 bp (Table 3.2). Sequences for the assembly as well as a more detailed analysis of this reference genome are forthcoming (unpublished).

Appendix

Appendix A: Results from Tukey Post Hoc Test of pair-wise comparisons of normalized protoplast absorbance throughout various time points discussed in Chapter 2.

Variant Comparison	HPI	Diff.	Adjusted p-value	Sig.	LCL	UCL
69SD657C-V1 - 69SD657C-V2	0.5	0.00632382	1		-0.1348714	0.14751906
69SD657C-V1 - 69SD657C-V3	0.5	0.0088109	1		-0.1323843	0.15000615
69SD657C-V1 - 9YS	0.5	0.07511134	0.8632		-0.0660839	0.21630659
69SD657C-V1 - AvrSr35	0.5	0.06844494	0.9263		-0.0727503	0.20964018
69SD657C-V1 - AvrSr35-Q72	0.5	0.03657853	0.9998		-0.1046167	0.17777378
69SD657C-V1 - QTHJC	0.5	0.04610896	0.9976		-0.0950863	0.18730421
69SD657C-V1 - RCRSC	0.5	0.04385244	0.9985		-0.0973428	0.18504769
69SD657C-V1 - TTKSF	0.5	-0.0069276	1		-0.1481228	0.13426766
69SD657C-V1 - TTKSK	0.5	-0.0228053	1		-0.1640006	0.11838994
69SD657C-V1 - TTKSP	0.5	-0.0463358	0.9975		-0.187531	0.09485945
69SD657C-V1 - TTKST	0.5	0.00481477	1		-0.1363805	0.14601002
69SD657C-V1 - TTTSK	0.5	0.0329602	0.9999		-0.108235	0.17415545
69SD657C-V1 - Water	0.5	0.09944042	0.4799		-0.0417548	0.24063566
69SD657C-V2 - 69SD657C-V3	0.5	0.00248709	1		-0.1387082	0.14368233
69SD657C-V2 - 9YS	0.5	0.06878753	0.9236		-0.0724077	0.20998277
69SD657C-V2 - AvrSr35	0.5	0.06212112	0.9644		-0.0790741	0.20331636
69SD657C-V2 - AvrSr35-Q72	0.5	0.03025472	1		-0.1109405	0.17144996
69SD657C-V2 - QTHJC	0.5	0.03978515	0.9995		-0.1014101	0.18098039
69SD657C-V2 - RCRSC	0.5	0.03752863	0.9997		-0.1036666	0.17872387
69SD657C-V2 - TTKSF	0.5	-0.0132514	1		-0.1544466	0.12794384
69SD657C-V2 - TTKSK	0.5	-0.0291291	1		-0.1703244	0.11206612
69SD657C-V2 - TTKSP	0.5	-0.0526596	0.9913		-0.1938549	0.08853563
69SD657C-V2 - TTKST	0.5	-0.001509	1		-0.1427043	0.1396862
69SD657C-V2 - TTTSK	0.5	0.02663639	1		-0.1145589	0.16783163
69SD657C-V2 - Water	0.5	0.0931166	0.5902		-0.0480786	0.23431184
69SD657C-V3 - 9YS	0.5	0.06630044	0.9414		-0.0748948	0.20749568
69SD657C-V3 - AvrSr35	0.5	0.05963403	0.9744		-0.0815612	0.20082928
69SD657C-V3 - AvrSr35-Q72	0.5	0.02776763	1		-0.1134276	0.16896287
69SD657C-V3 - QTHJC	0.5	0.03729806	0.9997		-0.1038972	0.17849331
69SD657C-V3 - RCRSC	0.5	0.03504154	0.9999		-0.1061537	0.17623678
69SD657C-V3 - TTKSF	0.5	-0.0157385	1		-0.1569337	0.12545675
69SD657C-V3 - TTKSK	0.5	-0.0316162	1		-0.1728115	0.10957903
69SD657C-V3 - TTKSP	0.5	-0.0551467	0.9869		-0.1963419	0.08604854

69SD657C-V3 - TTKST	0.5	-0.0039961	1		-0.1451914	0.13719911
69SD657C-V3 - TTTSK	0.5	0.0241493	1		-0.1170459	0.16534454
69SD657C-V3 - Water	0.5	0.09062951	0.6334		-0.0505657	0.23182476
9YS - AvrSr35	0.5	-0.0066664	1		-0.1478616	0.13452884
9YS - AvrSr35-Q72	0.5	-0.0385328	0.9996		-0.1797281	0.10266243
9YS - QTHJC	0.5	-0.0290024	1		-0.1701976	0.11219287
9YS - RCRSC	0.5	-0.0312589	1		-0.1724541	0.10993634
9YS - TTKSF	0.5	-0.0820389	0.7725		-0.2232342	0.05915631
9YS - TTKSK	0.5	-0.0979167	0.5062		-0.2391119	0.04327859
9YS - TTKSP	0.5	-0.1214471	0.1744		-0.2626424	0.0197481
9YS - TTKST	0.5	-0.0702966	0.9112		-0.2114918	0.07089867
9YS - TTTSK	0.5	-0.0421511	0.999		-0.1833464	0.0990441
9YS - Water	0.5	0.02432907	1		-0.1168662	0.16552432
AvrSr35 - AvrSr35-Q72	0.5	-0.0318664	1		-0.1730616	0.10932884
AvrSr35 - QTHJC	0.5	-0.022336	1		-0.1635312	0.11885927
AvrSr35 - RCRSC	0.5	-0.0245925	1		-0.1657877	0.11660275
AvrSr35 - TTKSF	0.5	-0.0753725	0.8602		-0.2165678	0.06582272
AvrSr35 - TTKSK	0.5	-0.0912502	0.6227		-0.2324455	0.049945
AvrSr35 - TTKSP	0.5	-0.1147807	0.2481		-0.255976	0.02641451
AvrSr35 - TTKST	0.5	-0.0636302	0.9571		-0.2048254	0.07756508
AvrSr35 - TTTSK	0.5	-0.0354847	0.9998		-0.17668	0.10571051
AvrSr35 - Water	0.5	0.03099548	1		-0.1101998	0.17219072
AvrSr35-Q72 - QTHJC	0.5	0.00953043	1		-0.1316648	0.15072567
AvrSr35-Q72 - RCRSC	0.5	0.00727391	1		-0.1339213	0.14846915
AvrSr35-Q72 - TTKSF	0.5	-0.0435061	0.9986		-0.1847014	0.09768912
AvrSr35-Q72 - TTKSK	0.5	-0.0593838	0.9753		-0.2005791	0.0818114
AvrSr35-Q72 - TTKSP	0.5	-0.0829143	0.7594		-0.2241096	0.05828091
AvrSr35-Q72 - TTKST	0.5	-0.0317638	1		-0.172959	0.10943148
AvrSr35-Q72 - TTTSK	0.5	-0.0036183	1		-0.1448136	0.13757691
AvrSr35-Q72 - Water	0.5	0.06286188	0.9609		-0.0783334	0.20405713
QTHJC - RCRSC	0.5	-0.0022565	1		-0.1434518	0.13893872
QTHJC - TTKSF	0.5	-0.0530366	0.9908		-0.1942318	0.08815869
QTHJC - TTKSK	0.5	-0.0689143	0.9226		-0.2101095	0.07228097
QTHJC - TTKSP	0.5	-0.0924448	0.6019		-0.23364	0.04875048
QTHJC - TTKST	0.5	-0.0412942	0.9992		-0.1824894	0.09990105
QTHJC - TTTSK	0.5	-0.0131488	1		-0.154344	0.12804648
QTHJC - Water	0.5	0.05333145	0.9903		-0.0878638	0.1945267
RCRSC - TTKSF	0.5	-0.05078	0.9938		-0.1919753	0.09041521
RCRSC - TTKSK	0.5	-0.0666578	0.9391		-0.207853	0.07453749

RCRSC - TTKSP	0.5	-0.0901882	0.641		-0.2313835	0.051007
RCRSC - TTKST	0.5	-0.0390377	0.9996		-0.1802329	0.10215757
RCRSC - TTTSK	0.5	-0.0108922	1		-0.1520875	0.130303
RCRSC - Water	0.5	0.05558797	0.9859		-0.0856073	0.19678322
TTKSF - TTKSK	0.5	-0.0158777	1		-0.157073	0.12531752
TTKSF - TTKSP	0.5	-0.0394082	0.9995		-0.1806035	0.10178703
TTKSF - TTKST	0.5	0.01174236	1		-0.1294529	0.1529376
TTKSF - TTTSK	0.5	0.03988779	0.9995		-0.1013075	0.18108303
TTKSF - Water	0.5	0.10636801	0.366		-0.0348272	0.24756325
TTKSK - TTKSP	0.5	-0.0235305	1		-0.1647257	0.11766475
TTKSK - TTKST	0.5	0.02762008	1		-0.1135752	0.16881532
TTKSK - TTTSK	0.5	0.05576551	0.9855		-0.0854297	0.19696075
TTKSK - Water	0.5	0.12224573	0.1668		-0.0189495	0.26344097
TTKSP - TTKST	0.5	0.05115057	0.9934		-0.0900447	0.19234581
TTKSP - TTTSK	0.5	0.079296	0.8112		-0.0618992	0.22049124
TTKSP - Water	0.5	0.14577621	0.036	*	0.00458097	0.28697146
TTKST - TTTSK	0.5	0.02814543	1		-0.1130498	0.16934067
TTKST - Water	0.5	0.09462564	0.5638		-0.0465696	0.23582089
TTTSK - Water	0.5	0.06648022	0.9402		-0.074715	0.20767546
69SD657C-V1 - 69SD657C-V2	12	0.24755671	0.1897		-0.0439218	0.53903519
69SD657C-V1 - 69SD657C-V3	12	-0.3115817	0.0244	*	-0.6030602	-0.0201033
69SD657C-V1 - 9YS	12	0.27922733	0.075	.	-0.0122511	0.5707058
69SD657C-V1 - AvrSr35	12	0.33259121	0.0109	*	0.04111273	0.62406968
69SD657C-V1 - AvrSr35-Q72	12	0.03154493	1		-0.2599335	0.32302341
69SD657C-V1 - QTHJC	12	0.29209976	0.049	*	0.00062128	0.58357823
69SD657C-V1 - RCRSC	12	0.0385933	1		-0.2528852	0.33007177
69SD657C-V1 - TTKSF	12	0.37786095	0.0016	**	0.08638248	0.66933943
69SD657C-V1 - TTKSK	12	0.34953607	0.0054	**	0.05805759	0.64101454
69SD657C-V1 - TTKSP	12	0.1727681	0.7476		-0.1187104	0.46424658
69SD657C-V1 - TTKST	12	0.23903749	0.2358		-0.052441	0.53051597
69SD657C-V1 - TTTSK	12	0.33556631	0.0096	**	0.04408783	0.62704478
69SD657C-V1 - Water	12	0.62865051	0	***	0.33717203	0.92012898
69SD657C-V2 - 69SD657C-V3	12	-0.5591385	0	***	-0.8506169	-0.26766
69SD657C-V2 - 9YS	12	0.03167062	1		-0.2598079	0.32314909
69SD657C-V2 - AvrSr35	12	0.0850345	0.9992		-0.206444	0.37651297
69SD657C-V2 - AvrSr35-Q72	12	-0.2160118	0.3933		-0.5074903	0.0754667
69SD657C-V2 - QTHJC	12	0.04454305	1		-0.2469354	0.33602152
69SD657C-V2 - RCRSC	12	-0.2089634	0.4495		-0.5004419	0.08251506
69SD657C-V2 - TTKSF	12	0.13030424	0.9597		-0.1611742	0.42178272

69SD657C-V2 - TTKSK	12	0.10197936	0.9952		-0.1894991	0.39345783
69SD657C-V2 - TTKSP	12	-0.0747886	0.9998		-0.3662671	0.21668987
69SD657C-V2 - TTKST	12	-0.0085192	1		-0.2999977	0.28295926
69SD657C-V2 - TTTSK	12	0.0880096	0.9989		-0.2034689	0.37948807
69SD657C-V2 - Water	12	0.3810938	0.0014	**	0.08961532	0.67257227
69SD657C-V3 - 9YS	12	0.59080908	0	***	0.2993306	0.88228755
69SD657C-V3 - AvrSr35	12	0.64417295	0	***	0.35269448	0.93565143
69SD657C-V3 - AvrSr35-Q72	12	0.34312668	0.0071	**	0.05164821	0.63460516
69SD657C-V3 - QTHJC	12	0.60368151	0	***	0.31220303	0.89515998
69SD657C-V3 - RCRSC	12	0.35017505	0.0053	**	0.05869657	0.64165352
69SD657C-V3 - TTKSF	12	0.6894427	0	***	0.39796423	0.98092118
69SD657C-V3 - TTKSK	12	0.66111781	0	***	0.36963934	0.95259629
69SD657C-V3 - TTKSP	12	0.48434985	0	***	0.19287138	0.77582833
69SD657C-V3 - TTKST	12	0.55061924	0	***	0.25914077	0.84209772
69SD657C-V3 - TTTSK	12	0.64714806	0	***	0.35566958	0.93862653
69SD657C-V3 - Water	12	0.94023226	0	***	0.64875378	1.23171073
9YS - AvrSr35	12	0.05336388	1		-0.2381146	0.34484235
9YS - AvrSr35-Q72	12	-0.2476824	0.1891		-0.5391609	0.04379608
9YS - QTHJC	12	0.01287243	1		-0.278606	0.30435091
9YS - RCRSC	12	-0.240634	0.2266		-0.5321125	0.05084445
9YS - TTKSF	12	0.09863363	0.9966		-0.1928449	0.3901121
9YS - TTKSK	12	0.07030874	0.9999		-0.2211697	0.36178721
9YS - TTKSP	12	-0.1064592	0.9929		-0.3979377	0.18501925
9YS - TTKST	12	-0.0401898	1		-0.3316683	0.25128864
9YS - TTTSK	12	0.05633898	1		-0.2351395	0.34781746
9YS - Water	12	0.34942318	0.0054	**	0.05794471	0.64090166
AvrSr35 - AvrSr35-Q72	12	-0.3010463	0.0358	*	-0.5925247	-0.0095678
AvrSr35 - QTHJC	12	-0.0404914	1		-0.3319699	0.25098703
AvrSr35 - RCRSC	12	-0.2939979	0.0459	*	-0.5854764	-0.0025194
AvrSr35 - TTKSF	12	0.04526975	1		-0.2462087	0.33674822
AvrSr35 - TTKSK	12	0.01694486	1		-0.2745336	0.30842333
AvrSr35 - TTKSP	12	-0.1598231	0.8356		-0.4513016	0.13165537
AvrSr35 - TTKST	12	-0.0935537	0.998		-0.3850322	0.19792476
AvrSr35 - TTTSK	12	0.0029751	1		-0.2885034	0.29445358
AvrSr35 - Water	12	0.2960593	0.0427	*	0.00458083	0.58753778
AvrSr35-Q72 - QTHJC	12	0.26055483	0.1325		-0.0309237	0.5520333
AvrSr35-Q72 - RCRSC	12	0.00704837	1		-0.2844301	0.29852684
AvrSr35-Q72 - TTKSF	12	0.34631602	0.0062	**	0.05483755	0.6377945
AvrSr35-Q72 - TTKSK	12	0.31799113	0.0192	*	0.02651266	0.60946961

AvrSr35-Q72 - TTKSP	12	0.14122317	0.9265		-0.1502553	0.43270164
AvrSr35-Q72 - TTKST	12	0.20749256	0.4616		-0.0839859	0.49897104
AvrSr35-Q72 - TTTSK	12	0.30402138	0.0322	*	0.0125429	0.59549985
AvrSr35-Q72 - Water	12	0.59710558	0	***	0.3056271	0.88858405
QTHJC - RCRSC	12	-0.2535065	0.1616		-0.5449849	0.03797202
QTHJC - TTKSF	12	0.0857612	0.9992		-0.2057173	0.37723967
QTHJC - TTKSK	12	0.05743631	1		-0.2340422	0.34891478
QTHJC - TTKSP	12	-0.1193317	0.9803		-0.4108101	0.17214682
QTHJC - TTKST	12	-0.0530623	1		-0.3445407	0.23841621
QTHJC - TTTSK	12	0.04346655	1		-0.2480119	0.33494503
QTHJC - Water	12	0.33655075	0.0093	**	0.04507228	0.62802923
RCRSC - TTKSF	12	0.33926766	0.0083	**	0.04778918	0.63074613
RCRSC - TTKSK	12	0.31094277	0.025	*	0.01946429	0.60242124
RCRSC - TTKSP	12	0.1341748	0.9495		-0.1573037	0.42565328
RCRSC - TTKST	12	0.2004442	0.5205		-0.0910343	0.49192267
RCRSC - TTTSK	12	0.29697301	0.0414	*	0.00549454	0.58845149
RCRSC - Water	12	0.59005721	0	***	0.29857873	0.88153568
TTKSF - TTKSK	12	-0.0283249	1		-0.3198034	0.26315359
TTKSF - TTKSP	12	-0.2050929	0.4815		-0.4965713	0.08638562
TTKSF - TTKST	12	-0.1388235	0.935		-0.4303019	0.15265502
TTKSF - TTTSK	12	-0.0422946	1		-0.3337731	0.24918383
TTKSF - Water	12	0.25078956	0.1741		-0.0406889	0.54226803
TTKSK - TTKSP	12	-0.176768	0.7171		-0.4682464	0.11471051
TTKSK - TTKST	12	-0.1104986	0.99		-0.401977	0.1809799
TTKSK - TTTSK	12	-0.0139698	1		-0.3054482	0.27750872
TTKSK - Water	12	0.27911444	0.0753	.	-0.012364	0.57059292
TTKSP - TTKST	12	0.06626939	1		-0.2252091	0.35774787
TTKSP - TTTSK	12	0.16279821	0.817		-0.1286803	0.45427668
TTKSP - Water	12	0.45588241	0	***	0.16440393	0.74736088
TTKST - TTTSK	12	0.09652881	0.9972		-0.1949497	0.38800729
TTKST - Water	12	0.38961301	9.00E-04	***	0.09813454	0.68109149
TTTSK - Water	12	0.2930842	0.0473	*	0.00160572	0.58456268
69SD657C-V1 - 69SD657C-V2	16	0.43023677	0.0402	*	0.0091078	0.85136575
69SD657C-V1 - 69SD657C-V3	16	-0.4191444	0.0524	.	-0.8402734	0.00198459
69SD657C-V1 - 9YS	16	0.45016919	0.0244	*	0.02904022	0.87129817
69SD657C-V1 - AvrSr35	16	0.51396312	0.0042	**	0.09283415	0.93509209
69SD657C-V1 - AvrSr35-Q72	16	0.06950576	1		-0.3516232	0.49063474
69SD657C-V1 - QTHJC	16	0.48291473	0.0102	*	0.06178575	0.9040437
69SD657C-V1 - RCRSC	16	0.10914508	0.9998		-0.3119839	0.53027406

69SD657C-V1 - TTKSF	16	0.64042595	1.00E-04	***	0.21929698	1.06155493
69SD657C-V1 - TTKSK	16	0.6326842	1.00E-04	***	0.21155523	1.05381317
69SD657C-V1 - TTKSP	16	0.29930678	0.4643		-0.1218222	0.72043575
69SD657C-V1 - TTKST	16	0.43590261	0.035	*	0.01477364	0.85703159
69SD657C-V1 - TTTSK	16	0.56698816	8.00E-04	***	0.14585919	0.98811714
69SD657C-V1 - Water	16	0.98263721	0	***	0.56150823	1.40376618
69SD657C-V2 - 69SD657C-V3	16	-0.8493812	0	***	-1.2705101	-0.4282522
69SD657C-V2 - 9YS	16	0.01993242	1		-0.4011966	0.44106139
69SD657C-V2 - AvrSr35	16	0.08372635	1		-0.3374026	0.50485532
69SD657C-V2 - AvrSr35-Q72	16	-0.360731	0.1793		-0.78186	0.06039796
69SD657C-V2 - QTHJC	16	0.05267795	1		-0.368451	0.47380693
69SD657C-V2 - RCRSC	16	-0.3210917	0.3463		-0.7422207	0.10003728
69SD657C-V2 - TTKSF	16	0.21018918	0.9097		-0.2109398	0.63131815
69SD657C-V2 - TTKSK	16	0.20244743	0.9305		-0.2186815	0.6235764
69SD657C-V2 - TTKSP	16	-0.13093	0.9985		-0.552059	0.29019898
69SD657C-V2 - TTKST	16	0.00566584	1		-0.4154631	0.42679481
69SD657C-V2 - TTTSK	16	0.13675139	0.9977		-0.2843776	0.55788036
69SD657C-V2 - Water	16	0.55240043	0.0013	**	0.13127146	0.97352941
69SD657C-V3 - 9YS	16	0.86931358	0	***	0.4481846	1.29044255
69SD657C-V3 - AvrSr35	16	0.9331075	0	***	0.51197853	1.35423648
69SD657C-V3 - AvrSr35-Q72	16	0.48865015	0.0087	**	0.06752118	0.90977912
69SD657C-V3 - QTHJC	16	0.90205911	0	***	0.48093014	1.32318808
69SD657C-V3 - RCRSC	16	0.52828947	0.0027	**	0.10716049	0.94941844
69SD657C-V3 - TTKSF	16	1.05957034	0	***	0.63844137	1.48069931
69SD657C-V3 - TTKSK	16	1.05182859	0	***	0.63069961	1.47295756
69SD657C-V3 - TTKSP	16	0.71845116	0	***	0.29732219	1.13958014
69SD657C-V3 - TTKST	16	0.855047	0	***	0.43391802	1.27617597
69SD657C-V3 - TTTSK	16	0.98613255	0	***	0.56500358	1.40726152
69SD657C-V3 - Water	16	1.40178159	0	***	0.98065262	1.82291056
9YS - AvrSr35	16	0.06379393	1		-0.357335	0.4849229
9YS - AvrSr35-Q72	16	-0.3806634	0.1218		-0.8017924	0.04046555
9YS - QTHJC	16	0.03274553	1		-0.3883834	0.45387451
9YS - RCRSC	16	-0.3410241	0.2536		-0.7621531	0.08010487
9YS - TTKSF	16	0.19025676	0.9562		-0.2308722	0.61138574
9YS - TTKSK	16	0.18251501	0.9684		-0.238614	0.60364398
9YS - TTKSP	16	-0.1508624	0.994		-0.5719914	0.27026656
9YS - TTKST	16	-0.0142666	1		-0.4353956	0.4068624
9YS - TTTSK	16	0.11681897	0.9996		-0.30431	0.53794795
9YS - Water	16	0.53246802	0.0024	**	0.11133904	0.95359699

AvrSr35 - AvrSr35-Q72	16	-0.4444574	0.0283	*	-0.8655863	-0.0233284
AvrSr35 - QTHJC	16	-0.0310484	1		-0.4521774	0.39008058
AvrSr35 - RCRSC	16	-0.404818	0.0727	.	-0.825947	0.01631094
AvrSr35 - TTKSF	16	0.12646283	0.999		-0.2946661	0.54759181
AvrSr35 - TTKSK	16	0.11872108	0.9995		-0.3024079	0.53985005
AvrSr35 - TTKSP	16	-0.2146563	0.896		-0.6357853	0.20647263
AvrSr35 - TTKST	16	-0.0780605	1		-0.4991895	0.34306847
AvrSr35 - TTTSK	16	0.05302505	1		-0.3681039	0.47415402
AvrSr35 - Water	16	0.46867409	0.015	*	0.04754511	0.88980306
AvrSr35-Q72 - QTHJC	16	0.41340896	0.0599	.	-0.00772	0.83453793
AvrSr35-Q72 - RCRSC	16	0.03963932	1		-0.3814897	0.46076829
AvrSr35-Q72 - TTKSF	16	0.57092019	7.00E-04	***	0.14979122	0.99204916
AvrSr35-Q72 - TTKSK	16	0.56317844	9.00E-04	***	0.14204946	0.98430741
AvrSr35-Q72 - TTKSP	16	0.22980101	0.8403		-0.191328	0.65092999
AvrSr35-Q72 - TTKST	16	0.36639685	0.1612		-0.0547321	0.78752582
AvrSr35-Q72 - TTTSK	16	0.4974824	0.0067	**	0.07635343	0.91861137
AvrSr35-Q72 - Water	16	0.91313144	0	***	0.49200247	1.33426042
QTHJC - RCRSC	16	-0.3737696	0.1398		-0.7948986	0.04735933
QTHJC - TTKSF	16	0.15751123	0.9911		-0.2636177	0.5786402
QTHJC - TTKSK	16	0.14976948	0.9944		-0.2713595	0.57089845
QTHJC - TTKSP	16	-0.1836079	0.9669		-0.6047369	0.23752103
QTHJC - TTKST	16	-0.0470121	1		-0.4681411	0.37411686
QTHJC - TTTSK	16	0.08407344	1		-0.3370555	0.50520241
QTHJC - Water	16	0.49972248	0.0063	**	0.07859351	0.92085145
RCRSC - TTKSF	16	0.53128087	0.0025	**	0.1101519	0.95240984
RCRSC - TTKSK	16	0.52353912	0.0031	**	0.10241014	0.94466809
RCRSC - TTKSP	16	0.1901617	0.9564		-0.2309673	0.61129067
RCRSC - TTKST	16	0.32675753	0.3183		-0.0943714	0.7478865
RCRSC - TTTSK	16	0.45784308	0.02	*	0.03671411	0.87897205
RCRSC - Water	16	0.87349212	0	***	0.45236315	1.2946211
TTKSF - TTKSK	16	-0.0077418	1		-0.4288707	0.41338722
TTKSF - TTKSP	16	-0.3411192	0.2532		-0.7622481	0.0800098
TTKSF - TTKST	16	-0.2045233	0.9253		-0.6256523	0.21660563
TTKSF - TTTSK	16	-0.0734378	1		-0.4945668	0.34769118
TTKSF - Water	16	0.34221125	0.2487		-0.0789177	0.76334023
TTKSK - TTKSP	16	-0.3333774	0.2872		-0.7545064	0.08775155
TTKSK - TTKST	16	-0.1967816	0.9435		-0.6179106	0.22434739
TTKSK - TTTSK	16	-0.065696	1		-0.486825	0.35543294
TTKSK - Water	16	0.34995301	0.2178		-0.071176	0.77108198

TTKSP - TTKST	16	0.13659584	0.9977		-0.2845331	0.55772481
TTKSP - TTTSK	16	0.26768139	0.6486		-0.1534476	0.68881036
TTKSP - Water	16	0.68333043	0	***	0.26220145	1.1044594
TTKST - TTTSK	16	0.13108555	0.9985		-0.2900434	0.55221452
TTKST - Water	16	0.54673459	0.0015	**	0.12560562	0.96786357
TTTSK - Water	16	0.41564904	0.0568	.	-0.0054799	0.83677802
69SD657C-V1 - 69SD657C-V2	20	0.54859702	0.0358	*	0.01748061	1.07971343
69SD657C-V1 - 69SD657C-V3	20	-0.6451894	0.0045	**	-1.1763058	-0.114073
69SD657C-V1 - 9YS	20	0.53148145	0.0497	*	0.00036504	1.06259786
69SD657C-V1 - AvrSr35	20	0.59831725	0.0129	*	0.06720084	1.12943366
69SD657C-V1 - AvrSr35-Q72	20	-0.0668233	1		-0.5979398	0.46429306
69SD657C-V1 - QTHJC	20	0.60180629	0.0119	*	0.07068988	1.1329227
69SD657C-V1 - RCRSC	20	0.05521339	1		-0.475903	0.5863298
69SD657C-V1 - TTKSF	20	0.78529956	1.00E-04	***	0.25418315	1.31641598
69SD657C-V1 - TTKSK	20	0.8199027	0	***	0.28878629	1.35101911
69SD657C-V1 - TTKSP	20	0.4045223	0.3481		-0.1265941	0.93563871
69SD657C-V1 - TTKST	20	0.52124237	0.06	.	-0.009874	1.05235878
69SD657C-V1 - TTTSK	20	0.70385852	0.0011	**	0.17274211	1.23497493
69SD657C-V1 - Water	20	1.22817605	0	***	0.69705964	1.75929246
69SD657C-V2 - 69SD657C-V3	20	-1.1937864	0	***	-1.7249028	-0.66267
69SD657C-V2 - 9YS	20	-0.0171156	1		-0.548232	0.51400084
69SD657C-V2 - AvrSr35	20	0.04972024	1		-0.4813962	0.58083665
69SD657C-V2 - AvrSr35-Q72	20	-0.6154204	0.0088	**	-1.1465368	-0.084304
69SD657C-V2 - QTHJC	20	0.05320927	1		-0.4779071	0.58432568
69SD657C-V2 - RCRSC	20	-0.4933836	0.0978	.	-1.0245	0.03773278
69SD657C-V2 - TTKSF	20	0.23670255	0.9606		-0.2944139	0.76781896
69SD657C-V2 - TTKSK	20	0.27130569	0.8945		-0.2598107	0.8024221
69SD657C-V2 - TTKSP	20	-0.1440747	0.9996		-0.6751911	0.3870417
69SD657C-V2 - TTKST	20	-0.0273547	1		-0.5584711	0.50376176
69SD657C-V2 - TTTSK	20	0.15526151	0.9992		-0.3758549	0.68637792
69SD657C-V2 - Water	20	0.67957904	0.002	**	0.14846263	1.21069545
69SD657C-V3 - 9YS	20	1.17667087	0	***	0.64555446	1.70778728
69SD657C-V3 - AvrSr35	20	1.24350667	0	***	0.71239026	1.77462308
69SD657C-V3 - AvrSr35-Q72	20	0.57836607	0.0196	*	0.04724966	1.10948248
69SD657C-V3 - QTHJC	20	1.2469957	0	***	0.71587929	1.77811211
69SD657C-V3 - RCRSC	20	0.70040281	0.0012	**	0.1692864	1.23151922
69SD657C-V3 - TTKSF	20	1.43048898	0	***	0.89937257	1.96160539
69SD657C-V3 - TTKSK	20	1.46509212	0	***	0.93397571	1.99620853
69SD657C-V3 - TTKSP	20	1.04971172	0	***	0.51859531	1.58082813

69SD657C-V3 - TTKST	20	1.16643178	0	***	0.63531537	1.69754819
69SD657C-V3 - TTTSK	20	1.34904794	0	***	0.81793153	1.88016435
69SD657C-V3 - Water	20	1.87336547	0	***	1.34224906	2.40448188
9YS - AvrSr35	20	0.06683581	1		-0.4642806	0.59795222
9YS - AvrSr35-Q72	20	-0.5983048	0.0129	*	-1.1294212	-0.0671884
9YS - QTHJC	20	0.07032484	1		-0.4607916	0.60144125
9YS - RCRSC	20	-0.4762681	0.1294		-1.0073845	0.05484835
9YS - TTKSF	20	0.25381812	0.9334		-0.2772983	0.78493453
9YS - TTKSK	20	0.28842125	0.8448		-0.2426952	0.81953766
9YS - TTKSP	20	-0.1269591	0.9999		-0.6580756	0.40415727
9YS - TTKST	20	-0.0102391	1		-0.5413555	0.52087733
9YS - TTTSK	20	0.17237708	0.9977		-0.3587393	0.70349349
9YS - Water	20	0.6966946	0.0013	**	0.16557819	1.22781101
AvrSr35 - AvrSr35-Q72	20	-0.6651406	0.0028	**	-1.196257	-0.1340242
AvrSr35 - QTHJC	20	0.00348903	1		-0.5276274	0.53460544
AvrSr35 - RCRSC	20	-0.5431039	0.0398	*	-1.0742203	-0.0119875
AvrSr35 - TTKSF	20	0.18698231	0.995		-0.3441341	0.71809872
AvrSr35 - TTKSK	20	0.22158545	0.9769		-0.309531	0.75270186
AvrSr35 - TTKSP	20	-0.193795	0.9929		-0.7249114	0.33732146
AvrSr35 - TTKST	20	-0.0770749	1		-0.6081913	0.45404152
AvrSr35 - TTTSK	20	0.10554127	1		-0.4255751	0.63665768
AvrSr35 - Water	20	0.6298588	0.0064	**	0.09874239	1.16097521
AvrSr35-Q72 - QTHJC	20	0.66862963	0.0026	**	0.13751322	1.19974604
AvrSr35-Q72 - RCRSC	20	0.12203674	0.9999		-0.4090797	0.65315315
AvrSr35-Q72 - TTKSF	20	0.85212291	0	***	0.3210065	1.38323932
AvrSr35-Q72 - TTKSK	20	0.88672605	0	***	0.35560964	1.41784246
AvrSr35-Q72 - TTKSP	20	0.47134565	0.1399		-0.0597708	1.00246206
AvrSr35-Q72 - TTKST	20	0.58806571	0.016	*	0.0569493	1.11918213
AvrSr35-Q72 - TTTSK	20	0.77068187	2.00E-04	***	0.23956546	1.30179828
AvrSr35-Q72 - Water	20	1.2949994	0	***	0.76388299	1.82611581
QTHJC - RCRSC	20	-0.5465929	0.0372	*	-1.0777093	-0.0154765
QTHJC - TTKSF	20	0.18349328	0.9958		-0.3476231	0.71460969
QTHJC - TTKSK	20	0.21809642	0.9798		-0.31302	0.74921283
QTHJC - TTKSP	20	-0.197284	0.9917		-0.7284004	0.33383243
QTHJC - TTKST	20	-0.0805639	1		-0.6116803	0.45055249
QTHJC - TTTSK	20	0.10205224	1		-0.4290642	0.63316865
QTHJC - Water	20	0.62636977	0.0069	**	0.09525336	1.15748618
RCRSC - TTKSF	20	0.73008618	5.00E-04	***	0.19896977	1.26120259
RCRSC - TTKSK	20	0.76468931	2.00E-04	***	0.2335729	1.29580572

RCRSC - TTKSP	20	0.34930892	0.5947		-0.1818075	0.88042533
RCRSC - TTKST	20	0.46602898	0.1519		-0.0650874	0.99714539
RCRSC - TTTSK	20	0.64864514	0.0041	**	0.11752873	1.17976155
RCRSC - Water	20	1.17296267	0	***	0.64184626	1.70407908
TTKSF - TTKSK	20	0.03460314	1		-0.4965133	0.56571955
TTKSF - TTKSP	20	-0.3807773	0.4495		-0.9118937	0.15033915
TTKSF - TTKST	20	-0.2640572	0.912		-0.7951736	0.26705921
TTKSF - TTTSK	20	-0.081441	1		-0.6125575	0.44967537
TTKSF - Water	20	0.44287649	0.2132		-0.0882399	0.9739929
TTKSK - TTKSP	20	-0.4153804	0.3058		-0.9464968	0.11573601
TTKSK - TTKST	20	-0.2986603	0.8098		-0.8297767	0.23245607
TTKSK - TTTSK	20	-0.1160442	1		-0.6471606	0.41507223
TTKSK - Water	20	0.40827335	0.3331		-0.1228431	0.93938976
TTKSP - TTKST	20	0.11672006	1		-0.4143963	0.64783647
TTKSP - TTTSK	20	0.29933622	0.8074		-0.2317802	0.83045263
TTKSP - Water	20	0.82365375	0	***	0.29253734	1.35477016
TTKST - TTTSK	20	0.18261616	0.996		-0.3485003	0.71373257
TTKST - Water	20	0.70693369	0.001	***	0.17581728	1.2380501
TTTSK - Water	20	0.52431753	0.0567	.	-0.0067989	1.05543394
69SD657C-V1 - 69SD657C-V2	24	0.57428715	0.135		-0.0697499	1.21832416
69SD657C-V1 - 69SD657C-V3	24	-0.8727568	7.00E-04	***	-1.5167938	-0.2287198
69SD657C-V1 - 9YS	24	0.46855139	0.4245		-0.1754856	1.11258839
69SD657C-V1 - AvrSr35	24	0.60611106	0.0876	.	-0.0379259	1.25014807
69SD657C-V1 - AvrSr35-Q72	24	-0.1680478	0.9998		-0.8120848	0.47598924
69SD657C-V1 - QTHJC	24	0.67543056	0.0303	*	0.03139356	1.31946757
69SD657C-V1 - RCRSC	24	0.09930974	1		-0.5447273	0.74334675
69SD657C-V1 - TTKSF	24	0.84907355	0.0012	**	0.20503654	1.49311056
69SD657C-V1 - TTKSK	24	0.84914609	0.0012	**	0.20510908	1.4931831
69SD657C-V1 - TTKSP	24	0.42525907	0.5882		-0.2187779	1.06929608
69SD657C-V1 - TTKST	24	0.53438057	0.2198		-0.1096564	1.17841758
69SD657C-V1 - TTTSK	24	0.75922692	0.0069	**	0.11518992	1.40326393
69SD657C-V1 - Water	24	1.37559414	0	***	0.73155713	2.01963115
69SD657C-V2 - 69SD657C-V3	24	-1.447044	0	***	-2.091081	-0.803007
69SD657C-V2 - 9YS	24	-0.1057358	1		-0.7497728	0.53830124
69SD657C-V2 - AvrSr35	24	0.03182391	1		-0.6122131	0.67586092
69SD657C-V2 - AvrSr35-Q72	24	-0.7423349	0.0095	**	-1.3863719	-0.0982979
69SD657C-V2 - QTHJC	24	0.10114341	1		-0.5428936	0.74518042
69SD657C-V2 - RCRSC	24	-0.4749774	0.4015		-1.1190144	0.16905959
69SD657C-V2 - TTKSF	24	0.2747864	0.9722		-0.3692506	0.9188234

69SD657C-V2 - TTKSK	24	0.27485894	0.9721		-0.3691781	0.91889595
69SD657C-V2 - TTKSP	24	-0.1490281	0.9999		-0.7930651	0.49500893
69SD657C-V2 - TTKST	24	-0.0399066	1		-0.6839436	0.60413042
69SD657C-V2 - TTTSK	24	0.18493977	0.9994		-0.4590972	0.82897678
69SD657C-V2 - Water	24	0.80130699	0.0031	**	0.15726998	1.445344
69SD657C-V3 - 9YS	24	1.34130823	0	***	0.69727122	1.98534523
69SD657C-V3 - AvrSr35	24	1.4788679	0	***	0.83483089	2.12290491
69SD657C-V3 - AvrSr35-Q72	24	0.70470907	0.0185	*	0.06067207	1.34874608
69SD657C-V3 - QTHJC	24	1.5481874	0	***	0.9041504	2.19222441
69SD657C-V3 - RCRSC	24	0.97206658	1.00E-04	***	0.32802957	1.61610358
69SD657C-V3 - TTKSF	24	1.72183039	0	***	1.07779338	2.36586739
69SD657C-V3 - TTKSK	24	1.72190293	0	***	1.07786592	2.36593994
69SD657C-V3 - TTKSP	24	1.29801591	0	***	0.6539789	1.94205292
69SD657C-V3 - TTKST	24	1.40713741	0	***	0.7631004	2.05117441
69SD657C-V3 - TTTSK	24	1.63198376	0	***	0.98794675	2.27602077
69SD657C-V3 - Water	24	2.24835098	0	***	1.60431397	2.89238799
9YS - AvrSr35	24	0.13755967	1		-0.5064773	0.78159668
9YS - AvrSr35-Q72	24	-0.6365992	0.056	.	-1.2806362	0.00743786
9YS - QTHJC	24	0.20687918	0.9979		-0.4371578	0.85091618
9YS - RCRSC	24	-0.3692417	0.7883		-1.0132787	0.27479536
9YS - TTKSF	24	0.38052216	0.7517		-0.2635148	1.02455917
9YS - TTKSK	24	0.3805947	0.7514		-0.2634423	1.02463171
9YS - TTKSP	24	-0.0432923	1		-0.6873293	0.60074469
9YS - TTKST	24	0.06582918	1		-0.5782078	0.70986619
9YS - TTTSK	24	0.29067554	0.9566		-0.3533615	0.93471254
9YS - Water	24	0.90704275	3.00E-04	***	0.26300575	1.55107976
AvrSr35 - AvrSr35-Q72	24	-0.7741588	0.0052	**	-1.4181958	-0.1301218
AvrSr35 - QTHJC	24	0.0693195	1		-0.5747175	0.71335651
AvrSr35 - RCRSC	24	-0.5068013	0.2963		-1.1508383	0.13723568
AvrSr35 - TTKSF	24	0.24296249	0.9904		-0.4010745	0.8869995
AvrSr35 - TTKSK	24	0.24303503	0.9904		-0.401002	0.88707204
AvrSr35 - TTKSP	24	-0.180852	0.9995		-0.824889	0.46318502
AvrSr35 - TTKST	24	-0.0717305	1		-0.7157675	0.57230652
AvrSr35 - TTTSK	24	0.15311586	0.9999		-0.4909211	0.79715287
AvrSr35 - Water	24	0.76948308	0.0057	**	0.12544607	1.41352009
AvrSr35-Q72 - QTHJC	24	0.84347833	0.0013	**	0.19944132	1.48751534
AvrSr35-Q72 - RCRSC	24	0.2673575	0.9778		-0.3766795	0.91139451
AvrSr35-Q72 - TTKSF	24	1.01712131	0	***	0.37308431	1.66115832
AvrSr35-Q72 - TTKSK	24	1.01719386	0	***	0.37315685	1.66123086

AvrSr35-Q72 - TTKSP	24	0.59330684	0.1048		-0.0507302	1.23734384
AvrSr35-Q72 - TTKST	24	0.70242833	0.0193	*	0.05839133	1.34646534
AvrSr35-Q72 - TTTSK	24	0.92727469	2.00E-04	***	0.28323768	1.57131117
AvrSr35-Q72 - Water	24	1.54364191	0	***	0.8996049	2.18767891
QTHJC - RCRSC	24	-0.5761208	0.1318		-1.2201578	0.06791618
QTHJC - TTKSF	24	0.17364299	0.9997		-0.470394	0.81767999
QTHJC - TTKSK	24	0.17371553	0.9997		-0.4703215	0.81775253
QTHJC - TTKSP	24	-0.2501715	0.9875		-0.8942085	0.39386552
QTHJC - TTKST	24	-0.14105	1		-0.785087	0.50298701
QTHJC - TTTSK	24	0.08379636	1		-0.5602406	0.72783337
QTHJC - Water	24	0.70016358	0.02	*	0.05612657	1.34420058
RCRSC - TTKSF	24	0.74976381	0.0083	**	0.1057268	1.39380082
RCRSC - TTKSK	24	0.74983635	0.0083	**	0.10579935	1.39387336
RCRSC - TTKSP	24	0.32594934	0.9008		-0.3180877	0.96998634
RCRSC - TTKST	24	0.43507083	0.5505		-0.2089662	1.07910784
RCRSC - TTTSK	24	0.65991719	0.039	*	0.01588018	1.30395419
RCRSC - Water	24	1.2762844	0	***	0.6322474	1.92032141
TTKSF - TTKSK	24	7.25E-05	1		-0.6439645	0.64410955
TTKSF - TTKSP	24	-0.4238145	0.5937		-1.0678515	0.22022253
TTKSF - TTKST	24	-0.314693	0.922		-0.95873	0.32934403
TTKSF - TTTSK	24	-0.0898466	1		-0.7338836	0.55419038
TTKSF - Water	24	0.52652059	0.2401		-0.1175164	1.1705576
TTKSK - TTKSP	24	-0.423887	0.5935		-1.067924	0.22014999
TTKSK - TTKST	24	-0.3147655	0.9219		-0.9588025	0.32927149
TTKSK - TTTSK	24	-0.0899192	1		-0.7339562	0.55411784
TTKSK - Water	24	0.52644805	0.2403		-0.117589	1.17048506
TTKSP - TTKST	24	0.1091215	1		-0.5349155	0.7531585
TTKSP - TTTSK	24	0.33396785	0.8836		-0.3100692	0.97800486
TTKSP - Water	24	0.95033507	1.00E-04	***	0.30629806	1.59437208
TTKST - TTTSK	24	0.22484636	0.9953		-0.4191907	0.86888336
TTKST - Water	24	0.84121357	0.0014	**	0.19717657	1.48525058
TTTSK - Water	24	0.61636722	0.0757	.	-0.0276698	1.26040423
69SD657C-V1 - 69SD657C-V2	36	0.54829305	0.3187		-0.1585174	1.2551035
69SD657C-V1 - 69SD657C-V3	36	-0.5026548	0.4633		-1.2094652	0.20415565
69SD657C-V1 - 9YS	36	0.37802311	0.8585		-0.3287873	1.08483356
69SD657C-V1 - AvrSr35	36	0.71238251	0.0462	*	0.00557206	1.41919296
69SD657C-V1 - AvrSr35-Q72	36	-0.1071307	1		-0.8139412	0.5996797
69SD657C-V1 - QTHJC	36	0.71811655	0.0426	*	0.0113061	1.424927
69SD657C-V1 - RCRSC	36	0.0580944	1		-0.648716	0.76490485

69SD657C-V1 - TTKSF	36	0.91665557	0.0016	**	0.20984512	1.62346602
69SD657C-V1 - TTKSK	36	0.82313534	0.0082	**	0.1163249	1.52994579
69SD657C-V1 - TTKSP	36	0.45021998	0.6453		-0.2565905	1.15703043
69SD657C-V1 - TTKST	36	0.72864434	0.0366	*	0.02183389	1.43545479
69SD657C-V1 - TTTSK	36	0.8111446	0.0101	*	0.10433415	1.51795505
69SD657C-V1 - Water	36	1.6422021	0	***	0.93539165	2.34901255
69SD657C-V2 - 69SD657C-V3	36	-1.0509478	1.00E-04	***	-1.7577583	-0.3441374
69SD657C-V2 - 9YS	36	-0.1702699	0.9999		-0.8770804	0.53654051
69SD657C-V2 - AvrSr35	36	0.16408946	0.9999		-0.542721	0.87089991
69SD657C-V2 - AvrSr35-Q72	36	-0.6554238	0.0993	.	-1.3622342	0.05138665
69SD657C-V2 - QTHJC	36	0.1698235	0.9999		-0.5369869	0.87663395
69SD657C-V2 - RCRSC	36	-0.4901987	0.5061		-1.1970091	0.2166118
69SD657C-V2 - TTKSF	36	0.36836252	0.8798		-0.3384479	1.07517297
69SD657C-V2 - TTKSK	36	0.2748423	0.9874		-0.4319682	0.98165274
69SD657C-V2 - TTKSP	36	-0.0980731	1		-0.8048835	0.60873738
69SD657C-V2 - TTKST	36	0.18035129	0.9998		-0.5264592	0.88716174
69SD657C-V2 - TTTSK	36	0.26285155	0.9916		-0.4439589	0.969662
69SD657C-V2 - Water	36	1.09390905	0	***	0.38709861	1.8007195
69SD657C-V3 - 9YS	36	0.88067791	0.003	**	0.17386746	1.58748836
69SD657C-V3 - AvrSr35	36	1.21503731	0	***	0.50822686	1.92184775
69SD657C-V3 - AvrSr35-Q72	36	0.39552405	0.815		-0.3112864	1.1023345
69SD657C-V3 - QTHJC	36	1.22077135	0	***	0.5139609	1.9275818
69SD657C-V3 - RCRSC	36	0.5607492	0.2839		-0.1460613	1.26755965
69SD657C-V3 - TTKSF	36	1.41931037	0	***	0.71249992	2.12612081
69SD657C-V3 - TTKSK	36	1.32579014	0	***	0.61897969	2.03260059
69SD657C-V3 - TTKSP	36	0.95287478	8.00E-04	***	0.24606433	1.65968523
69SD657C-V3 - TTKST	36	1.23129914	0	***	0.52448869	1.93810958
69SD657C-V3 - TTTSK	36	1.3137994	0	***	0.60698895	2.02060985
69SD657C-V3 - Water	36	2.1448569	0	***	1.43804645	2.85166735
9YS - AvrSr35	36	0.3343594	0.9382		-0.3724511	1.04116984
9YS - AvrSr35-Q72	36	-0.4851539	0.5237		-1.1919643	0.22165659
9YS - QTHJC	36	0.34009344	0.9301		-0.366717	1.04690389
9YS - RCRSC	36	-0.3199287	0.9556		-1.0267392	0.38688174
9YS - TTKSF	36	0.53863246	0.3472		-0.168178	1.2454429
9YS - TTKSK	36	0.44511223	0.6627		-0.2616982	1.15192268
9YS - TTKSP	36	0.07219687	1		-0.6346136	0.77900732
9YS - TTKST	36	0.35062123	0.9134		-0.3561892	1.05743167
9YS - TTTSK	36	0.43312149	0.7026		-0.273689	1.13993194
9YS - Water	36	1.26417899	0	***	0.55736854	1.97098944

AvrSr35 - AvrSr35-Q72	36	-0.8195133	0.0088	**	-1.5263237	-0.1127028
AvrSr35 - QTHJC	36	0.00573405	1		-0.7010764	0.71254449
AvrSr35 - RCRSC	36	-0.6542881	0.1007		-1.3610986	0.05252234
AvrSr35 - TTKSF	36	0.20427306	0.9993		-0.5025374	0.91108351
AvrSr35 - TTKSK	36	0.11075284	1		-0.5960576	0.81756328
AvrSr35 - TTKSP	36	-0.2621625	0.9918		-0.968973	0.44464792
AvrSr35 - TTKST	36	0.01626183	1		-0.6905486	0.72307228
AvrSr35 - TTTSK	36	0.09876209	1		-0.6080484	0.80557254
AvrSr35 - Water	36	0.9298196	0.0012	**	0.22300915	1.63663004
AvrSr35-Q72 - QTHJC	36	0.8252473	0.0079	**	0.11843685	1.53205775
AvrSr35-Q72 - RCRSC	36	0.16522515	0.9999		-0.5415853	0.87203559
AvrSr35-Q72 - TTKSF	36	1.02378632	2.00E-04	***	0.31697587	1.73059676
AvrSr35-Q72 - TTKSK	36	0.93026609	0.0012	**	0.22345564	1.63707654
AvrSr35-Q72 - TTKSP	36	0.55735073	0.2931		-0.1494597	1.26416118
AvrSr35-Q72 - TTKST	36	0.83577509	0.0066	**	0.12896464	1.54258553
AvrSr35-Q72 - TTTSK	36	0.91827535	0.0015	**	0.2114649	1.62508579
AvrSr35-Q72 - Water	36	1.74933285	0	***	1.0425224	2.4561433
QTHJC - RCRSC	36	-0.6600222	0.0936	.	-1.3668326	0.04678829
QTHJC - TTKSF	36	0.19853902	0.9995		-0.5082714	0.90534946
QTHJC - TTKSK	36	0.10501879	1		-0.6017917	0.81182924
QTHJC - TTKSP	36	-0.2678966	0.99		-0.974707	0.43891388
QTHJC - TTKST	36	0.01052779	1		-0.6962827	0.71733823
QTHJC - TTTSK	36	0.09302805	1		-0.6137824	0.7998385
QTHJC - Water	36	0.92408555	0.0014	**	0.2172751	1.630896
RCRSC - TTKSF	36	0.85856117	0.0045	**	0.15175072	1.56537162
RCRSC - TTKSK	36	0.76504095	0.0211	*	0.0582305	1.47185139
RCRSC - TTKSP	36	0.39212558	0.824		-0.3146849	1.09893603
RCRSC - TTKST	36	0.67054994	0.0818	.	-0.0362605	1.37736039
RCRSC - TTTSK	36	0.7530502	0.0254	*	0.04623975	1.45986065
RCRSC - Water	36	1.5841077	0	***	0.87729726	2.29091815
TTKSF - TTKSK	36	-0.0935202	1		-0.8003307	0.61329022
TTKSF - TTKSP	36	-0.4664356	0.5892		-1.173246	0.24037486
TTKSF - TTKST	36	-0.1880112	0.9997		-0.8948217	0.51879922
TTKSF - TTTSK	36	-0.105511	1		-0.8123214	0.60129948
TTKSF - Water	36	0.72554654	0.0382	*	0.01873609	1.43235698
TTKSK - TTKSP	36	-0.3729154	0.87		-1.0797258	0.33389509
TTKSK - TTKST	36	-0.094491	1		-0.8013015	0.61231944
TTKSK - TTTSK	36	-0.0119907	1		-0.7188012	0.6948197
TTKSK - Water	36	0.81906676	0.0088	**	0.11225631	1.52587721

TTKSP - TTKST	36	0.27842436	0.9859		-0.4283861	0.9852348
TTKSP - TTTSK	36	0.36092462	0.8947		-0.3458858	1.06773507
TTKSP - Water	36	1.19198212	0	***	0.48517167	1.89879257
TTKST - TTTSK	36	0.08250026	1		-0.6243102	0.78931071
TTKST - Water	36	0.91355777	0.0017	**	0.20674732	1.62036821
TTTSK - Water	36	0.8310575	0.0072	**	0.12424706	1.53786795
69SD657C-V1 - 69SD657C-V2	48	0.64370118	0.4301		-0.2439766	1.53137899
69SD657C-V1 - 69SD657C-V3	48	-0.6424902	0.4333		-1.530168	0.24518759
69SD657C-V1 - 9YS	48	0.45207629	0.8965		-0.4356015	1.3397541
69SD657C-V1 - AvrSr35	48	0.77944985	0.1511		-0.108228	1.66712766
69SD657C-V1 - AvrSr35-Q72	48	-0.1568059	1		-1.0444837	0.73087193
69SD657C-V1 - QTHJC	48	0.81297256	0.1098		-0.0747053	1.70065037
69SD657C-V1 - RCRSC	48	0.12135308	1		-0.7663247	1.00903089
69SD657C-V1 - TTKSF	48	1.04951487	0.0067	**	0.16183706	1.93719268
69SD657C-V1 - TTKSK	48	0.95023885	0.024	*	0.06256104	1.83791666
69SD657C-V1 - TTKSP	48	0.45351079	0.8944		-0.434167	1.3411886
69SD657C-V1 - TTKST	48	0.80361849	0.1203		-0.0840593	1.6912963
69SD657C-V1 - TTTSK	48	0.9227644	0.0334	*	0.03508659	1.81044221
69SD657C-V1 - Water	48	1.99150623	0	***	1.10382842	2.87918404
69SD657C-V2 - 69SD657C-V3	48	-1.2861914	2.00E-04	***	-2.1738692	-0.3985136
69SD657C-V2 - 9YS	48	-0.1916249	1		-1.0793027	0.69605293
69SD657C-V2 - AvrSr35	48	0.13574867	1		-0.7519291	1.02342648
69SD657C-V2 - AvrSr35-Q72	48	-0.8005071	0.124		-1.6881849	0.08717076
69SD657C-V2 - QTHJC	48	0.16927138	1		-0.7184064	1.05694919
69SD657C-V2 - RCRSC	48	-0.5223481	0.7568		-1.4100259	0.36532971
69SD657C-V2 - TTKSF	48	0.4058137	0.9521		-0.4818641	1.29349151
69SD657C-V2 - TTKSK	48	0.30653768	0.9958		-0.5811401	1.19421549
69SD657C-V2 - TTKSP	48	-0.1901904	1		-1.0778682	0.69748742
69SD657C-V2 - TTKST	48	0.15991731	1		-0.7277605	1.04759512
69SD657C-V2 - TTTSK	48	0.27906322	0.9983		-0.6086146	1.16674103
69SD657C-V2 - Water	48	1.34780505	1.00E-04	***	0.46012724	2.23548286
69SD657C-V3 - 9YS	48	1.09456651	0.0036	**	0.2068887	1.98224432
69SD657C-V3 - AvrSr35	48	1.42194007	0	***	0.53426226	2.30961788
69SD657C-V3 - AvrSr35-Q72	48	0.48568434	0.8377		-0.4019935	1.37336215
69SD657C-V3 - QTHJC	48	1.45546278	0	***	0.56778497	2.34314059
69SD657C-V3 - RCRSC	48	0.76384329	0.1739		-0.1238345	1.6515211
69SD657C-V3 - TTKSF	48	1.69200509	0	***	0.80432728	2.5796829
69SD657C-V3 - TTKSK	48	1.59272907	0	***	0.70505126	2.48040688
69SD657C-V3 - TTKSP	48	1.09600101	0.0035	**	0.2083232	1.98367882

69SD657C-V3 - TTKST	48	1.44610871	0	***	0.5584309	2.33378652
69SD657C-V3 - TTTSK	48	1.56525462	0	***	0.67757681	2.45293243
69SD657C-V3 - Water	48	2.63399644	0	***	1.74631863	3.52167425
9YS - AvrSr35	48	0.32737356	0.9922		-0.5603043	1.21505137
9YS - AvrSr35-Q72	48	-0.6088822	0.5248		-1.49656	0.27879564
9YS - QTHJC	48	0.36089627	0.9814		-0.5267815	1.24857408
9YS - RCRSC	48	-0.3307232	0.9914		-1.218401	0.55695459
9YS - TTKSF	48	0.59743858	0.5567		-0.2902392	1.48511639
9YS - TTKSK	48	0.49816256	0.812		-0.3895153	1.38584037
9YS - TTKSP	48	0.00143449	1		-0.8862433	0.8891123
9YS - TTKST	48	0.35154219	0.9852		-0.5361356	1.23922
9YS - TTTSK	48	0.47068811	0.8659		-0.4169897	1.35836592
9YS - Water	48	1.53942993	0	***	0.65175212	2.42710774
AvrSr35 - AvrSr35-Q72	48	-0.9362557	0.0285	*	-1.8239335	-0.0485779
AvrSr35 - QTHJC	48	0.03352271	1		-0.8541551	0.92120052
AvrSr35 - RCRSC	48	-0.6580968	0.3927		-1.5457746	0.22958104
AvrSr35 - TTKSF	48	0.27006502	0.9988		-0.6176128	1.15774283
AvrSr35 - TTKSK	48	0.170789	1		-0.7168888	1.05846681
AvrSr35 - TTKSP	48	-0.3259391	0.9925		-1.2136169	0.56173875
AvrSr35 - TTKST	48	0.02416864	1		-0.8635092	0.91184645
AvrSr35 - TTTSK	48	0.14331455	1		-0.7443633	1.03099236
AvrSr35 - Water	48	1.21205638	6.00E-04	***	0.32437857	2.09973419
AvrSr35-Q72 - QTHJC	48	0.96977844	0.0189	*	0.08210063	1.85745625
AvrSr35-Q72 - RCRSC	48	0.27815895	0.9984		-0.6095189	1.16583676
AvrSr35-Q72 - TTKSF	48	1.20632075	7.00E-04	***	0.31864294	2.09399856
AvrSr35-Q72 - TTKSK	48	1.10704473	0.003	**	0.21936692	1.99472254
AvrSr35-Q72 - TTKSP	48	0.61031666	0.5208		-0.2773611	1.49799447
AvrSr35-Q72 - TTKST	48	0.96042436	0.0212	*	0.07274655	1.84810217
AvrSr35-Q72 - TTTSK	48	1.07957028	0.0044	**	0.19189247	1.96724809
AvrSr35-Q72 - Water	48	2.1483121	0	***	1.26063429	3.03598991
QTHJC - RCRSC	48	-0.6916195	0.3118		-1.5792973	0.19605833
QTHJC - TTKSF	48	0.23654232	0.9997		-0.6511355	1.12422013
QTHJC - TTKSK	48	0.13726629	1		-0.7504115	1.0249441
QTHJC - TTKSP	48	-0.3594618	0.9821		-1.2471396	0.52821604
QTHJC - TTKST	48	-0.0093541	1		-0.8970319	0.87832374
QTHJC - TTTSK	48	0.10979184	1		-0.777886	0.99746965
QTHJC - Water	48	1.17853367	0.001	***	0.29085586	2.06621148
RCRSC - TTKSF	48	0.9281618	0.0313	*	0.04048399	1.81583961
RCRSC - TTKSK	48	0.82888578	0.0937	.	-0.058792	1.71656359

RCRSC - TTKSP	48	0.33215771	0.9911		-0.5555201	1.21983552
RCRSC - TTKST	48	0.68226541	0.3334		-0.2054124	1.56994322
RCRSC - TTTSK	48	0.80141132	0.1229		-0.0862665	1.68908913
RCRSC - Water	48	1.87015315	0	***	0.98247534	2.75783096
TTKSF - TTKSK	48	-0.099276	1		-0.9869538	0.78840179
TTKSF - TTKSP	48	-0.5960041	0.5607		-1.4836819	0.29167372
TTKSF - TTKST	48	-0.2458964	0.9996		-1.1335742	0.64178142
TTKSF - TTTSK	48	-0.1267505	1		-1.0144283	0.76092734
TTKSF - Water	48	0.94199135	0.0266	*	0.05431354	1.82966916
TTKSK - TTKSP	48	-0.4967281	0.815		-1.3844059	0.39094974
TTKSK - TTKST	48	-0.1466204	1		-1.0342982	0.74105745
TTKSK - TTTSK	48	-0.0274745	1		-0.9151523	0.86020336
TTKSK - Water	48	1.04126737	0.0074	**	0.15358956	1.92894518
TTKSP - TTKST	48	0.3501077	0.9857		-0.5375701	1.23778551
TTKSP - TTTSK	48	0.46925361	0.8684		-0.4184242	1.35693142
TTKSP - Water	48	1.53799544	0	***	0.65031763	2.42567325
TTKST - TTTSK	48	0.11914591	1		-0.7685319	1.00682372
TTKST - Water	48	1.18788774	9.00E-04	***	0.30020993	2.07556555
TTTSK - Water	48	1.06874183	0.0051	**	0.18106402	1.95641964
69SD657C-V1 - 69SD657C-V2	60	0.56963904	0.8437		-0.4781074	1.61738547
69SD657C-V1 - 69SD657C-V3	60	-0.8232511	0.2986		-1.8709975	0.22449533
69SD657C-V1 - 9YS	60	0.53892819	0.8896		-0.5088182	1.58667462
69SD657C-V1 - AvrSr35	60	0.89896866	0.1774		-0.1487778	1.94671508
69SD657C-V1 - AvrSr35-Q72	60	-0.1922824	1		-1.2400288	0.85546402
69SD657C-V1 - QTHJC	60	0.84002878	0.2682		-0.2077176	1.88777521
69SD657C-V1 - RCRSC	60	0.24682473	0.9999		-0.8009217	1.29457115
69SD657C-V1 - TTKSF	60	1.01129831	0.0701	.	-0.0364481	2.05904474
69SD657C-V1 - TTKSK	60	0.94062116	0.1283		-0.1071253	1.98836759
69SD657C-V1 - TTKSP	60	0.40422935	0.9883		-0.6435171	1.45197578
69SD657C-V1 - TTKST	60	0.67783105	0.6211		-0.3699154	1.72557747
69SD657C-V1 - TTTSK	60	0.91406191	0.1582		-0.1336845	1.96180833
69SD657C-V1 - Water	60	2.05997593	0	***	1.0122295	3.10772235
69SD657C-V2 - 69SD657C-V3	60	-1.3928901	0.001	***	-2.4406366	-0.3451437
69SD657C-V2 - 9YS	60	-0.0307109	1		-1.0784573	1.01703558
69SD657C-V2 - AvrSr35	60	0.32932961	0.9983		-0.7184168	1.37707604
69SD657C-V2 - AvrSr35-Q72	60	-0.7619214	0.4253		-1.8096679	0.28582498
69SD657C-V2 - QTHJC	60	0.27038974	0.9998		-0.7773567	1.31813617
69SD657C-V2 - RCRSC	60	-0.3228143	0.9987		-1.3705607	0.72493211
69SD657C-V2 - TTKSF	60	0.44165927	0.9748		-0.6060872	1.4894057

69SD657C-V2 - TTKSK	60	0.37098212	0.9947		-0.6767643	1.41872854
69SD657C-V2 - TTKSP	60	-0.1654097	1		-1.2131561	0.88233674
69SD657C-V2 - TTKST	60	0.10819201	1		-0.9395544	1.15593843
69SD657C-V2 - TTTSK	60	0.34442287	0.9974		-0.7033236	1.39216929
69SD657C-V2 - Water	60	1.49033688	3.00E-04	***	0.44259046	2.53808331
69SD657C-V3 - 9YS	60	1.36217929	0.0015	**	0.31443286	2.40992572
69SD657C-V3 - AvrSr35	60	1.72221976	0	***	0.67447333	2.76996618
69SD657C-V3 - AvrSr35-Q72	60	0.6309687	0.7266		-0.4167777	1.67871512
69SD657C-V3 - QTHJC	60	1.66327988	0	***	0.61553346	2.71102631
69SD657C-V3 - RCRSC	60	1.07007583	0.0403	*	0.0223294	2.11782225
69SD657C-V3 - TTKSF	60	1.83454941	0	***	0.78680299	2.88229584
69SD657C-V3 - TTKSK	60	1.76387226	0	***	0.71612583	2.81161869
69SD657C-V3 - TTKSP	60	1.22748045	0.0076	**	0.17973403	2.27522688
69SD657C-V3 - TTKST	60	1.50108215	2.00E-04	***	0.45333572	2.54882857
69SD657C-V3 - TTTSK	60	1.73731301	0	***	0.68956658	2.78505943
69SD657C-V3 - Water	60	2.88322702	0	***	1.8354806	3.93097345
9YS - AvrSr35	60	0.36004047	0.996		-0.687706	1.40778689
9YS - AvrSr35-Q72	60	-0.7312106	0.4955		-1.778957	0.31653583
9YS - QTHJC	60	0.30110059	0.9993		-0.7466458	1.34884702
9YS - RCRSC	60	-0.2921035	0.9995		-1.3398499	0.75564296
9YS - TTKSF	60	0.47237012	0.9569		-0.5753763	1.52011655
9YS - TTKSK	60	0.40169297	0.9889		-0.6460535	1.4494394
9YS - TTKSP	60	-0.1346988	1		-1.1824453	0.91304759
9YS - TTKST	60	0.13890286	1		-0.9088436	1.18664928
9YS - TTTSK	60	0.37513372	0.9941		-0.6726127	1.42288014
9YS - Water	60	1.52104774	2.00E-04	***	0.47330131	2.56879416
AvrSr35 - AvrSr35-Q72	60	-1.0912511	0.0327	*	-2.1389975	-0.0435046
AvrSr35 - QTHJC	60	-0.0589399	1		-1.1066863	0.98880655
AvrSr35 - RCRSC	60	-0.6521439	0.6801		-1.6998904	0.3956025
AvrSr35 - TTKSF	60	0.11232966	1		-0.9354168	1.16007608
AvrSr35 - TTKSK	60	0.0416525	1		-1.0060939	1.08939893
AvrSr35 - TTKSP	60	-0.4947393	0.939		-1.5424857	0.55300713
AvrSr35 - TTKST	60	-0.2211376	1		-1.268884	0.82660882
AvrSr35 - TTTSK	60	0.01509325	1		-1.0326532	1.06283968
AvrSr35 - Water	60	1.16100727	0.0159	*	0.11326084	2.2087537
AvrSr35-Q72 - QTHJC	60	1.03231119	0.0578	.	-0.0154352	2.08005761
AvrSr35-Q72 - RCRSC	60	0.43910713	0.976		-0.6086393	1.48685356
AvrSr35-Q72 - TTKSF	60	1.20358072	0.0099	**	0.15583429	2.25132714
AvrSr35-Q72 - TTKSK	60	1.13290356	0.0214	*	0.08515714	2.18064999

AvrSr35-Q72 - TTKSP	60	0.59651176	0.7962		-0.4512347	1.64425818
AvrSr35-Q72 - TTKST	60	0.87011345	0.2186		-0.177633	1.91785988
AvrSr35-Q72 - TTTSK	60	1.10634431	0.0281	*	0.05859788	2.15409074
AvrSr35-Q72 - Water	60	2.25225833	0	***	1.2045119	3.30000475
QTHJC - RCRSC	60	-0.5932041	0.8024		-1.6409505	0.45454237
QTHJC - TTKSF	60	0.17126953	1		-0.8764769	1.21901596
QTHJC - TTKSK	60	0.10059238	1		-0.947154	1.1483388
QTHJC - TTKSP	60	-0.4357994	0.9775		-1.4835459	0.611947
QTHJC - TTKST	60	-0.1621977	1		-1.2099442	0.88554869
QTHJC - TTTSK	60	0.07403313	1		-0.9737133	1.12177955
QTHJC - Water	60	1.21994714	0.0083	**	0.17220072	2.26769357
RCRSC - TTKSF	60	0.76447358	0.4196		-0.2832728	1.81222001
RCRSC - TTKSK	60	0.69379643	0.5836		-0.35395	1.74154286
RCRSC - TTKSP	60	0.15740463	1		-0.8903418	1.20515105
RCRSC - TTKST	60	0.43100632	0.9795		-0.6167401	1.47875275
RCRSC - TTTSK	60	0.66723718	0.6457		-0.3805092	1.71498361
RCRSC - Water	60	1.8131512	0	***	0.76540477	2.86089762
TTKSF - TTKSK	60	-0.0706772	1		-1.1184236	0.97706927
TTKSF - TTKSP	60	-0.607069	0.7759		-1.6548154	0.44067747
TTKSF - TTKST	60	-0.3334673	0.9981		-1.3812137	0.71427916
TTKSF - TTTSK	60	-0.0972364	1		-1.1449828	0.95051002
TTKSF - Water	60	1.04867761	0.0496	*	0.00093119	2.09642404
TTKSK - TTKSP	60	-0.5363918	0.8929		-1.5841382	0.51135462
TTKSK - TTKST	60	-0.2627901	0.9999		-1.3105365	0.78495631
TTKSK - TTTSK	60	-0.0265593	1		-1.0743057	1.02118717
TTKSK - Water	60	1.11935477	0.0246	*	0.07160834	2.16710119
TTKSP - TTKST	60	0.27360169	0.9998		-0.7741447	1.32134812
TTKSP - TTTSK	60	0.50983255	0.9243		-0.5379139	1.55757898
TTKSP - Water	60	1.65574657	0	***	0.60800015	2.703493
TTKST - TTTSK	60	0.23623086	1		-0.8115156	1.28397729
TTKST - Water	60	1.38214488	0.0012	**	0.33439845	2.42989131
TTTSK - Water	60	1.14591402	0.0186	*	0.09816759	2.19366044